THE ROLE OF RNA POLYMERASE II SUBUNIT RPB9: IN AND OUT OF THE ACTIVE SITE

A Dissertation

by

BENJAMIN CATLIN KASTER

Submitted to the Office of Graduate Studies of
Texas A&M University
in partial fulfillment of the requirements for the degree of

DOCTOR OF PHILOSOPHY

Chair of Committee,	David O. Peterson
Committee Members,	Craig D. Kaplan
	Geoffrey M. Kapler
	Hays S. Rye
Head of Department,	G.D. Reinhardt

May 2016

Major Subject: Biochemistry

ABSTRACT

Rpb9 is a conserved RNA polymerase II (pol II) subunit, the absence of which confers alterations to pol II enzymatic properties and transcription fidelity. It has been suggested previously that Rpb9 affects mobility of the trigger loop (TL), a structural element of Rpb1 that moves in and out of the active site with each elongation cycle. However, a biochemical mechanism for this effect has not been defined. We find that the mushroom toxin α-amanitin, which inhibits TL mobility, suppresses the effect of Rpb9 on NTP misincorporation consistent with a role for Rpb9 in this process. Furthermore, we have identified missense alleles of *RPB9* in yeast that suppress the severe growth defect caused by *rpb1-G730D*, a substitution within Rpb1 α-helix 21. These alleles suggest a model in which Rpb9 indirectly affects TL mobility by anchoring the position of α21, with which the TL directly interacts during opening and closing. Amino acid substitutions in Rpb9 or Rpb1 that disrupt proposed anchoring interactions resulted in phenotypes shared by *rpb9*Δ strains, including increased elongation rate *in vitro*. Combinations of *rpb9*Δ with the fast *rpb1* alleles that we identified did not result in significantly faster *in vitro* misincorporation rates than those resulting from the *RPB1* mutations alone, and this epistasis is consistent with the idea that defects caused by the *rpb1* alleles are related mechanistically to the defects caused by *rpb9*Δ. We conclude that Rpb9 supports intra-pol II interactions that modulate TL function and thus pol II enzymatic properties, which distinguishes Rpb9 from its counterparts in pol I and III. In addition, we also find that several of the genetic interactions between *RPB9* and genes

encoding components of chromatin modifying complexes are dependent on the first 11-16 amino acids of the Rpb9 N-terminal domain. This same region also interacts with the transcription factor Bye1, and may be important for TFIIF association with pol II. This suggests that there are two distinct modes of Rpb9 function—one at the active site, and one on the exterior of pol II.

TABLE OF CONTENTS

Page

LIST OF FIGURES

Page

LIST OF TABLES

Page

CHAPTER I

INTRODUCTION

From the discovery of the fundamental molecular structure of the gene in 1953 by Watson and Crick (Watson and Crick, 1953), the interpretation and utilization of the information encoded and stored inside DNA has been sought. From the Central Dogma, we understand that DNA is made tractable through RNA, the functional message that is not only used to translate proteins, but also can be used in various other gene regulatory pathways as seen in gene down-regulation with interfering RNAs and gene processing with non-coding RNAs (for a review see (Jonas and Izaurralde, 2015; Morris and Mattick, 2014)). The act of transcribing a RNA is a highly regulated process carried out by RNA polymerase (RNAP), with the regulation and complexity increasing as evolutionary diversity increases. RNAP provides the catalytic scaffold for the phosphodiester bond formation to occur between ribonucleotides as dictated by the DNA template strand, as well as serving as a landing pad for a myriad of regulatory factors that decide the outcome and final character of the RNA being transcribed. In eukaryotes, transcription is carried out by three different RNAPs termed RNA polymerase I, II, and III (pol I, II, and III), which is in contrast to the single RNAP utilized in prokaryotic RNA synthesis. Pol I is the polymerase responsible for transcribing the specialized, large ribosomal RNA transcripts rather than a protein-coding RNA, and interestingly, its activity accounts for more than half of all transcription in the cell. Pol II, in contrast, is responsible for transcribing the most diverse population of RNAs—the protein-coding

messenger RNAs. And finally, similar to pol I, pol III is also responsible for the transcription of specialized RNAs, specifically the 5S ribosomal RNA and the transfer RNAs. It is interesting to point out that though these RNAPs transcribe very different products, they have many similarities in their structure, sharing 3 of the same subunits, and mechanistically as they all have three distinct phases (termed initiation, elongation, and termination) in the generation of their product RNAs.

Of the three eukaryotic polymerases, pol II in particular has been the paradigm for studying the mechanism of transcription. Indeed, at the time of writing this work, of the peer-reviewed literature that exists on any of the three polymerases, ~89% is dedicated to pol II. This may not be particularly surprising with consideration of the fact that pol II is responsible for manufacturing the blueprints for virtually every molecular machine that exists in the cell, and that the timing, usage, and degradation of those blueprints are highly regulated. However, though much study had been devoted to understanding core structural, biochemical and regulatory mechanisms of pol II, less is known about how pol II faithfully transcribes (approximately 1 mistake out of every 100,000 bases) each of the protein blue prints from a DNA template. Maintenance of accurate mRNA transcription inside the cell is essential to life. Errors that occur during transcription can potentially lead to misfolded, truncated, or non-functional proteins that can have deleterious effects in the cell. Therefore, it is vital to understand the fundamental attributes and intrinsic, mechanistic accuracy that pol II utilizes to polymerize ribonucletides from a DNA template.

In this work, I focus on how structural elements of the budding yeast (Saccharomyces cerevisiae) pol II subunit Rpb9 can interact with and directly modulate the function of the pol II core catalytic domain termed the Trigger Loop (TL), which has been shown through various biochemical and genetic studies to affect the accuracy of transcription. In addition, I will describe some interactions of Rpb9 with non-polymerase complexes that relate to chromatin and the cellular response to stress. *S. cerevisiae* was used as the model organism for these studies in particular because it provides several advantages. Yeast pol II is homologous to all eukaryotic pol II both in sequence and structure. In addition, yeast provides a genetically tractable platform and can be grown in sufficient quantities to satisfy the demands of biochemical experiments, which have led to its extensive use in the study of various aspects of general pol II dynamics.

RNA polymerase II introduction

The first step in the utilization of genetic information is transcription of the DNA template to synthesize a complementary RNA. In eukaryotes, protein-coding genes are transcribed by RNA polymerase II, a complex and highly regulated process in which pol II transiently interacts with distinct sets of proteins during transcription initiation, elongation, and termination (Hampsey, 1998). Pol II in *Saccharomyces cerevisiae* consists of twelve subunits encoded by genes *RPB1* through *RPB12* (Woychik, 1994). Among eukaryotic pol II there is extensive structural homology. Indeed, so much homology that six subunits of human pol II can effectively replace their orthologous

counterparts in yeast (McKune, 1995). The Rpb1, Rpb2, Rpb3, Rpb4, Rpb7, Rpb9, and Rpb11 subunits of pol II have homologs in RNA pol I and III. An additional five subunits, Rpb5, Rpb6, Rpb8, Rpb10, and Rpb12 are shared by all three polymerases (Woychik, 1994; Woychik et al., 1990; Young, 1991). Rpb9 and Rpb4 are the only non-essential subunits, though each confers a growth phenotype upon removal. The two largest subunits, Rpb1 and Rpb2 (β′ and β in bacteria), which form the main body of the polymerase, are the most conserved. Rpb1 and Rpb2 are similar to their bacterial homologs not only in structure, but also in function, as Rpb1/β′ is involved in DNA binding, and Rpb2/β is involved in nucleotide substrate binding. Such commonality in structure and function suggests a common mechanism for nucleotide addition between bacterial polymerase and pol II (Cramer, 2002).

Several high–resolution crystal structures have been solved for yeast pol II that include bound templates, product RNA, and substrate NTPs. These structures have yielded much information about molecular contacts occurring within the polymerase during the process of transcription. Fig. 1.1 (left panel) depicts a crystal structure (Kettenberger, 2003) of 12 subunit pol II in an orientation known as the "top view." A large part of the structure is made up of Rpb1 and Rpb2, in tan and green, respectively. They form the primary channel, which cradles the downstream DNA, entering on the right of the polymerase, and subsequently turning 90^{o} at the active site where the template DNA (blue) is in complex with the growing RNA chain (red). Rotating the top view of the polymerase 180^{o} (Fig. 1.1, right panel) exposes other features of the enzyme such as the "funnel" domain, which flanks the active site at the 90^{o} turn of the template

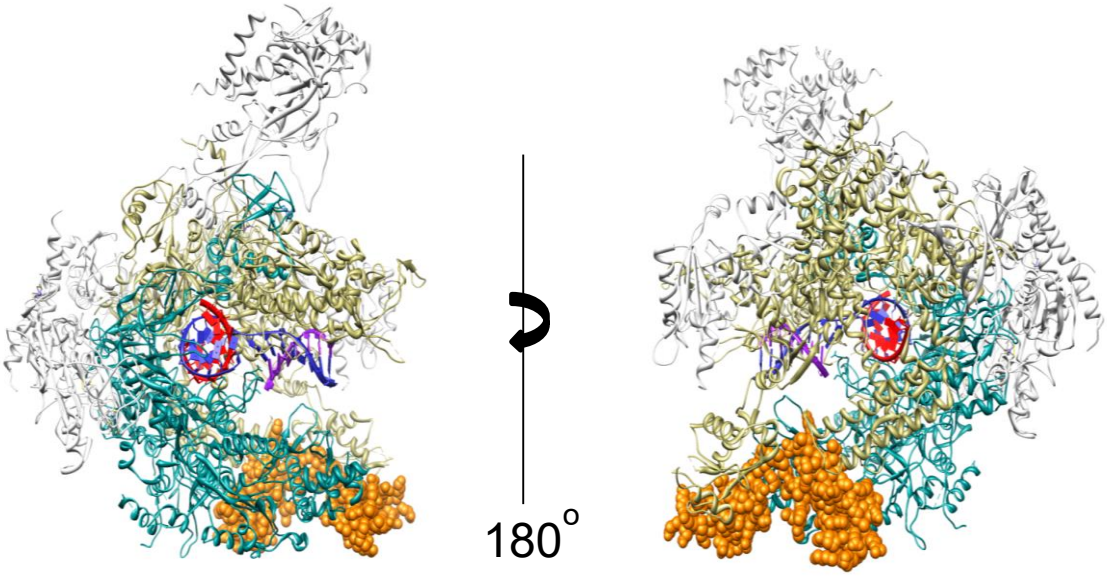

Figure 1.1: Structure of 12 subunit RNA pol II from yeast

Pictured is the crystal structure of 12 subunit, elongating RNA pol II (PDB code 1Y1W). The structure seen in the first panel is positioned in the "top view." Polymerase movement is from left to right on the template DNA (blue). Downstream DNA would extend out right from the polymerase; upstream DNA would extend out of the page. A portion of the nascent RNA transcript is pictured in red. The orange space-fill model is subunit Rpb9 located between Rpb1 and Rpb2 in tan and green respectively. The second panel is a clock-wise 180° rotation of the first panel, exposing the secondary channel of the polymerase which can be located by following the helical axis of the RNA/DNA hybrid out of the page. The "funnel" domain is to the left of the secondary channel which flanks the active site.

DNA and is proposed to be the path of incoming nucleotides (Kettenberger, 2003; Zhang, 1999). In the orange, space-fill representation is the Rpb9 subunit, which is located on the leading edge of the polymerase, and, along with Rpb1, forms a portion of the "jaw" and primary channel (Conaway, 2000). Most of the work reported here relates to the function of Rpb9.

Movement of pol II does not occur across the template DNA at a constant rate. Rather, the polymerase can pause, stop, and backtrack. The reasons underlying this attenuation are various, including physical barriers (Orphanides, 2000), damage to template DNA, and specific pause sites intrinsic to the template sequence (Bai, 2004). The most substantial of these hindrances is the presence of chromatin. Nucleosome blocks can be overcome through various mechanisms such as histone tail modifications (Roth, 2001), nucleosome remodeling via remodeling complexes like Swi/Snf and RSC (Liu, 2011), and the synergistic action of multiple polymerases on a template (Jin, 2011). In addition, transcriptional arrest can occur when pol II becomes stuck in a backtracked state. This may be remedied by the nuclease activity of pol II (Wang, 1993), which aligns a new 3′ end of the RNA with the catalytic center, leading to the continuation of transcription (Izban, 1993, 1992; Kulish, 2001; Reins, 1999). This nuclease activity is intrinsic to pol II; however, it is enhanced by the extrinsic transcription factor TFIIS, which distinguishes pol II from pol I and pol III, where efficient cleavage does not require an extrinsic protein (Izban, 1992; Kettenberger, 2003; Ruan, 2011). Extrinsic cleavage stimulation in yeast, as well as all eukaryotes, is thought to be a conserved trait from bacteria, where a protein orthologous to TFIIS (GreA in *E. coli*) is required

(Borukhov et al., 1993; Opalka et al., 2003). Several crystal structures of TFIIS in complex with pol II reveal that a C-terminal zinc ribbon domain of TFIIS enters through the funnel of pol II to contact the active site, where it is thought that acidic residues of TFIIS help to coordinate active site-bound Mg^{2+}, changing the active site environment for nuclease activity (Fish and Kane, 2002; Kettenberger, 2003).

Mechanism of RNA polymerase II catalysis

All DNA-dependent RNA polymerases have a commonality in that their first catalytic step is the transfer of a nucleotidy1-moeity from a matched substrate NTP to the 3′-hydroxyl group located on the ribose base of the ultimate nucleotide on the nascent RNA end. This requires not only that the active site of RNAP be spatially accommodating to a transcription bubble containing an RNA/DNA hybrid, but also must contain a binding site for the 3′-end of the nascent RNA and the incoming substrate. In addition, every round of phosphodiester bond synthesis must be accompanied with the forward progress of translocation of the polymerase from one position to the next. Extensive study of both bacterial RNAP and yeast RNA pol II crystal structures has identified specific conformation states that describes this progressive cycling referred to as the nucleotide addition cycle (NAC) (See Fig. 1.2A) (Martinez-Rucobo and Cramer, 2013).

The NAC begins with the polymerase in a post-translocated state. In this state the DNA template base that is immediately 5′ to the DNA base currently paired to the 3′

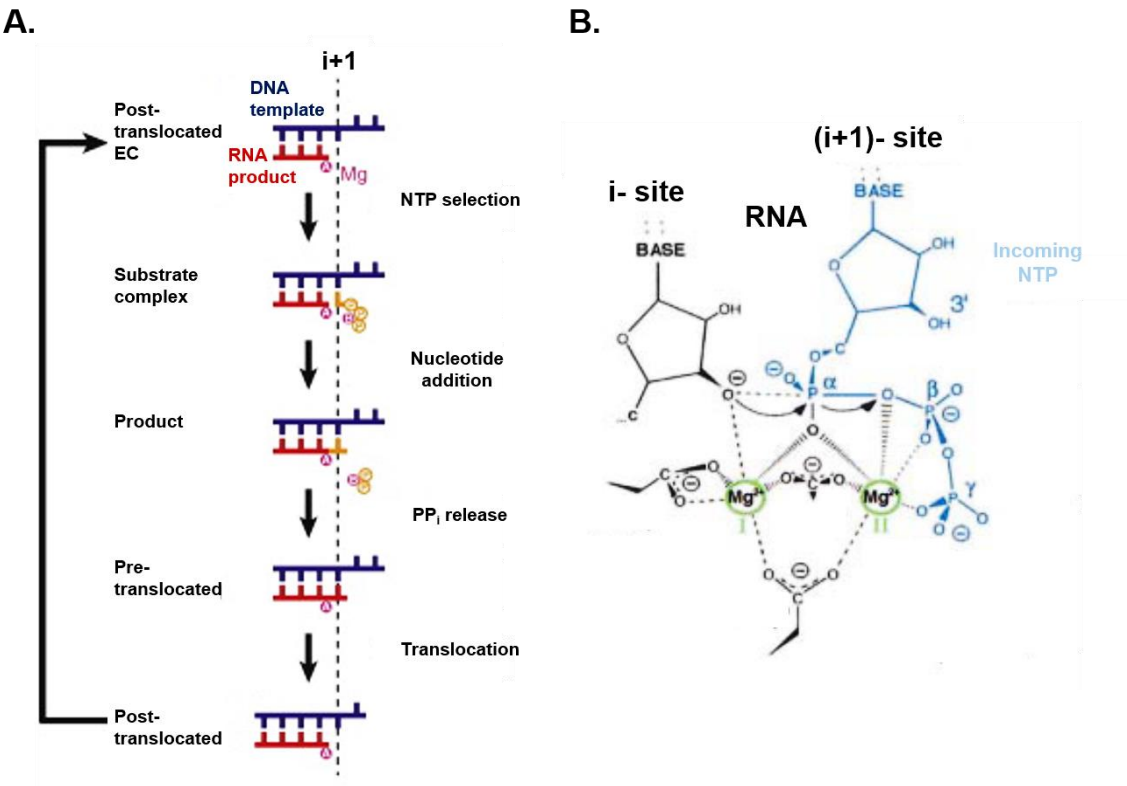

Figure 1.2: NAC and mechanism of catalysis of RNA pol II

Illustrated in (A) is the nucleotide addition cycle modified from Martinez-Rucobo, F.W., and Cramer, P. (2013). Template DNA and nascent RNA is shown in blue and red respectively. The dashed line represents the position of the i+1 site or A-site. Active site magnesium ions are colored in magenta, with the incoming substrate nucleotide colored in orange. (B) Illustrates the two metal mechanism of catalysis for all RNAPs (Sosunov et al., 2003). Colored in blue is the substrate base and in green, the coordinated active site magnesium ions. The 3′-OH on the ribose base of the RNA 3′ end nucleophilically attacks the α- phosphate of the substrate, evolving pyrophosphate.

base of the nascent RNA transcript is free to be bound by the next correct nucleotide. The position on the DNA template that would correspond to the RNA chain being extended to i+1 nucleotides in length is referred to as the A, (i+1), or insertion site. It is at this point that correct or incorrect nucleotides approach the active site through the secondary or primary cleft of pol II and are selected for or against (Wang, 2006). Once a matched NTP is paired with the template in the insertion site, nucleotide addition can occur. The generally accepted two-metal ion catalytic mechanism illustrated in Fig. 1.2 B is an S_N2 mechanism facilitated by two Mg^{2+} (colored in green and coordinated by conserved aspartate residues) and is accomplished through attack of the α-phosphate on the matched nucleotide by the 3′-OH group on the ribose base of 3′- most RNA nucleotide (Sosunov et al., 2003). The new phosphodiester bond formation is followed by pyrophosphate release with the polymerase in a pre-translocated state and the RNA 3′-end occupying the insertion site. RNAP then translocates (pre- to post- translocated) freeing the insertion site for new round of nucleotide addition. Single molecule studies have suggested that the three stages of pol II elongation—substrate selection, translocation, and catalysis—are consistent with a 'Brownian ratchet' model. In this model, the substrate can bind either translocation state of pol II, and the actual transition from pre- and post-translocated state is governed by a mobile element at the active site termed the Trigger Loop, which will be discussed in later sections (Bar-Nahum et al., 2005; Brueckner and Cramer, 2008; Gnatt et al., 2001).

In addition to the canonical A-site, high-resolution crystallographic studies have suggested multiple substrate binding sites that in some instances occupy some of the

same spatial area as the A-site (Kettenberger et al., 2004; Sosunov et al., 2003; Westover et al., 2004). One interpretation is that the process of substrate positioning within the active site is a multi-step, coordinated process that gives rise to intermediate conformations that could potentially be check points for fidelity (discussed further in later sections). The other alternative is that they represent non-native states that are synthetically caused by artifacts of pol II complexes assembled with unnatural substrates. However, these proposed sites observed in crystal structures of pol II do deserve scrutiny. One putative site was based on a crystal structure that was solved with a non-hydrolyzable substrate. Though the substrate was non-complementary, and the triphosphate of the analog was still coordinated with the active site magnesium molecules, the base was flipped facing away from the template DNA and occupying what was proposed as the E-site. This site was suggested to be important for a base discrimination check point during catalysis (Westover et al., 2004). Another site was suggested by a differing experimental approach using a different complementary NTP analog that was unable to be incorporated into the RNA chain. In this crystallographic study, the resulting elongation complex (EC) co-crystal suggested an alternative NTP pre-insertion site which largely overlaps the characterized A-site (Kettenberger et al., 2004; Wang, 2006; Westover et al., 2004).

The NAC in all RNA polymerases is dictated in part by two common, dynamic structural features—the Trigger Loop (TL), and the Bridge Helix (BH). These mobile domains have been implicated in various roles for nucleotide selection, binding, and the translocation step (Gnatt et al., 2001; Larson et al., 2012; Toulokhonov et al., 2007;

Vassylyev, 2007; Wang, 2006). The TL is a highly mobile domain in the active site and has been studied in essentially two main conformations within the crystal structure—the 'closed' state and the 'open' state. The closed state is characterized as the state in which the TL is closed down on the active site trapping the substrate at the A-site and providing acidic residues for catalysis (Kaplan, 2008; Vassylyev, 2007; Wang, 2006). In addition, it is thought that in the closed state the TL, in conjunction with the BH, work together to facilitate substrate binding and selection through a complex coordination of the ribose sugar, base, and triphosphate group (Kaplan, 2008; Kireeva et al., 2008; Larson et al., 2012; Vassylyev, 2007). This ensures that a matched substrate has bound at the A-site allowing for the closing and folding of the TL on the active site, which sequesters the substrate and provides an optimal conformation for catalysis and accurate transcription. The sequestration of the active-site-bound NTP and exclusion of other substrates by the closed state of the TL have also been observed with EDTA-quenching, which identified EDTA-resistant and sensitive pol II conformations, again suggesting a closed and open state (Kireeva et al., 2008; Walmacq et al., 2009). The 'open' conformation of the TL allows for the NTP to enter and bind the active site, potentially at the pre-insertion site. The substrate NTP has been proposed to approach the active site either through the secondary pore flanking the active site, or alternatively through the main cleft. However, there is some debate over which one is the actual pathway (Batada et al., 2004; Burton et al., 2005). If the substrate NTP base-pairs appropriately with the DNA at the A-site, the TL can then transition to the closed state. The open state of the TL is also important for the extrinsic factor TFIIS to gain access to the active site. TFIIS

is a cleavage factor that is critical for rescuing pol II when it becomes arrested or is in a back-tracked state due to DNA damage, mistakes in the RNA, or encounters with nucleosomes, as will be discussed in later sections. Much biochemical, genetic, and computational study has been devoted to understanding the transition of the TL between its various states. The obvious implication of the mobility of the TL is that changing the rate at which the TL is in or out of the active site affects not only the rate of transcription, but also its accuracy.

As seen in Fig. 1.2, the NAC is also dependent on the translocation state of the polymerase. The elongating polymerase is constantly shifting between a post-translocated (competent for elongation, exposed A-site), pre-translocated (occupied A-site, inactive), and backtracked states. In addition to their roles in selection and catalysis, the TL and BH also play a role in shifting through these various translocation states, which appears to be independent of NTP hydrolysis (Fig. 1.3) (Abbondanzieri et al., 2005; Bar-Nahum et al., 2005; Brueckner and Cramer, 2008; Larson et al., 2012). The current model for understanding the translocation process is a combination of two previously described models. The first model was proposed based on several crystal structures of both yeast and bacterial RNAPs in which the bending of the BH after NTP incorporation at the A-site provided the motive force to move the RNAP position by one nucleotide. That is, that the BH acts as a reciprocating claw that aligns the RNAP off of the incoming NTP at the active site, causing the shift between pre- and post-translocated states with the TL playing a supplementa l coordinating role (Gnatt et al., 2001). The alternate model proposes that the TL, as opposed to the BH, plays the major role in

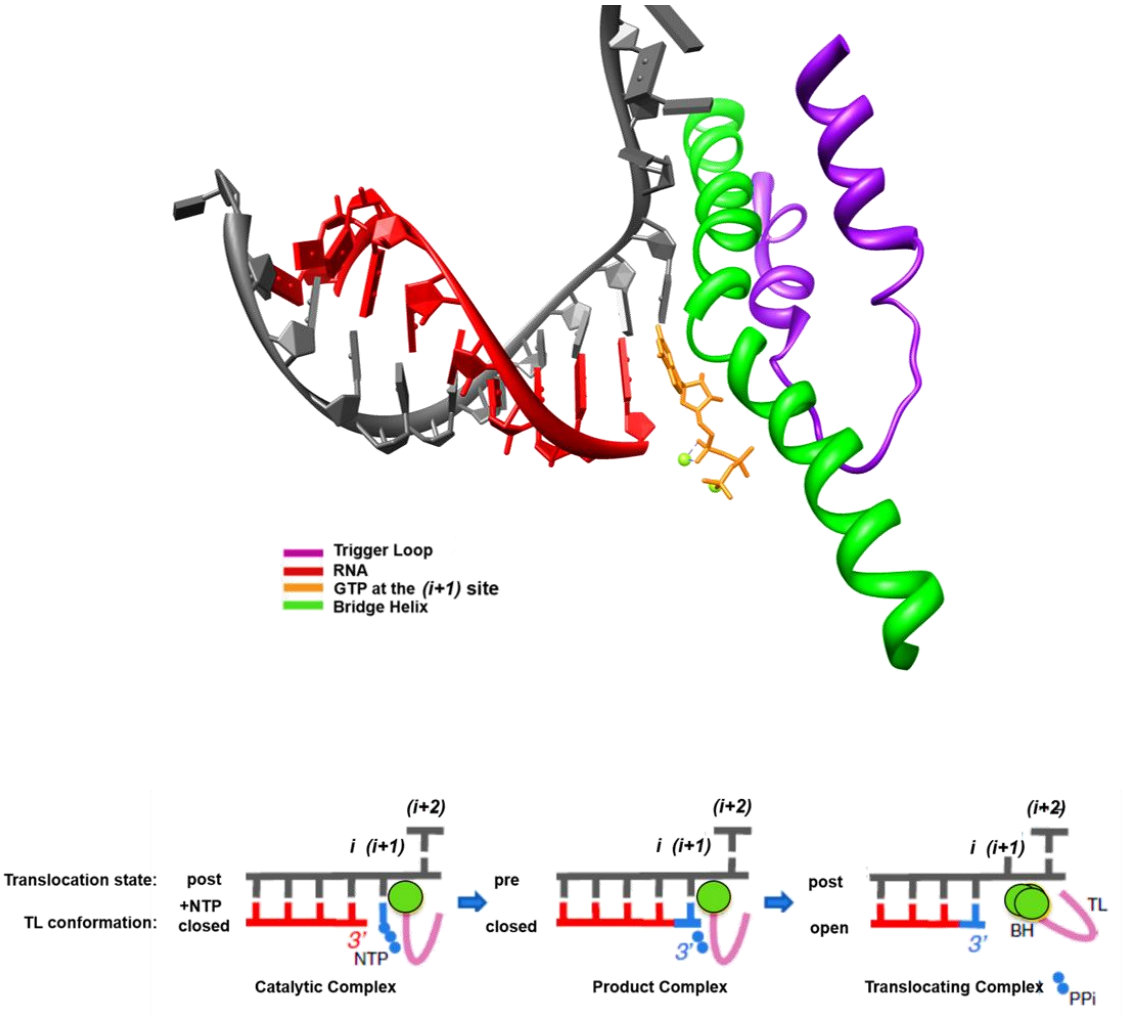

Figure 1.3: **Trigger Loop/Bridge Helix active site location and movement during NAC**

Above is a rendering of the relative positions of the TL (purple) and BH (green) in relation to the RNA end (red) at the active center pol II (modified from (Kireeva et al., 2012; Wang, 2006)). Lines between residues indicate interaction pairs. Bottom panel shows the stages of opening and closing of the TL and movement of the BH during the NAC. See text for more details.

translocation (Toulokhonov et al., 2007; Vassylyev, 2007). The model proposed that lateral movement of the RNAP is restricted upon the binding of a matched substrate. The subsequent folding of the TL on the active site further stabilizes the bound NTP, favoring the forward movement of the RNAP by preventing backtracking. However, this model does not explain the effects of the TL on RNAP translocation state independent of substrate (Bar-Nahum et al., 2005). In reality the translocation mechanism is most likely a combination of both models, such that the TL and BH act in concert by actively blocking backtracking, and favoring forward translocation (Brueckner and Cramer, 2008). Single-molecule studies with mutations in the TL of yeast pol II are in agreement with this. The closure of the TL on the bound NTP inhibits translocation. This can be exacerbated by an amino acid substitution in the TL (Rpb1-E1103G) that affects movement of the TL between different conformations, causing the TL to prefer the pre-translocated state (Larson et al., 2012). However, it is thought that after incorporation into the 3′-end of the RNA, translocation is allowed by the opening of the TL along with conformation changes in the BH via a two-ratchet mechanism (Fig. 1.3 bottom panel) (Burton et al., 2005; Kireeva et al., 2012). It's clear from the current interpretation of the NAC based on structural and biochemical data, that the TL plays a central role in both translocation, and as discussed in the next section, transcriptional fidelity.

RNA polymerase II Fidelity

The accurate production of a transcript by pol II is important at all levels of cellular function. Erroneous transcription can lead to non-functional, truncated, and mis-folded proteins that manifest themselves in deleterious ways across the cell (Saxowsky, 2006; van Leeuwen et al., 2000). Two basic processes determine how RNA polymerases maintain faithful transcription: (a) the stringent selection of substrate, and (b) recognition and removal of an error. Within pol II, the mobile TL domain plays a critical role in these processes, and can be affected through altering its ability to transition in and out of the active site.

Selectivity and Trigger Loop mobility

The first step in maintaining accurate transcription in pol II is the selection of the correct, matched, template-specified nucleotide. The *selectivity* of pol II refers to the ability of the polymerase to differentiate between ribonucleotides as well as deoxy-ribonucleotides that may be complementary to the template (for a review see (Brueckner, 2009)). The incoming NTP enters the open polymerase active site and binds to an insertion site. At this site, the DNA template is exposed establishing the Watson-Crick base pairing for the incoming nucleotide. The mobile TL then folds down on the active site and catalysis occurs. This mobile element, as well as some surrounding residues, have been implicated in transcriptional fidelity (for review see (Kaplan, 2010)). From

various crystallographic studies it has been shown that the TL takes on a stable conformation, making contacts with the substrate, when the correct NTP is in position to be added to the RNA chain. The TL in this conformation at the active center is proposed to promote catalysis through a histidine residue (Rpb1-H1085) (Wang, 2006). Analysis of mutations within the TL have implicated several residues that are important for fidelity. Mutation of residue E1103, affecting the hinging of the TL around residue G1097, has been shown to significantly increase the rate of pol II misincorporation by affecting the movement of the loop, as have other mutations that occur in the same structural area such as Rpb1-L1101S and G1097D (See Fig. 1.4) (Kaplan et al., 2012). It has also been demonstrated that a highly conserved histidine (H1085) is important for the discrimination of incorrect NTPs and matched 2'-dGTP. Other mutations in the TL vary in their effects on transcription. Mutations have been identified that increase (E1103G) or decrease (H1085Y) the incorporation of all nucleotide substrates or selectively affect only incorrect substrates (Kaplan, 2008). This suggests that the TL has dual roles in transcription, both in selection of substrate and promotion of efficient catalysis. Single molecule and computational analysis is also consistent with an effect of the TL on fidelity and speed (Kireeva et al., 2012; Larson et al., 2012; Wang et al., 2015; Wang et al., 2013). Specifically, the E1103G mutation has been shown to increase the observed catalytic rate, but also to increase the binding affinity of NTPs in general (Larson et al., 2012). Interestingly, in the same study, combination of E1103G with a mutation in H1085, which is important for catalysis and stabilization of the closed TL, reverts pol II to near wild-type function for translocation and substrate binding, but not

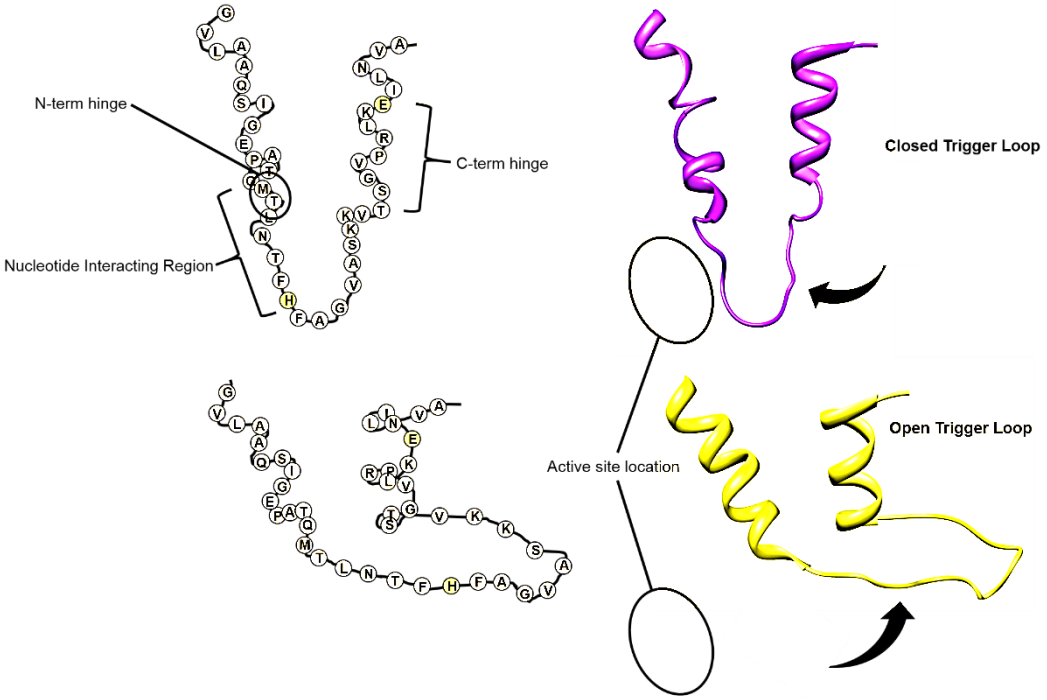

Figure 1.4: Key structural elements of the open and closed TL

The panels on the left represent the relative positions of the amino acids in the closed (top) and open (bottom) conformations of the TL from the crystal structures on the right (PDB: 2E2H and 1Y1V). Also indicated are the hinging areas and the nucleotide interaction regions, as well as the relative location of the active site. Highlighted in yellow are residues H1085 which has been shown to be critical for catalysis, and E1103 which is thought to be important for TL mobility. Black arrows indicate the direction of movement for the TL.

for catalytic rate. This suggests that TL conformations that support substrate binding and translocation are separable from those necessary for catalysis.

Other residues surrounding the TL have also been proposed to participate in substrate selection, such as Rpb1-N479, which has counterparts in prokaryotic polymerases. In the closed TL structure N479 resides opposite to TL residue Q1078, which makes contacts with the triphosphate group of the incoming nucleotide (Sydow, 2009b; Wang, 2006). The ability of pol II to distinguish between NTPs and dNTPs is based on interactions between the 2'-OH (Kettenberger, 2003) or 3′-O of the ribose base of the incoming nucleotide (Wang, 2006). Mutation of the N469 to a serine resulted in a reduction in differentiation between NTPs and dNTPs and was attributed to the loss of the contact between the 3′-OH of the ribose base (Wang, 2006), which is consistent with proposed mechanisms for the corresponding residues in *T. thermophilis* and *E. coli* (Svetlov, 2004; Vassylyev, 2007).

There are two factors that affect the selectivity of RNAPs. One is the overall catalytic efficiency for any given substrate, and the other is the propensity of the RNAP to bind a given substrate. Given that the dynamics of the TL of pol II affect both of these aspects based on mutational analysis and single molecule experimentation (Kireeva et al., 2012; Larson et al., 2012; Wang et al., 2015; Wang et al., 2013), it is important to understand the structural elements within pol II that govern the transition of the TL through its various states between open and closed. A mutation in the TL of pol II from yeast, Rpb1-E1103G has been commonly studied as a paradigm for the affect perturbations on TL mobility on pol II activity. Through computer modeling, *in vitro*

transcription assays, and stop-flow kinetics, The E1103G mutation has been shown to increase sequestration of substrate NTPs at the active site both for correct and incorrect NTPs (Walmacq et al., 2009). E1103G resides in a portion of the TL that 'hinges' based on whether the TL is in the open or closed conformation (Refer to Fig. 1.4). Systematic mutational analysis of the C-terminal hinge area where E1103 resides has been consistent in that mutations in the same area such as L1101S and G1097D increase the overall elongation rate, similar to E1103G (Kaplan et al., 2012). These mutations presumably stabilize the closed conformation of the TL such that the likelihood of pol II to incorporate any substrate is increased. Interestingly, this increase in pol II activity has been associated with changes in pol II start-site selection. It has been suggested that during initiation, a catalytically more active polymerase will be more likely to overcome the initial energy barrier of synthesis of ~5 nucleotides and will be more likely to start from an upstream start site (Braberg et al., 2013; Jin and Kaplan, 2015; Kaplan et al., 2012). The opposite is true for mutations in the nucleotide interacting region (NIR) of the TL, which contains residues important for positioning the substrate base at the A-site, stabilizing the closed TL, and catalysis. Mutations in this region of the TL (such as H1085Y and N1082S) generally are transcriptionally slow and utilize downstream sites more frequently (Kaplan et al., 2012b). Intriguingly, combinations of mutations, fast and slow, within the TL can mutually suppress the phenotypes of either single mutant (Kaplan et al., 2012).

In addition to intrinsic TL mutations, other mutations and subunits of the polymerase have been suggested to affect the movement of the TL in and out of the

active site. One study in particular modeled various transitions of the TL moving from the open to closed conformation using known crystal structures as a guide (Wang et al., 2015). Using crystal structures of pol II, as well as RNAPs of *T. thermophilus* and *E. coli*, this study identified conserved residues that would be important for the stabilization of the various TL states. TL residues E1103 and K1092 and the non-TL residue D1309 were identified as important for stabilizing the 'open' conformation of the TL. Interestingly, residues K1092 and its interacting partner E712 were proposed to form a salt bridge that affects one of the transition states of the TL. E712 resides near a loop connecting two α-helices in the 'funnel' domain of pol II, proximal to the C-terminal domain of the pol II subunit Rpb9 (See Fig. 1.5). Curiously, Rpb9 has been proposed to affect TL movement similar to the E1103 residue in the TL, though no direct molecular evidence has been provided (Walmacq et al., 2009). Nevertheless, it is clear from the literature that understanding how the TL transitions in and out of the active site is vital in our understanding of how pol II maintains a homeostatic speed that is efficient in meeting cellular demands but, provides enough time during the NAC to allow for fidelity check points either through base selection by the TL or through pol II proofreading mechanisms discussed in the next section.

Proofreading

Despite selectivity mechanisms that minimize incorporation of an incorrectly templated base, errors do occur in the course of transcription. Pol II must be able to

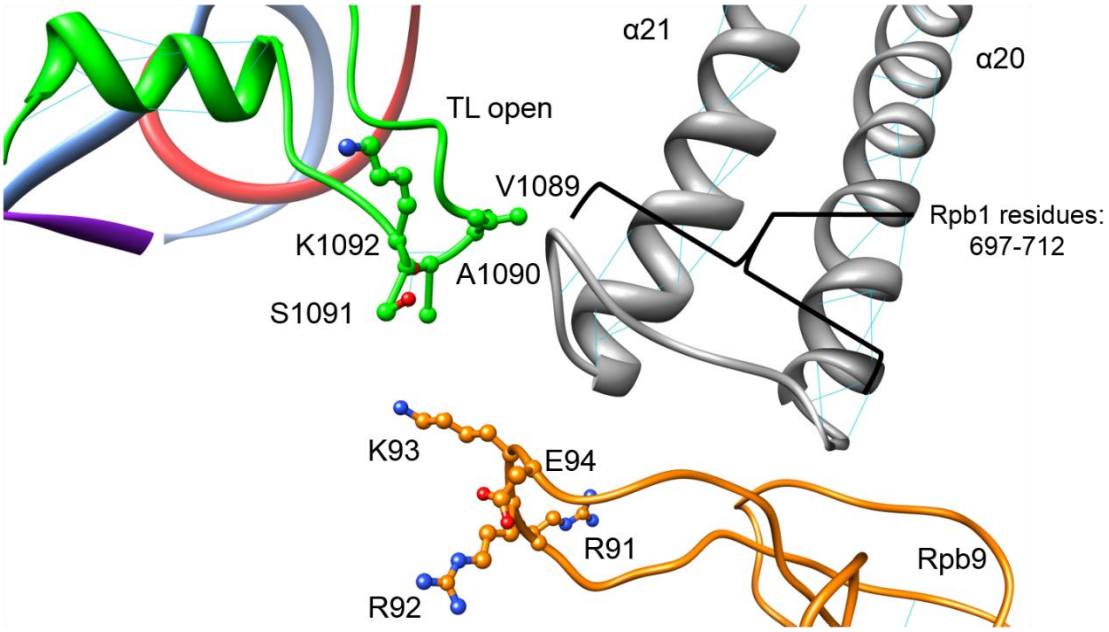

Figure 1.5: Local structural environment of open TL

Above is a rendering of a crystal structure (PDB: 1Y1V) showing the open conformation of the TL (green) and its proximity to the Rpb9 C-terminal domain (orange) and a loop connecting helices α- 20/-21 (grey) which forms part of the Funnel domain of pol II in yeast. See text for more details.

detect the error, slow transcription to allow for proofreading, and remove the mistake. Pol II incorporates incorrect substrates with varying efficiencies depending on sequence context and, regardless of the type of misincorporation, extension of the mismatch is slow (Sydow, 2009a). Mismatches can cause the polymerase to stall as a result of disrupting the competent active center conformation (Erie, 1993), which is attributed to the "frayed," mismatched end of the RNA occupying the site where an incoming nucleotide would bind (Sydow, 2009a). The distortion caused by a misincorporated nucleotide at the 3′-end of the RNA can cause pol II to pause and subsequently enter into a backtracked state. The backtracking of the pol II moves the frayed end of the RNA to another defined site in the pol II active center known as the P- (proofreading) site (Martinez-Rucobo and Cramer, 2013). In order to resume productive transcription, pol II must remove the misincorporated nucleotide from the nascent RNA and realign the 3′-end of the transcript with the active site. Pol II corrects its mistakes via an intrinsic nuclease activity, which can be stimulated by TFIIS, though the TFIIS stimulated cleavage is much more efficient than the intrinsic nuclease activity of pol II (Sigurdsson et al., 2010). Cleavage of a mismatch yields a new 3′-OH group at the end of the transcript that allows for RNA synthesis to continue. Removal of a mismatch occurs in dinucleotide steps, which removes both the terminal mismatch and the preceding nucleotide (Thomas, 1998). In order for this cleavage to take place, the polymerase must align the phosphodiester bond that will be cleaved with the active site by back-tracking such that the mismatched nucleotide moves from the (+1) to (+2) nucleotide position at the active site. TFIIS-mediated cleavage is then coordinated by the binding of TFIIS

through its pol II binding domain (domain II) to the "jaw" of pol II, followed by the insertion of domain III of TFIIS displacing the TL as demonstrated by the co-crystal of TFIIS bound with pol II (Kettenberger et al., 2004). Domain III of TFIIS has two acidic residues (D290 and E291 in *S. cerevisiae*) that are required the dinucleotide cleavage or a mismatched frayed RNA end, or the cleavage of a backtracked RNA.

Though TFIIS clearly increases fidelity *in vitro* by enhancing proofreading, *in vivo* fidelity assays have yielded conflicting results (Nesser et al., 2006; Shaw et al., 2002). *In vitro*, mutation of Domain III of TFIIS, which includes the acidic residues required for transcript cleavage completely abrogates cleavage activity (Sigurdsson et al., 2010) It is interesting to note that single molecule experiments have shown that TFIIS can suppress pausing and backtracks induced by mechanical or nucleosomal barriers by decreasing their lifetime (Ishibashi et al., 2014; Schweikhard et al., 2014), and at least some of this activity seems to operate by a cleavage-independent mechanism. In addition, absence of the pol II subunit Rpb9 increases the rate of nucleotide addition to a RNA with a mismatched nucleotide at its 3′-end or immediately adjacent to its 3'-end and decreases the efficiency of TFIIS-mediated cleavage, decreasing the likelihood that transcription errors will be excised (Knippa and Peterson, 2013). It would interesting to know whether transcriptionally fast mutations in the TL or the absence of Rpb9 increase competition with TFIIS for occupancy of the active site, as has been proposed in the bacterial system (Dangkulwanich et al., 2014; Roghanian et al., 2011). II fidelity.

A simple but useful fidelity model that incorporates pol II selectivity and

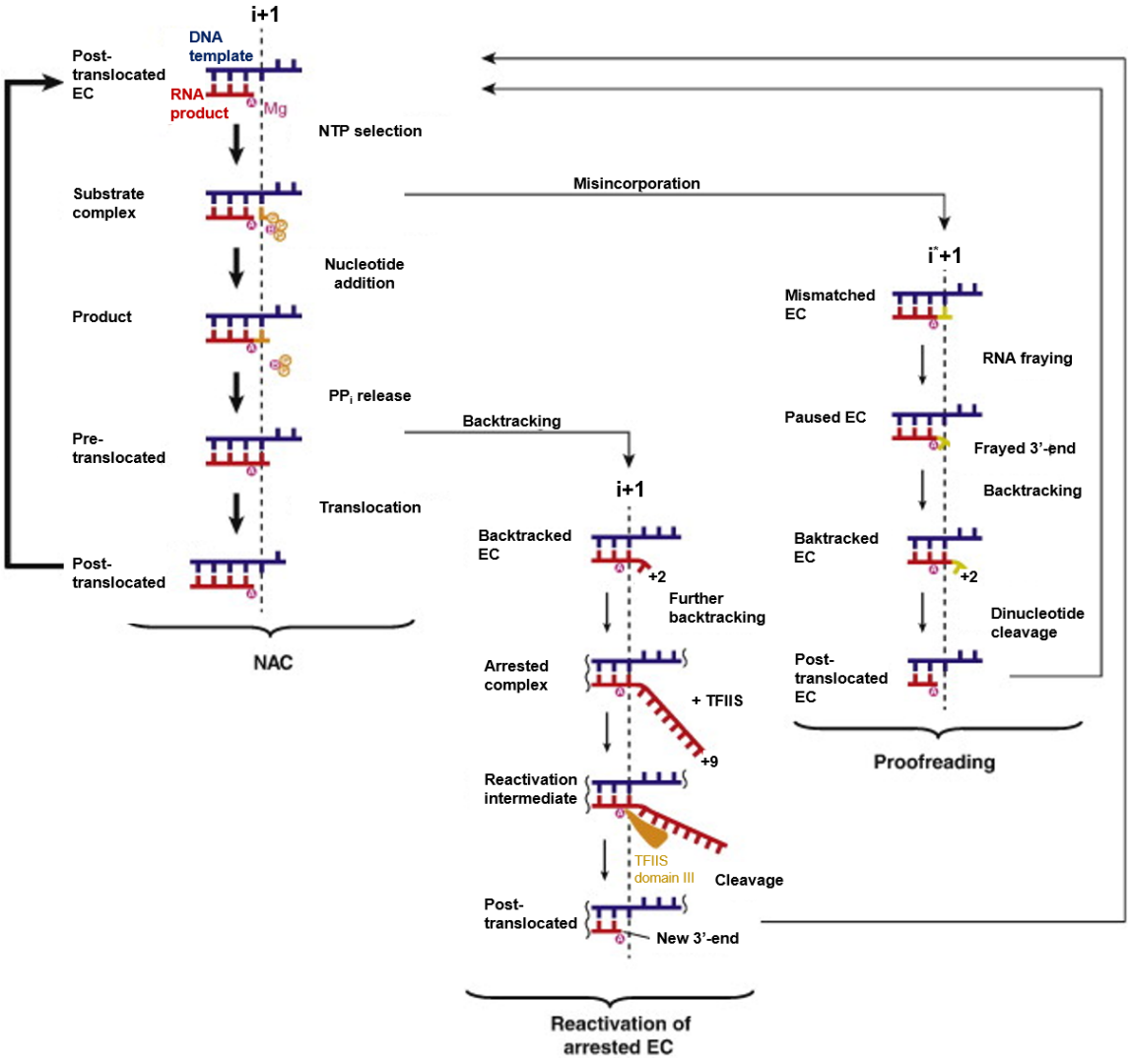

Figure 1.6: Integrated model for NAC, proofreading, and backtracking

Normal transcription occurs via the various steps of the NAC which requires correct NTP selection, addition, and pol II translocation. If initial fidelity checkpoints fail and a misincorporation event occurs, it results in a frayed RNA 3′ end. This may subsequently result in a paused elongation complex (EC) which can result in backtracking of pol II. In order to remove the misincorporation and rescue the backtracked pol II complex (Proofreading), TFIIS is recruited to pol II which stimulates cleavage of a dinucleotide from the frayed RNA 3′ end which allows transcription to begin again. Backtracking that occurs independent of transcription errors is similarly reactivated by TFIIS mediated cleavage (adapted from Martinez-Rucobo, F.W., and Cramer, P. (2013)).

proofreading is shown in Fig. 1.6 (Martinez-Rucobo and Cramer, 2013). Pol II with a transcript (i) nucleotides in length can be extended by either a correct nucleotide to a transcript (i+1) nucleotides long, or by an incorrect nucleotide to a transcript (i^* +1) nucleotides long. In the first path the correct nucleotide is added, which results in accurate transcription, demonstrated by the left, NAC panel. The second path illustrates how an incorrect nucleotide is added to the 3′-end of the RNA chain, resulting in a mismatch with the template DNA and backtracking. Selectivity can be described as the ratio of the rates of incorporation of correct and incorrect NTPs, while transcriptional proofreading depends on the ratio of the rates of mismatch extension and removal. The product of these ratios defines fidelity in a quantitative way. For pol II, incorporation of an incorrect nucleotide occurs at a rate anywhere from 500 to 4000 times slower than the incorporation of a correct nucleotide (Kaplan, 2008; Thomas, 1998). After a misincorporation event, the rate of extension slows dramatically (Knippa and Peterson, 2013; Thomas, 1998), providing a window that allows for removal of the incorrect nucleotide. Fig. 1.6 also illustrates that backtracking can occur due transcriptional arrest of pol II caused by long-term pausing or blocks to transcription such as nucleosomal barriers. An arrested pol II complex can be rescued by cleavage of the nascent RNA yielding a new, aligned 3′-end from which pol II can resume productive transcription.

The RNA polymerase II subunit Rpb9

Rpb9, a small 122 amino acid protein located on the leading edge of pol II, is

highly conserved among eukaryotes. In fact, the human homolog of Rpb9 can suppress the growth defect associated with the loss of Rpb9 in yeast (McKune et al., 1995). Indeed, the conservation of Rpb9 is not limited to pol II, as Rpb9 homologs A12.2 and C11 are present in pol I and III, respectively. Structurally, Rpb9 consists of three separate domains, two zinc-ribbon folds that are connected by a linker that forms a β motif with β28 of Rpb1 (Fig. 1.7). Zn1 and Zn2 each contain 2 cysteines (colored green) that coordinate Zn^{2+} (colored red) with a sequence context of $CX_2CX_nCX_2C$. The C-terminal zinc-ribbon fold (Zn2) is buried between the Rpb1 funnel domain and the lobe domain of Rpb2 (Fig. 1.1). The N- terminal domain (Zn1) extends from the main body of the polymerase, and, along with Rpb1, helps form part of the "jaw" that cradles the incoming DNA. The zinc-ribbon fold domain is not unique to Rpb9, but is a feature shared with various transcriptionally related proteins such as TFIIB and TFIIS. Interestingly, the C-terminal zinc-ribbon motif of TFIIS is shared with Rpb9's counterparts in pol I and pol III. Furthermore, it has been demonstrated that substituting the C-terminal domain of Rpb9 with the C-terminal domain from pol III subunit C11, which is the domain of C11 responsible for stimulating nucleolytic cleavage, conveys a strong cleavage activity to pol II. This suggests that the system that pol II utilizes for transcript cleavage diverged during its evolution allowing for a remote system of cleavage stimulation while maintaining Rpb9 and its function in transcription (Ruan, 2011).

In vivo assays in budding yeast have suggested roles for Rpb9 in transcriptional fidelity. This was done through several assays that assessed fidelity *in vivo* by examining

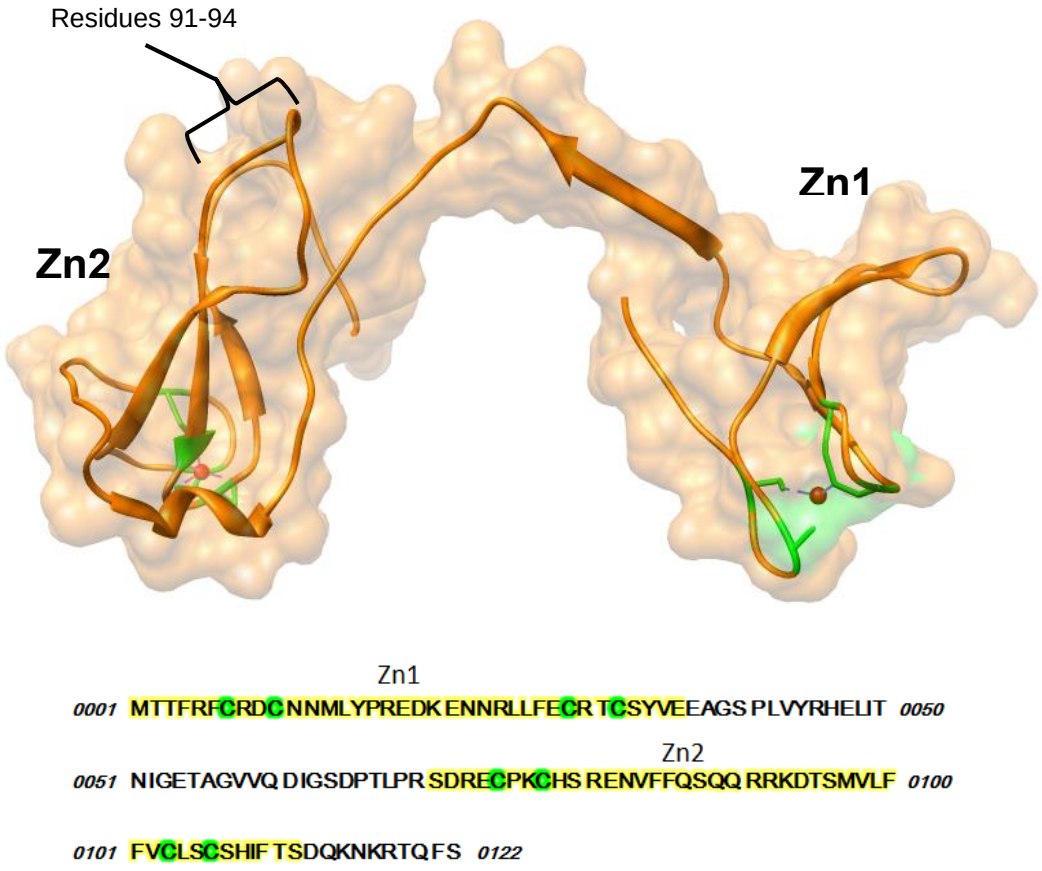

Figure 1.7: The RNA pol II subunit Rpb9

The secondary structure and protein sequence of Rpb9. Zinc-ribbon fold domains are indicated by Zn1 or Zn2 in the structure, and highlighted in yellow in the protein sequence. Cysteines chelating the zinc atoms (red) are shown in green on the structure and highlighted in green in the sequence. Residues that are nearest the active site in pol II on a C-terminal loop of Rpb9 are indicated. The relative position of the Rpb9 structure is the same as depicted in Fig 1.1. (PDB file 1Y1W)

misincorporation-based correction of a stop codon inserted into a reporter gene demonstrated that reporter gene expression increased when *RPB9* was deleted (Koyama, 2007; Nesser et al., 2006). This correlates well with phenotypes of strains lacking Rpb9 such as hypersensitivity to oxidative stress induced by menadione, which potentially leads to a need for increased discrimination or proofreading of oxidized nucleotides (Koyama, 2007). This is also consistent with *in vitro* observations that the absence of Rpb9 enhances error propagation and decreases the efficiency of TFIIS-mediated proofreading (Knippa and Peterson, 2013). A study that employed rapid-quench kinetics (Walmacq et al., 2009a) showed that the lack of Rpb9 promotes increased sequestration of substrate NTP at the active site, suggesting that one function of Rpb9 is to delay closure of the TL. It was proposed that TL mobility is restrained through interaction with K93 of Rpb9 (see Figs. 1.5 and 1.7), but mutations in K93 did not provide evidence for this idea. This study also reported evidence for an effect of Rpb9 on substrate selectivity, but these results were not confirmed in work from our lab (Knippa and Peterson, 2013).

In addition to a synthetic lethal interaction with the TL mutation *rpb1-Ell03G* (described previously), *rpb9Δ* also has genetic interactions with other mutations in pol II. *Sit* (suppressor of initiation of transcription) mutations were first isolated by Arndt et al. (Arndt et al., 1989) through a genetic screen that identified mutations that increased transcription of *HIS4* in the absence of activating transcription factors normally required in wild type cells. Interestingly, these mutations, *sit1* or *sit2*, were shown to be clustered in *RPB1* and *RPB2*, encoding the two largest subunits of RNA pol II. Further analysis revealed that *sit1* mutations cluster in 3 conserved regions of Rpb1: Region D, which

contains amino acids important for magnesium coordination in the active site; Region F, which is a portion of Rpb1 that not only interacts with Rpb9, but also forms part of the "funnel" domain of pol II; and Region G, which contains the TL (Archambault et al., 1998). Much more recently, one of the *sit1* mutants (*sit 1-7 or rpb1-G730D*) was re-isolated in a screen for mutations that suppress oxidative stress in yeast (Koyama et al., 2010). *rpb1-G730D* also caused suppression of many of the phenotypes associated with *rpb9Δ* strains (Koyama, 2007; Koyama et al., 2010).

Besides its interactions with many mutations of pol II, *RPB9* also has various interactions with non-polymerase genes (See Table 4.1). These genes serve various roles. Deletion of genes encoding proteins belonging to the SAGA (*ADA2*, *GCN5*, *SPT3/7*) and Paf1C complexes, which are important for pol II promoter escape and elongation, have been shown to be synthetic lethal with *rpb9Δ*, as have various alleles of the Mediator, Elongator, and basal initiation factors. To date, no satisfactory molecular interpretation has been given for the interactions of these distinct complex components and *RPB9*.

Rpb9 has been implicated as a key participant in processes beyond its roles in elongation and transcriptional fidelity, including transcription start site selection (Awrey, 1997) and transcription-coupled repair (Li et al., 2006), one of the two specialized branches of nucleotide excision repair pathway. Transcription-coupled repair (TCR) occurs when pol II encounters DNA damage, such as pyrimidine dimers caused by UV light. At this point the polymerase stalls, which is a signal for the recruitment of various DNA repair factors to the actively transcribing gene (for a review see (Mullenders,

2015)). During long-term stalling, Rpb9 has been shown to promote Rpb1 ubiquitylation and degradation, independent of TCR. Interestingly, the promotion of Rpb1 degradation has been localized to the Zn2 domain, and TCR functions of Rpb9 are unaffected by the loss of Zn2 (Chen et al., 2007) which suggest that Rpb9's TCR functions reside in the Zn1 domain and are independent of its function in Rpb1 degradation.

Functional differences and similarities in pol I and III

In addition to the wealth of structural information gained from crystallographic studies of pol I and II (as well as a 17 Å EM pol III structure), a recent study (Viktorovskaya et al., 2013) that generated chimeric pol II enzymes with substitutions of the pol II TL and BH with their pol I and pol III counterparts, has provided insight into the similarities and differences between RNA pol active sites (recent pol I structure (Fernandez-Tornero et al., 2013) and review of pol II and III structures (Cramer et al., 2008)). In every case the substitutions allowed growth. However, the pol II enzyme containing the pol I TL did exhibit a growth defect, and, in some instances, analogous mutations in active site functional domains do not behave the same way in the three polymerases. For example, a mutation in the pol I TL (*rpa190-E1224G*), which corresponds to the well-studied *rpb1-E1103G* mutation in the pol II TL, had opposite effects. While *rpb1-E1103G* negatively affects translocation and yet increases the overall transcription rate of pol II, *rpa190-E1224G* decreases the rate of transcription

and increases pol I pausing (Viktorovskaya et al., 2013). The results with pol I, though opposite to what was expected (transcriptionally slow, as opposed to pol II E1103G (which is transcriptionally fast), were interpreted as still likely affecting the TL mobility. It was proposed that any increase in elongation rate due to the E1224G mutation might be masked by a limiting defect in translocation (Viktorovskaya et al., 2013).

One of the most interesting mechanistic differences among the three eukaryotic polymerases is the way they proofread their mistakes. Compared to pol I and III, pol II has minimal intrinsic cleavage activity and requires the extrinsic factor TFIIS to stimulate cleavage of nucleotides from an RNA end. This lack of strong intrinsic cleavage activity is observed *in vitro* with transcription assays with purified pol II that measure the rate of misincorporation, which can be exacerbated by the lack of Rpb9 or the presence of the E1103G mutation in the TL (Knippa and Peterson, 2013; Walmacq et al., 2009). However, with pol I and III, there is no observable rate of misincorporation *in vitro*, even with the addition of the analogous E1103G mutation in the pol I TL (Viktorovskaya et al., 2013). This is due to the fact that the Rpb9 homologs of pol I and III, A12 and C11 respectively, have a C-terminal domain more closely related to TFIIS domain III, which can gain access to the active site directly and strongly stimulate cleavage, unlike the C-terminal domain of Rpb9 (Alic et al., 2007; Kuhn et al., 2007). However, it should be noted that Rpb9 is important for TFIIS mediated cleavage (Knippa and Peterson, 2013; Koyama, 2007; Koyama et al., 2010; Nesser et al., 2006). Not surprisingly, both the pol II mutation E1103G as well as its counterpart in pol I (E1124G) are synthetic lethal with the loss of Rpb9 or A12 (Viktorovskaya et al., 2013;

Walmacq et al., 2009). The E1103G mutation is also synthetic lethal with deletion of the gene encoding TFIIS, suggesting that the synthetic lethality resulting from the combination of E1103G and *rpb9Δ* is derived from a similar mechanism as its counterparts in pol I and III (Malagon et al., 2006).

It is interesting to speculate on why enzymes that have high sequence identity at their active sites (43% between pol I, II, and III TLs) should have such different mechanisms for dealing with transcription errors. For pol I, it is possible that having a strong intrinsic cleavage activity is critical because of its high initiation rate and fast elongation (twice that of pol II (Mason and Struhl, 2005; Turowski and Tollervey, 2015)). If pol I is paused on an rDNA template with a high polymerase density, it would be advantageous to have an intrinsic ability to overcome pauses rather than a remote system comparable to TFIIS recruitment. For pol III, not only is its strong intrinsic cleavage important for the proofreading response, but it is also important for termination, though a lack of a high resolution crystal structure limits more detailed investigation of the active site structural differences among the polymerases (Cramer et al., 2008). In the case of pol II, the variety of promoters, templates, and chromatin states it might encounter may demand an ability to have a multi-layered situational response. For instance, TFIIS, in addition to its role at the pol II active site, has been implicated in a role with the chromatin modifying SAGA complex, as well as with the Mediator complex, which binds upstream activating sequences in some pol II promoters and helps to coordinate pre-initiation complex formation (Wery et al., 2004). However, it should

be emphasized that all three polymerases still maintain a dependence on the TL and BH domains, as well as a necessity for cleavage activity, despite their template differences.

Structural conservation can also be observed in peripheral sub-complexes of each of the three polymerases. For example, pol I and III contain a homologous pol II Rpb4/7 sub-complex, but there is little sequence conservation for these heterodimers (Cramer et al., 2008). In pol II this complex, which can dissociate from the body of the polymerase and shuttle between the nucleus and cystoplasm, has been implicated in mRNA decay, as well as translation initiation (Duan et al., 2013). In the other two polymerases, these complexes have been suggested to be more important for interactions with initiation factors that are class-specific (Cramer et al., 2008). In addition, there is evidence that both pol I and pol III have TFIIF-like subunit complexes as integral parts of the polymerase (Fernandez-Tornero et al., 2013; Iben et al., 2011; Kuhn et al., 2007). TFIIF in pol II has been implicated in pause suppression, transcription start-site selection, and termination (Ghazy et al., 2004; Ishibashi et al., 2014; Kubicek et al., 2013; Schweikhard et al., 2014). Interestingly, the TFIIF-like sub-complex in pol III (C53/37) has also been implicated in the termination step of pol III along with the N-terminal domain of the Rpb9 homologous subunit C11 (Iben et al., 2011). It is also significant to point out that these polymerases, which differ greatly in their promoter organization, also require initiation factors such as TBP and TFIIB (homologous subunits Rrn3 and TFIIIB in pol I and III, respectively) in addition to their TFIIF-like subunits. Thus it seems though there is strong similarity between the three eukaryotic polymerases, each polymerase has evolved template-specific differences in structure and function in order to fulfill its

cellular role without necessarily “reinventing” the transcription wheel. Some of the significant differences and structural features of pol I, II, and III are detailed in Table 1.1.

Summary of introduction

Transcriptional fidelity is vital to faithfully utilizing the coded information stored in DNA, and understanding how fidelity is maintained is essential to the greater understanding of this basic component of life. Experiments in both prokaryotic and eukaryotic systems have identified certain structural elements within RNAPs that govern aspects of transcriptional fidelity. One of those elements is the TL, which moves in and out of the active site helping to ensure selection of the correct substrate nucleotide and providing a means for maintaining an evolutionarily tuned speed of transcription. Appropriate TL mobility is thus critical to all aspects of transcription.

In the chapters that follow, I provide evidence for a mechanism to explain how the small pol II subunit Rpb9 could affect the mobility of the TL. In addition, I present initial experiments designed to formulate and better understanding of the genetic interactions between RPB9 and genes that encode various co-transcriptional complexes.

Table 1.1: Notable differences of yeast nuclear polymerases

***S. cerevisiae* RNA polymerase**	**Pol I**	**Pol II**	**Pol III**
Core enzyme	A190	Rpb1	C160
	A135	Rpb2	C128
	A40	Rpb3	A40
	A19	Rpb11	A19
	A12.2	Rpb9	C11
	Rpb5	Rpb5	Rpb5
	Rpb6	Rpb6	Rpb6
	Rpb8	Rpb8	Rpb8
	Rpb10	Rpb10	Rpb10
	Rpb12	Rpb12	Rpb12
Rpb4/7 subcomplex	A14	Rpb4	C17
	A43	Rpb7	C25
TFIIF-like subcomplex	A49	(Tfg1)	C37
	A34.5	(Tfg2)	C53
Pol III-specific subcomplex	-	-	C82
	-	-	C34
	-	-	C31
Extrinsic factor required for transcript cleavage?	No (A12.2)	Yes (TFIIS)	No (C11)
Estimated *in vivo* transcription rate (nucleotides/second) [a]	~50	~30	-
Estimated *in vitro* transcription rate (nucleotides/second) [b]	~20	~12	~20
Intrinsic cleavage activity required for termination? [c]	No	No	Yes
Presence of TL and BH in active center? [d]	Yes	Yes	Yes

([a]) (Mason and Struhl, 2005; Turowski and Tollervey, 2015) ([b]) (Kaplan, 2008; Matsuzaki et al., 1994; Viktorovskaya et al., 2013) ([c] and [d]) (Cramer et al., 2008)

CHAPTER II

MATERIALS AND METHODS

Yeast strains, media, cloning, and preparations of whole cell extracts

Yeast strains and media

All yeast strains utilized were derived from three different parental strains obtained from different sources. One parental strain (generously provided by Mikhail Kashlev) was derived from the protease-deficient BJ5464 strain (Kireeva et al., 2003) with the *RPB3* ORF modified to contain a 6X-His tag and a BirA binding sequence. This strain was the source of purified pol II and pol IIΔ9, which were isolated as described (Knippa and Peterson), and it was also utilized in *in vitro* experiments in which pol II was immobilized from whole cell extracts using Ni^{2+}-NTA beads. A second parental strain (generously provided by Craig Kaplan) was derived from a *GAL2*$^{+}$ S288C strain containing a TAP-tag in the ORF of *RPB3*, *rpb1Δ::cloNATMx* supplemented with a *CEN URA3 RPB1* plasmid, and the *lys2-126δ* allele (Simchen et al., 1984). This background also harbored the *gal10Δ56* allele which contains a mutation in the *GAL10* polyadenylation signal used to report on the Gal^{S} phenotype (Greger and Proudfoot, 1998). The third strain was BY4741, also derived from S288C, which is the strain in which the yeast knockout collection was constructed.

Gene deletions were generated by PCR-generated gene disruption as described (Baudin et al., 1993; Brachmann et al., 1998) or obtained as haploids from the yeast deletion library (Dharmacon). Gene deletions that are synthetic lethal with *rpb9Δ* were generated by genetic cross of *rpb9Δ::HIS3* or *rpb9::TRP1* (supplemented with a single-copy *URA3*-marked plasmid containing *RPB9*) with a strain containing the *KanMX4* knockout of *HTZ1*, *GCN5*, *SPT7*, or *SCW5*, and screening random spores for the desired genotype.

Media

Growth and general manipulation of yeast strains were done using standard protocols (Spencer, 1989). All media was prepared using standard protocols (Spencer, 1989). Media used for phenotyping was supplemented with drugs where indicated. Media used for Gal^S phenotyping (Kaplan, 2008) contained either 2% Raffinose, or 2% Raffinose/ 1% Galactose supplemented with antimycin A (1μg/mL).

Cloning

RPB9 mutations were constructed by site-directed mutagenesis (Baudin et al., 1993; Brachmann et al., 1998), as were *RPB1* mutations *rpb1-R711A*, *-E712A*, and *-(707-709A*). *RPB1* mutations at residue S713, or any other TL residue were the generous gift of Craig Kaplan. Shuffles of various *rpb1* mutations were performed as in (Kaplan,

2008). Briefly, *rpb1* mutations were sub-cloned from a plasmid containing only a portion of the *RPB1* ORF, ligated into the full-length *RPB1* ORF on a plasmid marked with *LEU2*, and confirmed by sequencing. Plasmids containing the *rpb1* mutation of interest was then transformed into the *rpb1Δ* background via plasmid shuffle.

Whole cell extracts

All WCEs were prepared as described previously by (Kireeva et al., 2003; Knippa and Peterson, 2013).

Rpb9 purification of recombinant Rpb9

Rpb9 and the Rpb9 variant were purified essentially as in (Ruan, 2011) with several minor changes. DNA encoding N-terminal Flag-tagged Rpb9 or Rpb9-(95-97)A was amplified by PCR, digested with NdeI and XhoI, and ligated into the pET28a expression vector (Novagen), which added a 6X-His tag onto the N-terminus of each ORF. Plasmid construction was verified by sequencing. BL21(DE3) *E. coli* cells were transformed with plasmids containing Rpb9, Rpb9-(95-97)A, or the empty vector. Cells were then grown to A_{600} =0.6 at 37°C. Cells were then shifted to 18°C and induced overnight by the addition of 40 μM IPTG. Cells were lysed by sonication in PBS supplement with a protease inhibitor cocktail 1:1000 (Calbiochem) and 10 μM $ZnCl_2$. The lysate was subsequently clarified by several rounds of centrifugation at 4°C. Crude

lysate was applied to a 1 mL Histrap column (GE Healthcare) that had previously been washed with 100 mM $NiSO_4$ solution and equilibrated in purification buffer as described (Ruan, 2011). The column was washed with 10 column volumes of equilibrating buffer, buffer containing 2M NaCl and 10mM imidazole, followed by buffer containing 100mM NaCl and 40 mM imidazole, and finally by buffer containing 100mM NaCl and 100 mM imidazole. Protein was then eluted from the column by addition of purification buffer containing 300mM imidazole. Fractions containing eluted proteins were concentrated with a 30 kDa cut-off spin concentration, followed by further concentration with a 10 kDa cut-off spin concentrator. SDS-polyacrylamide gel electrophoresis of the concentrate (~0.1 mg/mL) showed only a single band, which was of the size expected for recombinant Rpb9 and which contained the flag epitope as revealed by Western blot with a flag antibody.

In vitro **transcription assays**

RNA/DNA hybrid formation and RNA labeling

Template, non-template, and RNA oligomers were either purchased from Integrated DNA Technologies or graciously supplied by Craig Kaplan (long template assays). RNAs were labeled at the 5'-end in transcription buffer (TB) 40 [20 mM Tris-HCl (pH 7.9), 40 mM KCl, 5 mM MgCl2, 2mM 2-mercaptoethanol] using T4 polynucleotide kinase and 16.7 pmol of [γ-32P] ATP (Perkin-Elmer). The labeled RNA was then

annealed to the template DNA (16.7 pmol) as described (Kireeva et al., 2003). Substrate NTPs used for misincorporation and correct nucleotide extension assays were obtained from GE Healthcare.

Assembly of elongation complexes

Elongation complexes were assembled identical to those described by (Knippa and Peterson, 2013) For assays using purified polymerase, pol II or pol II lacking Rpb9 (250 ng) was added to 25 μL of Ni^{2+}-NTA beads, which had been equilibrated in transcription buffer. For assays using WCEs, 25-50 μL was added to the same amount of Ni^{2+}-NTA or human IgG-agarose beads for strains carrying the Rpb3 TAP-tag. Purified pol II or pol II from WCEs was then allowed to bind the beads for 30 minutes at room temperature in an orbital shaker. After the initial incubation, beads were washed with 1 mL of transcription buffer identical to TB(40) except with 1 mM KCl [TB(1000)] for 10 min, followed by three 1 mL washes with TB(40). The pre-annealed RNA/DNA hybrid (1 pmol) was then added to the beads in a total volume of 100-150 μL and incubated for 10 min, followed by the addition of the non-template strand which was allowed to incubate for an addition 10 min. Elongation complexes (ECs) were then washed with 1 mL of TB(1000) for 10 min followed by 3 washes of TB(40). Final volume of washed elongation complexes was 100- 200 μL. Substrate NTPs were added, and aliquots (10μL) of the reaction mixture were removed at various time intervals (10 μL) and added to 10 μL of 2X loading buffer, which stopped the treaction. Resulting extension

products were resolved in 13.5% (long templates) or 20% polyacrylamide gels as described in (Kaplan, 2008; Knippa and Peterson, 2013). For assays with recombinant Rpb9 or Rpb9-(95-97)A, an additional wash step with 1 mL of Sarkosyl (0.035%) was incorporated between the initial TB(40) and TB(1000) washes during EC assembly. The amount of purified Rpb9 or Rpb9- (95-97)A added to the complexes is an amount to make the concentration of Rpb9 in solution (500 nM), ~20 times higher than that of the published binding constant of wild-type Rpb9 (Hemming and Edwards, 2000). For assays using α-amanitin (Calbiochem), assembled complexes were incubated with α-amanitin for 15 min before addition of NTPs. Quantification of extension products for all assays was done using Bio-Rad PharosFX Plus, and curve plots were prepared using Kaleidagraph graphing utility.

Western blotting

WCEs derived from strains with an empty vector (pRS413), or the same vector containing DNA encoding either Rpb9 or the Rpb9- (95-97)A, were added to 10 μL of Ni^{2+}-NTA beads for 30 minutes and washed as described for preparation of ECs. After the washes, most of the final wash buffer was removed to reduce the volume to approximately 20-30 μL, and 20 μL of 2X Laemmli buffer (120 mM Tris-HCl at pH 6.8, 20% glycerol, 4% SDS, 0.005% bromophenol blue, and 5% 2-mercaptoethanol) was added. Samples were boiled for 2 minutes and loaded onto a 4-20% SDS polyacrylamide gel along with molecular weight size standards. The resolved proteins were transferred

to a PVDF membrane overnight at room temperature. The membrane was then blocked in a 3% non-fat dry milk/TBS solution for 1 hour followed by an overnight incubation at 4 ^{o}C with anti-Flag antibody (Sigma) (diluted 1:1,000 in 3% non-fat dry milk/TBS). After the incubation, the blot was rinsed several times in H_2O, followed by 5 washes with TBS. Anti-mouse IgG 1:30,000 was then added to the blot and incubated for 30 minutes at room temperature, followed by 5 washes with TBS. The blot was visualized with incubation of Supersignal West Femto (Thermo) for 5 minutes, with the signal detected by a chemiluminescent imager (Bio-Rad ChemiDoc XRS). In order to compare the ratios of Rpb9 and Rpb9- (95-97)A to the Rpb1 subunit to address possible defects in association, blots were washed and blocked as described previously, probed with anti-RNA pol II 8WG16 1:500 at 4 ^{o}C overnight, and imaged as above.

CHAPTER III

A STRUCTURAL MODEL FOR TRIGGER LOOP-DEPENDENT RPB9 FUNCTION IN TRANSCRIPTION

Summary

The small RNA polymerase II (pol II) subunit Rpb9, though nonessential, has been shown to contribute to polymerase activity in several ways. The loss of Rpb9 (pol IIΔ9) results in a faster polymerase, as well as one with a decreased ability to proofread mistakes in the RNA chain, rendering it more error-prone. In addition, though far from the active center, the loss of Rpb9 increases NTP sequestration at the active site prior to new phosphodiester bond formation. This suggested that Rpb9 may act by delaying the closure of the Trigger Loop (TL), a mobile element within the interior of the polymerase important for correct nucleotide selection and catalysis. To test whether Rpb9 functions by affecting TL movement, we took advantage of the RNA polymerase inhibitor α-amanitin, which binds tightly to the polymerase, preventing closure of the TL. If there are any effects on TL movement due to the loss of Rpb9, the expectation was that in the presence of α-amanitin, these effects should disappear. Using this approach, we showed that the rates of misincorporation for a non-complementary NTP, normally 2- to 3-fold faster for pol IIΔ9 compared to pol II, become identical in the presence of the inhibitor, suggesting that the faster rate of misincorporation for pol IIΔ9 is dependent on the TL. However, a faster rate for correct NTP incorporation was still observed in pol IIΔ9, even

in the presence of α-amanitin, also suggesting a TL-independent role for Rpb9. Insights into the structural mechanism of this Rpb9-TL interaction were gained through utilizing a previously described *sit1* mutation, *rpb1-G730D*, which has been shown to have a negative *in vivo* interaction with *RPB9*. In particular, we have identified a mutation, *rpb9-(95-97)A*, that relieves this negative interaction and mimics behavior of *rpb9Δ in vivo*, and *in vitro*. Upon close examination of the structure of pol II and the position of Rpb9 residues 95-97, we identified potential interaction interfaces between Rpb9 and a loop of Rpb1 positioned between the Rpb9 C-terminal domain and the TL, termed the Anchor Loop (AL). Using site-directed mutagenesis, we targeted residues that affected Rpb9-AL and AL-TL interactions. Mutations that mimicked the *in vivo* and *in vitro* traits of *rpb9Δ* were found at each interface which was unchanged when these mutations were combined with *rpb9Δ*. Moreover, in a NTP misincorporation assay, the effects of all these mutations disappeared in the presence of α-amanitin, indicating that they depend on TL movement. Taken together, these data demonstrate a molecular pathway for TL-dependent effects of Rpb9 on transcription.

Introduction

Rpb9 is a small (122 amino acids in *S. cerevisiae*) subunit of RNA polymerase II (pol II) that is highly conserved among eukaryotes. It is composed of two zinc ribbon domains characterized by the zinc-chelating motif ($CX_2CX_nCX_2C$). Although Rpb9 is not essential for growth in yeast, *rpb9* null mutants have a number of phenotypes,

including slow growth (Li et al., 2006), hypersensitivity to several drugs (Gibney et al., 2008; Koyama, 2007; Li et al., 2006), upstream shifts in transcription start site (Hull et al., 1995; Sun et al., 1996), defects in transcription-coupled repair that result in enhanced sensitivity to UV light (Chen et al., 2007), and decreased transcriptional fidelity *in vivo* (Koyama, 2007; Nesser et al., 2006) and *in vitro* (Knippa and Peterson, 2013; Walmacq et al., 2009).

The fidelity defect of pol II that is lacking Rpb9 (pol IIΔ9) has been examined in several studies. Decreased selectivity for correct (complementary to the DNA template) versus incorrect NTP substrates has been observed (Walmacq et al., 2009). However, our published experiments did not provide evidence for a selectivity defect, and, in our hands, the decreased fidelity of pol IIΔ9 appears to be the result of inefficient proofreading caused by an increased rate of RNA extension from a mismatched 3'-end combined with a decreased efficiency of TFIIS-mediated mismatch removal (Knippa and Peterson, 2013). A role for Rpb9 in fidelity is consistent with reported roles for the corresponding subunits in RNA polymerases I and III (A12.2 and C11, respectively) (Chedin et al., 1998; Kuhn et al., 2007), as well as the related archaeal protein TFS (Hausner et al., 2000; Lange and Hausner, 2004).

Rpb9 is located on the leading edge of the elongating polymerase at a position that is not in immediate proximity to the active site (Kettenberger, 2003), and the absence of Rpb9 has little or no effect on the binding affinity of TFIIS with the polymerase (Awrey, 1997). This leaves open the question of how Rpb9 exerts its effects on elongation and cleavage. Using rapid quench-flow kinetic techniques, Walmacq, et al.

(Walmacq et al., 2009) demonstrated that Rpb9 promotes the sequestration of NTP substrates in the active site prior to formation of a new phosphodiester bond. This behavior was similar to that observed with pol II containing Rpb1-E1103G (hereafter abbreviated pol II-(Rpb1E1103G), a mutation within the trigger loop (TL), a mobile structural element that closes on the pol II active site and interacts with the substrate NTP reviewed in (Kaplan, 2010). Based on the similar behavior of pol IIΔ9 and pol II-(Rpb1E1103G), it was proposed that the C-terminal domain of Rpb9 interacts directly with the open pol II TL (Walmacq et al., 2009). However, in this same study, direct mutational analysis of an amino acid (Rpb9-K93) thought to interact with the TL showed no fidelity defect.

As discussed in Chapter I, the TL has been implicated in several functions during the transcription cycle, including, start-site selection, transcriptional fidelity, and determination of the overall catalytic rate (Brueckner and Cramer, 2008; Jin and Kaplan, 2015; Kaplan et al., 2012; Kaplan, 2008; Mejia et al., 2015; Sydow, 2009a; Sydow, 2009b; Wang et al., 2013). Effects on the transition of the TL from the open to closed state have been suggested to impact all of these processes (Wang et al., 2015; Wang et al., 2013). Genetic, single-molecule, and computational analyses have at least partially defined structural features of the TL that are important for its transition into and out of the active site. In addition to E1103, several other residues in the C-terminal hinge area of the TL, such as G1097, P1099, and L1101, also exhibit behavior consistent with an effect on TL mobility (Kaplan et al., 2012; Kireeva et al., 2012) . Intriguingly, these

mutations also demonstrate *in vivo* and *in vitro* phenotypes similar to *rpb9*Δ, and as we have found in many cases, are similarly synthetically lethal (Appendix Fig. 1).

Based on the similarities between *rpb9*Δ and mutations in the TL that have been predicted to affect TL mobility, it is very likely that Rpb9 does affect TL movement. However, to date, no biochemical mechanism for such an effect has been defined. In this study we provide additional genetic and biochemical evidence that Rpb9 affects pol II activity through the TL, describe a plausible biochemical model for how this could occur, and confirm predictions suggested by this model related to the phenotypes of certain alleles of *RPB9* and *RBP1*.

Results

Effect of Rpb9 on pol II activity in the presence of α-amanitin

While previous work had shown that the absence of Rpb9 promotes NTP sequestration in the pol II active site, the proposed mechanism, in which sequestration is increased through altered mobility of the TL, was without direct experimental support (Walmacq et al., 2009). We decided to test the general idea that Rpb9 affects TL mobility using an experimental approach that exploits the mushroom toxin α-amanitin, which has been shown to inhibit pol II by locking the TL in a position where it cannot participate directly in active site chemistry (Kaplan, 2008). We reasoned that if Rpb9

affects TL mobility, then, by immobilizing the TL with α-amanitin, the effects of Rpb9 on pol II activity would be markedly affected.

We have previously reported that the absence of Rpb9 increases the rate of pol II-catalyzed RNA synthesis in a single-nucleotide misincorporation assay (Knippa and Peterson, 2013). To assess the effect of α-amanitin on misincorporation, purified pol II or pol IIΔ9 was immobilized on Ni^{2+}-NTA beads via a 6x-His tag on Rpb3, and elongation complexes (ECs) were assembled with DNA and RNA oligonucleotides in which the 10 nt RNA was completely complementary to the template DNA and was 5'-end labeled with ^{32}P (Fig. 3.1A). Instead of the template-specified CTP, ATP (1 mM) was added, and the time course of A-for-C misincorporation was followed in the presence or absence of α-amanitin (Fig. 3.1, B and C). The fraction extended to 11 nt was plotted against time, and the data were fit to a single exponential equation. We confirmed that the extension to 11 nt was the result of misincorporation, and not the result of contaminating CTP, as the 11 nt product was not rapidly extended by addition of CTP, GTP, and UTP (data not shown), consistent with a mismatched 3'-end. In the absence of α-amanitin, the misincorporation rate for pol II was about half that observed for pol IIΔ9 (Fig. 3.1D), consistent with our previously reported observations (Knippa and Peterson, 2013), but in the presence of α-amanitin (160 μg/mL), the rates for pol II and pol IIΔ9 were almost identical (Fig. 3.1E). This concentration of α-amanitin was saturating, as concentrations as high as 640 μg/mL had no increased effect on the rate. Overall, the misincorporation reaction was not very sensitive to α-amanitin (2.3-fold and 4.8-fold for pol II and pol IIΔ9, respectively), consistent with previous observations

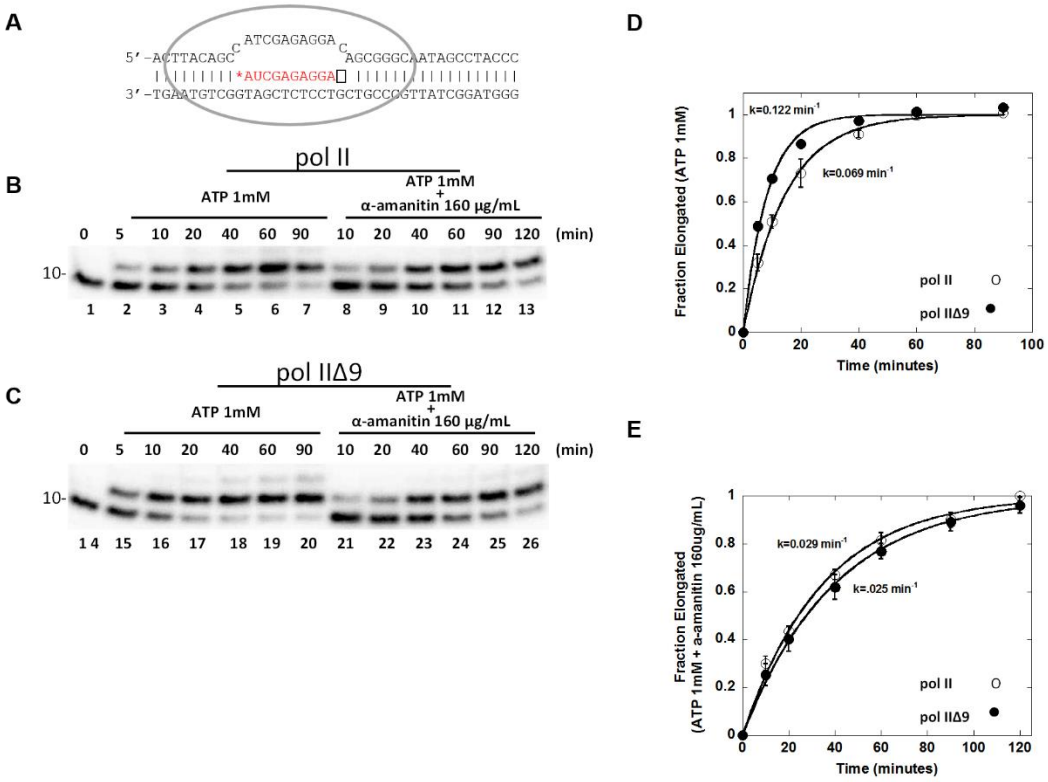

Figure 3.1: Pol IIΔ9 rate increase for an ATP misincorporation is dependent on α-amanitin

(A) The EC complex with template/non-template DNA combinations used for misincorporation assay as well as the pre-annealed 5'-^{32}P labeled RNA (red). Complexes were formed as described in material and methods with purified pol II. The gray circle indicates the approximate position of pol II and the black box indicates the i+1 nucleotide positon (CTP per the template). (B and C) ATP 1mM was added to ECs with pol II or pol IIΔ9 alone or ECs pre-incubated with α-amanitin, and the extension of the RNA to 11 nucleotides (nt) or greater was monitored over time via a 20% polyacrylamide gel. (D and E)The fraction extended to 11 nts in B and C was plotted and fit to a single exponential function to obtain an observed rate for misincorporation, indicated by each curve. The fraction elongated was divided by the extent of the reaction as determined by curve fit. Experiments here and in Fig. 3.2 were performed by Knippa, K.C.

(Kaplan, 2008), but immobilization of the TL by α-amanitin completely eliminated the effect of Rpb9 on the rate. This observation is consistent with the idea that the effect of Rpb9 on the rate of misincorporation is mediated, at least in part, by affecting the TL.

To assess the effect of α-amanitin on the much more rapid rate of elongation with template-matched NTPs, we took advantage of a method in which the rate of elongation was estimated as the average rate at which the polymerase completes transcription across a relatively long DNA template (Kaplan, 2008). ECs were assembled as shown in Fig. 3.2A, all four NTPs were added simultaneously, and transcription was monitored over time. After gel electrophoresis of the RNA products, the halftime for the appearance of products greater than 60 nt in length was estimated, and the average rate of elongation was calculated by dividing the actual number of nt synthesized (51 nt) by the halftime. At NTP concentrations of 1mM each, which was near saturation for both pol II and pol IIΔ9, the average rate of elongation was about 2.5 times faster in the absence of Rpb9 (11.5 $nt \bullet s^{-1}$ versus 4.5 $nt \bullet s^{-1}$), and remained about twice as fast in the presence of saturating α-amanitin. Overall, however, this assay was much more sensitive to α-amanitin inhibition than the misincorporation assay (about 50-fold for both pol II and pol IIΔ9) (Fig. 3.2B). This observation does not provide support for the idea that Rbp9 affects the TL. However, this pattern of differential α-amanitin sensitivity for template-matched and mismatched NTP substrates has also been observed with pol II-(Rpb1E1103G), a polymerase with a substitution at one of the TL hinge regions that, like the absence of Rpb9, results in a faster elongation rate (Kaplan, 2008), presumably by affecting TL mobility (Walmacq et al., 2009). This somewhat unexpected behavior of

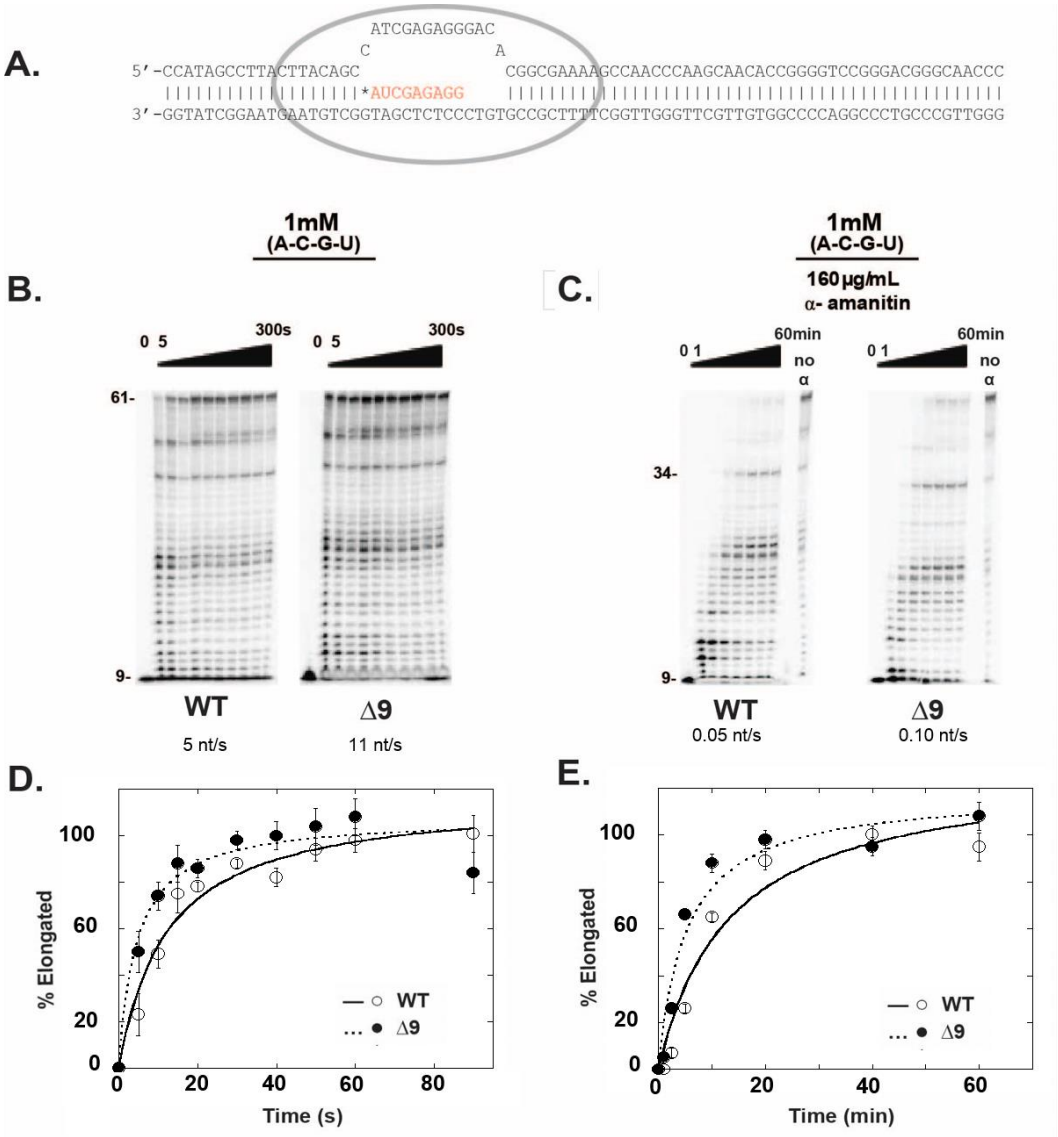

Figure 3.2: Pol IIΔ9 average correct nucleotide extension rate is not dependent on α-amanitin

(A) The EC complex with template/non-template DNA combinations used to determine the average correct nucleotide extension rate as in Fig. 3.1 except that a much longer template/non-template DNA (80 nt) was used in order to extend the measurable time period for pol II extension. (B and C) A-, C,-, G, and UTP 1mM were simultaneously added to ECs with pol II or pol IIΔ9 alone or ECs pre-incubated with α-amanitin. The fraction of RNA extended to 61 nt (or 34 nts or greater for α-amanitin experiments), forming a product of 51nt, was plotted and fit with a non-linear equation to determine the half-time (D and E). The extension rate in nt/s was determined by dividing the length of the extension product n- nucleotides long by the half-time.

pol II-(Rpb1E1103G) (and perhaps that of pol IIΔ9) may be due to effects that are independent of the TL, but this seems unlikely for E1103G, as the amino acid substitution is actually within a hinge region of the TL. Alternatively, it is possible that the rapid rate of elongation with template-matched NTPs could compete with the "on" rate of α-amanitin binding such that the small amount of free pol II in equilibrium with α-amanitin-bound pol II could, during its brief period of freedom from the inhibitor, sometimes elongate, and this would be more likely to occur in a variant with a faster elongation rate.

Overall, the α-amanitin experiments were not conclusive with regard to a potential effect of Rpb9 on the TL. The effect of α-amanitin in the misincorporation assay was consistent with the idea that the effect of Rpb9 on pol II activity is dependent on TL mobility, but its effect on elongation with template-matched NTPs was not. However, pol II-(Rpb1E1103G), a fast polymerase with an alteration in TL mobility, and pol IIΔ9 responded almost identically to α-amanitin.

Rpb9 mutations that suppress sit1-7 *(*rpb1-G730D*)*

Concurrent with the α-amanitin experiments described above, we took a more general approach to identify mutations that affect Rpb9 function. The *sit1-7* mutation (S*uppressor of* I*nitiation of* T*ranscription*), an allele of *RPB1* (*rpb1-G730D*) was originally isolated based on its ability to support low level transcription from the *HIS4* gene in the absence of normally required activating factors, and later implicated in

transcriptional elongation based on its location in a region of Rpb1 that was associated with α-amanitin resistance (Archambault et al., 1998). Subsequently, this mutation was re-isolated by Koyama, *et al.* (Koyama et al., 2010) as a suppressor of the menadione hypersensitivity of *rpb9*Δ strains. A severe growth defect is conferred by *rpb1-G730D* in the presence of *RPB9*, but near wild-type growth can be restored by deletion of Rpb9 residues 48-122, 65-70, or 89-95 (Koyama et al., 2010). Previous experiments had shown that these deletions do not prevent binding of Rpb9 to pol II (Chen et al., 2007; Hemming and Edwards, 2000), and thus it is likely that some kind of negative interaction between *RPB9* and *rpb1-G730D* is mediated through the C-terminal half of the 122-residue Rpb9. Pol II carrying the Rpb1-G730D alteration was subsequently shown to be very slow, with an elongation rate only about 10% that of wild-type pol II (Walmacq et al., 2012). We observed that the absence of Rpb9 restores a near wild-type *in vitro* elongation rate to pol II (Rpb1-G730D) (Appendix Fig. 2A-D), suggesting that specific *rpb9* alleles that relieve the negative genetic interaction with *rpb1-G730D*, such as those that delete Rpb9 residues 48-122, 65-70, or 89-95, might also have this effect. Therefore, we decided to screen additional *rpb9* alleles for their ability to relieve the negative interaction between *RPB9* and *rpb1-G730D.*

Our initial results are consistent with the results of Koyama, *et al.* (Koyama et al., 2010) (Fig. 3.3A). The severe growth defect in *rpb1-G730D RPB9* strains was partially relieved when *RPB9* was deleted, and the *rpb1-G730D rpb9*Δ strain retained only the growth defect caused by *rpb9*Δ. Providing *RPB9* on a single-copy plasmid restored the negative interaction with *rpb1-G730D*, as did an allele that changed Rpb9

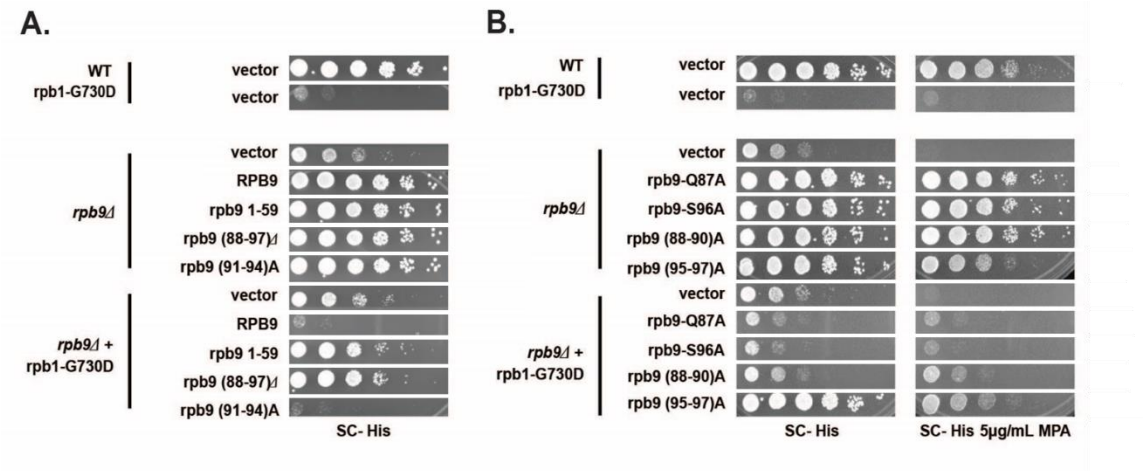

Figure 3.3: The *rpb9- (95-97)A* mutation relieves the negative interaction of the Rpb9 C-terminal domain with the *sit1* mutant *rpb1- G730D*

(A) 10-fold serial dilutions of various plasmid-borne Rpb9 mutants in the context of the rpb1- G730D mutation were spotted on the indicated media from saturated liquid cultures, and monitored for growth for several days. The C-terminal truncation mutant *rpb9- (1-59)* and the deletion mutant *rpb9- (88-97)Δ* relieve the negative interaction of *RPB9* and *rpb1- G730D*. (B) Mutations in the regions of Rpb9 thought to be important for the *rpb1- G730D* interaction were introduced via site-directed mutagenesis, combined in the context of the *rpb1* mutations, and spotted on synthetic media, or media containing MPA (5 µg/mL). Rpb9- (95-97)A relieves the negative interaction with *rpb1- G730D*, while restoring wild-type growth.

amino acids 91-94 to alanine (*rpb9-(91-94)A*). However, deletion of amino acids 88-97 (*rpb9-(88-97)*Δ) or an allele encoding only the N-terminal 59 amino acids of Rpb9 (*rpb9-(1-59)*) did not restore this negative interaction. Rpb9 encoded by all of the tested alleles appeared to be expressed and capable of associating with pol II, as all of them restored near wild-type growth to a *RPB1 rpb9*Δ strain, and in the *rpb1-G730D rpb9*Δ background, both *rpb9-(1-59)* and *rpb9-(88-97)*Δ grew significantly better than when the vector alone was present. These results strongly suggest that Rpb9 residues 88-90 and/or 95-97 play a major role in the negative interaction between *RPB9* and *rpb1-G730D.*

Additional *rpb9* alleles were constructed to further dissect this region of the protein (Fig. 3.3B, left panel). *rpb9-Q87A*, *rpb9-S96A*, *rpb9-(88-90)A*, and *rpb9-(95-97)A* all restore wild-type growth to a *rpb9*Δ strain, but only *rpb9-(95-97)A* also completely avoids the negative interaction with *rpb1-G730D* (Fig. 3.3B, left panel). *rpb9-(95-97)A* is also unique among these alleles in that it confers moderate hypersensitivity to mycophenolic acid (MPA) in a *RPB1* background (Fig. 3.3B, right panel). MPA is a potent inhibitor of IMP dehydrogenase, an enzyme important in purine biosynthesis. It has been widely assumed that MPA hypersensitivity in yeast is indicative of a defect in transcription elongation. However, a number of studies strongly indicate that the hypersensitivity is almost always a much more specific defect that results from the failure of low concentrations of GTP to cause induction of the yeast *IMD2* gene, which encodes a relatively MPA-resistant form of IMP dehydrogenase (Hyle et al., 2003; Kaplan et al., 2012). Induction is caused by a downstream shift in transcription initiation site that is required to generate the long, stable transcript that includes the

ORF. Thus, strains with mutations that prevent the efficient shift from the upstream start site (which begins with GTP) to the downstream site (which begins with ATP) when GTP concentrations are low become MPA hypersensitive. Recent evidence suggests that one (but certainly not the only) determinant of transcription initiation site selection in yeast is the elongation rate of pol II, the faster the elongation rate, the more hypersensitive to MPA, presumably because the fast polymerases constitutively initiate at the upstream start site even in the presence of low GTP concentrations (Kaplan et al., 2012). These results indicate that Rpb9-(95-97)A is missing a function that is required for both the negative interaction with Rpb1-G730D and for the efficient induction of *IMD2* transcription. However, hypersensitivity to MPA is significantly higher in a *rpb9*Δ strain compared to *rpb9-(95-97)A*, suggesting that there may be more than one function in Rpb9 that contributes to MPA resistance, as will be discussed in Chapter IV. This is consistent with observations that the N-terminal domain of Rpb9 alone (amino acids 1-57 (Van Mullem et al., 2002) or 1-59 (our unpublished observation) is sufficient to partially relieve the MPA hypersensitivity of *rpb9*Δ strains. The ability of Rpb9-(95-97)A to mimic the absence of Rpb9 in some contexts appears not to be the result of an inability of Rpb9-(95-97)A to bind the polymerase, as some contexts (e.g. in a *rpb1-G730D* strain) create phenotypes unique to *rpb9-(95-97)A*. This is consistent with published work in which amino acid substitutions near this region of Rpb9 do not affect pol II binding (Hemming and Edwards, 2000), but we address this issue more directly below.

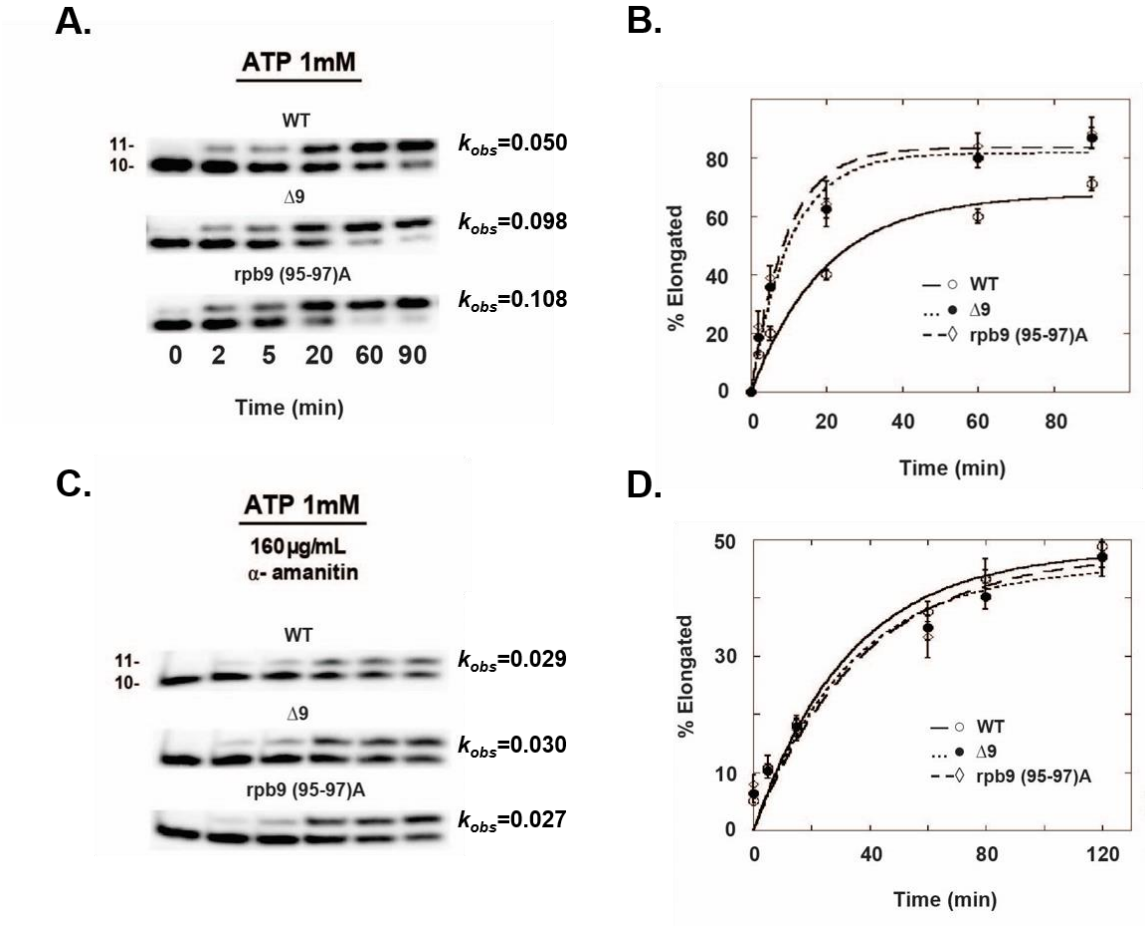

Figure 3.4: ECs derived from a strain with the Rpb9- (95-97)A variant mimic *in vitro* behavior of pol IIΔ9 for an ATP misincorporation

(A) ATP 1mM was added to ECs immobilized from WCEs with pol II (WT), *rpb9-(95-97)A* pol II, and pol IIΔ9 and the extension of the RNA to 11 nucleotides (nt) or greater was monitored over time via a 20% polyacrylamide gel. (B)The fraction extended to 11 nts in A was plotted and fit to a single exponential function to obtain an observed rate for misincorporation, indicated by each representative assay. (C) as in A, except ECs pre-incubated with α-amanitin for 15 minutes. (D) Same as B.

*Rpb9- (95-97)A mimics the behavior of pol II*Δ*9* in vitro

The *rpb9-(95-97)A* and *rpb9*Δ strains share a number of *in vivo* phenotypes, (Fig. 3.3), and we sought to determine whether *in vitro* properties of pol II are affected when Rpb9 is replaced by Rpb9- (95-97)A. In these assays we immobilized pol II from whole cell extracts (WCE) from a *rpb9*Δ strain carrying a plasmid-born *rpb9-(95-97)A* by exploiting a TAP tag on Rpb3 (Kaplan, 2008). In an A-for-C misincorporation experiment performed at a near saturating concentration of ATP (1 mM), the Rpb9- (95-97)A substitutions resulted in a misincorporation rate almost twice that of pol II immobilized from wild-type WCE and essentially identical to the rate of pol II from WCE of *rpb9*Δ cells (Fig. 3.4, A and B). In the presence of α-amanitin, the rates of misincorporation for polymerase immobilized from all three strains were essentially identical, consistent with a possible effect of the (95-97)A substitutions on TL function.

We directly addressed the possibility that the alterations in Rpb9 amino acids 95-97 might affect the binding of Rpb9 to pol II in two ways. In a pull-down assay, we exploited a *rpb9*Δ strain with a 6x-His tag on Rpb3 that contained a plasmid-borne copy of either *RPB9* or *rpb9-(95-97)A*, each of which was flag-epitope tagged at its N-terminus. Pol II was immobilized from WCEs derived from these strains using Ni^{2+}-NTA beads, and the beads were washed just as they would be for an *in vitro* transcription assay. Bead-bound proteins were dissolved in SDS, fractionated by SDS-PAGE, and Rpb9 was identified by Western blot analysis with an anti-flag antibody

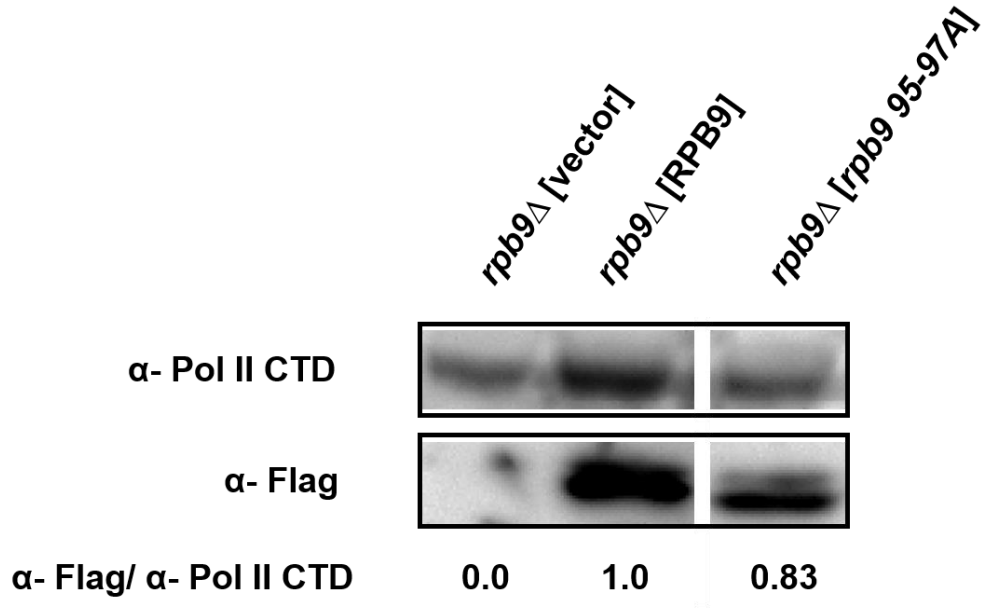

Figure 3.5: Association of Rpb9- (95-97)A with pol II

WCEs containing N-terminally Flag-tagged Rpb9 or Rpb9- (95-97)A expressed from a single-copy plasmid were analyzed with a Western blot under the same conditions used for *in vitro* transcription assays. This was done in order to determined their association with pol II based on signal from a probe detecting the Flag-epitope (upper box) and the CTD of pol II (8WG16) (lower box) as described in the materials and methods chapter. The ratio of the signal of α- Flag to α- Pol II CTD under each lane is normalized to the *RPB9* strain (n=1).

(Fig. 3.5). A protein band of approximately 14 kDa, consistent with the size of Rpb9, was detected in lanes derived from extracts from cells with the *RPB9* or *rpb9-(95-97)A* plasmid, but not the control extract made from cells carrying only the empty vector. The membrane was also probed with an antibody against the Rpb1 C-terminal domain (Fig. 3.5, upper box). Quantitation yielded a ratio of Rpb1 to Rpb9 for *rpb9- (95-97)A* was very similar to that of wild-type Rpb9, indicating there is no major defect for binding in the Rpb9 variant. This is not surprising , as the area critical for Rpb9 binding resides in residues nearer to the linker of Rpb9 (Hemming and Edwards, 2000). These results were not affected by the presence of the eight amino acid flag-epitope tag, as all of the *RPB9* alleles shown in Fig. 3.3 contain it.

Our second approach was based on *in vitro* experiments with pol II, where the slow *rpb1-G730D* mutation could suppress the fast misincorporation rate of pol IIΔ9, but not the fast rate of pol II-(Rpb9-(95-97)A). We took advantage of published methods for bacterial expression and purification of Rpb9 that were developed for x-ray crystallographic studies of Rpb9 and its pol II counterpart C11 (Ruan, 2011). Our preparations contained highly purified Rbp9 (Appendix Fig. 5). When we attempted to reconstitute wild-type pol II behavior with purified Rpb9 and pol IIΔ9 that had been immobilized from WCE with a 6x His-tag on Rpb3, we found that the best protocol was to assemble ECs with pol IIΔ9 and then add the purified Rpb9. In addition, we found that in order for the added Rpb9 to affect the activity of pol IIΔ9 ECs, the presence of a low concentration of Sarkosyl (0.035%) was required. However, the Sarkosyl addition had no effect on the activity of ECs containing pol II or pol IIΔ9 in the absence of added

recombinant Rpb9 (Appendix Fig. 6). The activity of ECs reconstituted in this way exactly mimicked that of the ECs prepared directly from cell extracts derived from *RPB1 RPB9, RPB1 rpb9(95-97)A, rpb1-G730D RPB9,* and *rpb1-G730Drpb9-(95-97)A* strains, consistent with the idea that Rpb9-(95-97)A efficiently associates with pol II.

A model for interaction between Rpb9 and the TL

Examination of the location of Rpb9 in numerous pol II crystal structures revealed that Rpb9 and the TL are never in sufficiently close proximity to allow for a direct interaction. However, the positions of Rpb9 amino acids 95-97 are in position to interact with the ends of Rpb1 α-helices 20 and 21, which form part of the "jaw" domain of pol II, as well as the small loop that connects them. Furthermore, in a crystal structure containing TFIIS in which the TL is captured in the most open conformation that has been observed (PDB 1Y1V) (Kettenberger et al., 2004), the TL is also positioned to interact with α-helix 21, which may stabilize the open state. Potential interacting residues are shown in Fig. 3.6. The model that emerges from this analysis is that Rpb9 may anchor the ends of α-helices 20 and 21, as well as the loop between them, which we have termed the anchor loop (AL), so that the open TL position is stabilized. This provides time for binding of NTP substrate or proofreading of errors without TL interference. This is similar to a model proposed by Walmacq et al. (Walmacq et al., 2009), but it does not involve direct interaction between Rpb9 and the TL, which Walmacq, et al. were not able to demonstrate. Instead, our model requires two

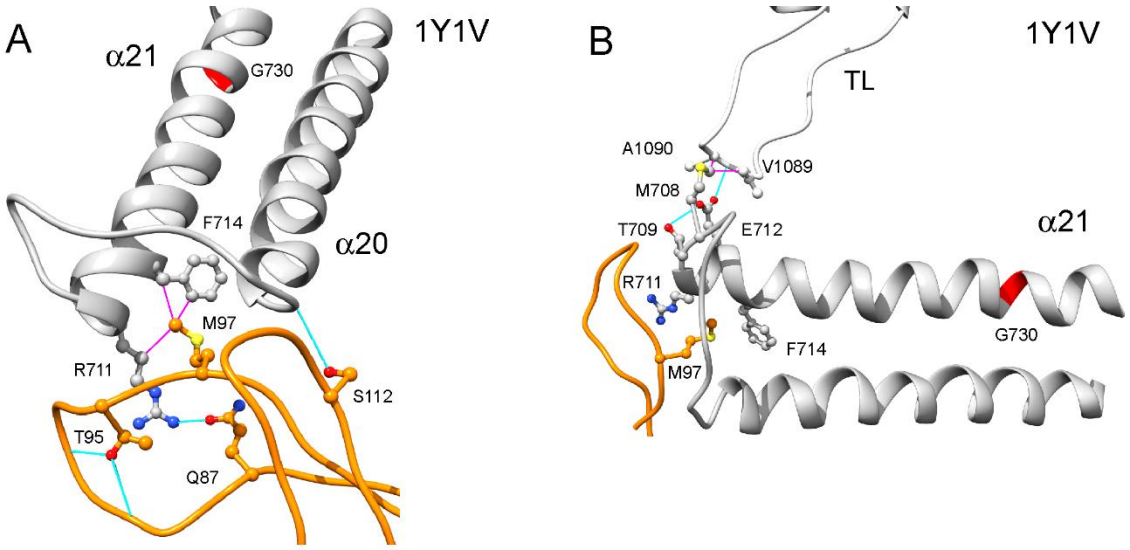

Figure 3.6: A new interaction model for Rpb9 and the TL

The crystal structure on the left (PDB: 1Y1V) indicates the relative positions of Rpb9 C-terminal domain residues 95-97 and 112 (orange), the open TL conformation, and their proximity to the Anchor Loop (AL). The AL is located on α-21 distal to the *rpb1-G730D* mutation (red), and interacts with open conformation of the TL. Rpb9 may serve to optimize to the conformation of the AL necessary to stabilize the open TL, instead of a direct interaction between Rpb9 and the TL as proposed by Walmaq *et al.* 2009. Purple lines indicate hydrophobic interactions, while blue lines indicate hydrogen bonds. See text for further details.

interaction interfaces, one between Rpb9 and the AL, and a second between the AL and the TL. Interestingly, Rpb1-G730 is also in α-helix 21, and our model provides a plausible explanation for the negative genetic interaction between *RPB9* and *rpb1-G730D*. Substitution of glycine with the larger and negatively charged aspartate might disrupt the orientation of α-helix 21 and thereby affect the proposed interactions of the AL with Rpb9 and the open TL at the other end of the helix.

If the intramolecular interactions are as predicted, mutations that alter them should result in *in vivo* phenotypes that mimic at least some of the phenotypes of *rpb9*Δ strains. Some published observations are consistent with this idea. For example, *rpb1-S713P*, in which the proline would disrupt the N-terminus of α-helix 21 and potentially alter both Rpb9-AL and AL-TL interactions, causes an upstream shift in transcription start site of *ADH1*, a trait shared by *rpb9*Δ strains (Braberg et al., 2013) and one that is common to mutations that increase the pol II transcription rate (Kaplan et al., 2012). In addition, a screen for suppressors of the downstream shift in transcription initiation site caused by *sua7-1*, an allele of the gene that encodes TFIIB, identified an allele of *RPB9* that encodes only amino acids 1-107, possibly disrupting Rpb9-AL interactions, specifically the hydrogen bond between Rpb9 S112 and the tip of α-helix 20.

In vivo phenotypes across the Rpb9-AL-TL interfaces

To address our hypothesized model, we made a series of mutations throughout each Rpb9-AL-TL interface that could disrupt potential interactions at the Rpb9-AL-TL

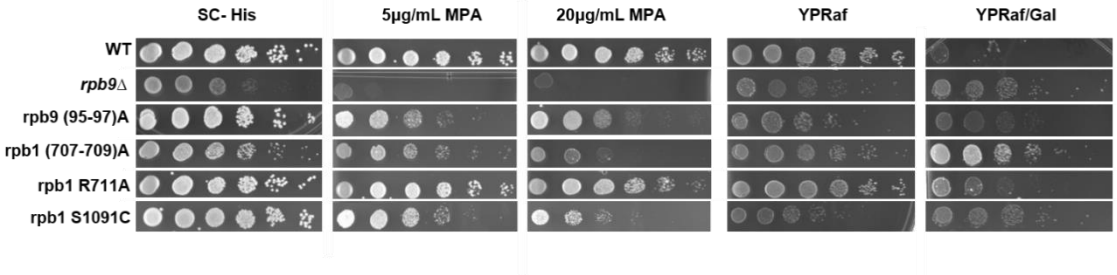

Figure 3.7: Selected phenotypes of mutations located across the Rpb9-AL-TL interfaces

10-fold serial dilutions of mutations in Rpb9 (*rpb9- (95-97)A*), the AL (*rpb1- (707-709)A*, *R711A*) and the TL (*rpb1- S1091C*) which are at each interaction interface described in Fig. 3.6 and in the text. Rpb1 mutations were introduced as in Fig. A1, and the Rpb9 mutation was carried on a single-copy plasmid marked with *HIS3*. Strains were growth for 3 days on synthetic media or media with indicated concentrations of MPA, and 4 days for rich media with either raffinose or galactose and supplemented with antimycin A (1 µg/ mL).

interfaces. Mutations were characterized using three phenotypes of *rpb9*Δ strains, decreased growth, hypersensitivity to MPA, and suppression of galactose sensitivity in a *gal10*Δ*56* background (Gal^R). The Gal^R phenotype assesses transcriptional interference (Kaplan, 2008). In wild-type cells, *GAL10* and *GAL7* are located in tandem on chromosome II (Greger and Proudfoot, 1998). These genes encode UDP-glucose-4-epimerase and galactose-1-P uridylyltransferase, respectively, which are required for galactose to enter the glycolytic pathway. A small deletion in *GAL10* (*gal10*Δ*56)* compromises its major polyadenylation signal, and the resulting read-through transcription interferes with transcription initiation at *GAL7*. This leads to a build-up of galactose-1-P, one of the substrates of the uridylyltransferase encoded by *GAL7*, which is toxic to yeast. Toxicity is modulated by certain mutations in pol II (including *rpb9*Δ), as well as mutations in pol II elongation factors and mRNA processing factors (Bucheli and Buratowski, 2005; Bucheli et al., 2007; Greger et al., 2000; Greger and Proudfoot, 1998; Kaplan et al., 2005). No specific molecular defect can necessarily be inferred from altered galactose sensitivity, but it is a readout directly related to transcription that is characteristic of *rpb9*Δ strains.

As seen in Fig. 3.7, mutations that are on either side of an interface, i.e. Rpb9-AL or AL-TL, exhibit some spectrum of MPA^S and Gal^R. For MPA^S, the range is from a slight sensitivity in *rpb1-R711A,* the moderate sensitivity of *rpb9- (95-97)A* and *rpb1-S1091C,* to the well documented hypersensitivity of *rpb9Δ*(Li et al., 2006; Van Mullem et al., 2002). It should be pointed out that the MPA sensitivity exhibited by the *rpb9-*

(95-97)A mutation is unique. Previous studies have indicated that the MPA hypersensitivity of *rpb9Δ* is associated with the first 17 residues of Rpb9, and that residues 1-53 can suppress the majority of the MPA sensitivity (Li et al., 2006). The MPA sensitivity associated with residues 95-97 may be related to a specific C-terminal mechanism of Rpb9 that is TL-dependent, which is intriguing as most transcriptionally fast mutations in the TL (Kaplan et al., 2012; Kaplan, 2008), as well as mutations *rpb1-(707-709)A* and *S1091C*, also share a sensitivity to MPA. In addition, while suppression of the *gal10Δ56* allele seen with the selected mutations in Fig. 3.7 is varied, mutations (707-709)A, R711A, and S1091C all have some spectrum of Gal^R. It is worth pointing out that in addition to the mutations in Fig. 3.7 which we chose to study more extensively, we also observed various spectrums of decreased growth, Gal^R, and MPA sensitivity phenotypes in the Rpb9 point mutants Q87A and S96A, the AL mutant *rpb1-S713P*, and in several mutants (*rpb1-V1089Δ, S1091C/W, K1092E/W*) from a pool of Rpb1 TL mutants generously provided to us from the Kaplan Lab (Appendix Fig. 7-9). This reinforces our conclusion that mutations that are in each proposed interaction interface result in phenotypes shared by *rpb9Δ*.

Anchor Loop mutations are epistatic with rpb9Δ

Earlier we had shown that there is a two-fold increase in the misincorporation rate for pol IIΔ9 and for pol II with Rpb9- (95-97)A. Similar to pol IIΔ9, Rpb9- (95-97)A also causes a two-fold increase in the average rate of correct nucleotide extension

(Appendix Fig. 10A). If the proposed model is correct, then *rpb1* mutations at the Rpb9-AL and AL-TL interfaces that result in phenotypes that are similar to those of *rpb9*Δ strains would be expected to mimic the fast elongation rate of pol IIΔ9 and Rpb9- (95-97)A. Using pol II immobilized from WCE derived from cells expressing Rpb1 (707-709)A, Rpb1-R711A, and Rpb1-S1091C, the rates of A-for-C misincorporation (Fig. 3.8A) , as well as the average rates of elongation with template-matched NTPs (Appendix Fig. 10B), were all essentially identical to the fast rates observed with pol IIΔ9 and Rpb9- (95-97)A (Refer to Table 3.1 for all determined observed rates). In addition, just as with pol IIΔ9 and Rpb9- (95-97)A, the presence of saturating amounts of α-amanitin collapsed the misincorporation rate to that observed with wild-type pol II (Table 3.1 and Appendix Fig. 11), consistent with the idea that the mutations may be affecting a TL-related function.

TL mutations that affect the rate of elongation tend to be additive when combined. Fast, gain-of-function alleles combined with slow, loss-of-function alleles tend to have an elongation rate between the two extremes, while combinations of two fast or two slow alleles are many times lethal (Kaplan et al., 2012). In contrast, when we combined the fast *rpb1* alleles associated with the Rpb9-AL-TL interaction network with *rpb9*Δ, the combinations were no faster than the single mutations in the A-for-C misincorporation assay (Fig. 3.8B and Table 3.1). This epistasis strongly suggests that the defect imposed by the *rpb1* alleles *R711A, (707-709)A,* and *S1091C* is related mechanistically to the defect caused by *rpb9Δ* and *rpb9- (95-97)A*.

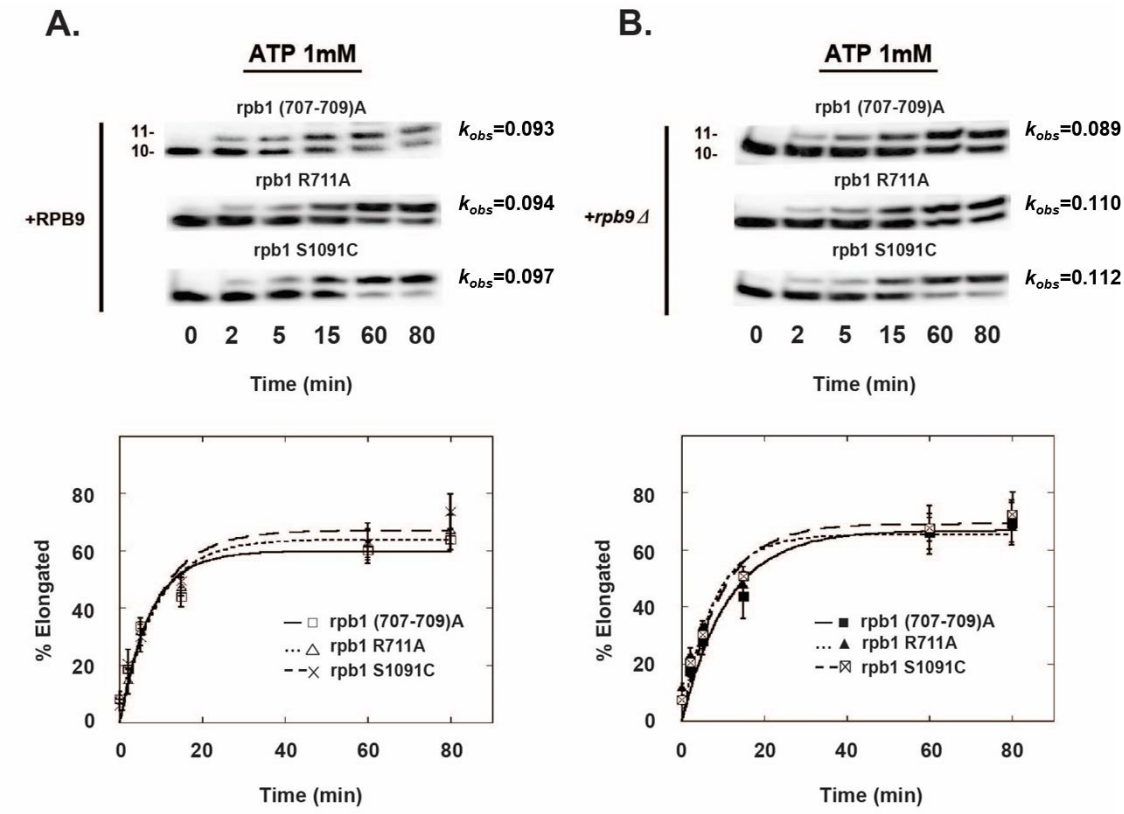

Figure 3.8: AL and TL mutations are epistatic *in vitro* with *rpb9*Δ for an ATP misincorporation

(A) ATP 1mM was added to ECs immobilized from WCEs with the *rpb1- (707-709)A*, -*R711A*, or *S1091C* mutation, and the extension of the RNA to 11 nucleotides (nt) or greater was monitored over time via a 20% polyacrylamide gel. The fraction extended to 11 nts in A was plotted and fit to a single exponential function to obtain an observed rate for misincorporation, indicated by each representative assay. (B) The pol II mutations in A were combined into a *rpb9*Δ and challenged with the same misincorporation assay. Rates are indicated as in A, and compiled in Chapter III, Table 1.

Discussion

A mobile element at the core of RNA pol II known as the trigger loop, is important for both catalytic coordination and for transcriptional fidelity (Larson et al., 2012). As discussed in Chapter I, The movement in and out of the active site determines the extent to which the TL can fulfil these functions, many of which are conserved both in bacterial as well as RNAPs (Kireeva et al., 2012; Wang et al., 2013). In terms of transcriptionally fidelity, mutations in the TL which reside in hinging areas based on crystal structures, such as the well-studied hinge mutant E1103G, seem to affect not only the likelihood of incorporating a mismatched NTP, but also decrease pol II's ability to induce pauses which is important for the proof-reading response (Larson et al., 2012). In addition, residues that have been identified as being critical for substrate selection in the area of the TL that makes contacts with the substrate NTP, can also be indirectly affected by changing the time to which they occupy the catalytic center. Therefore it is important for us to understand, not only in terms of pol II mechanism, but also in terms of accuracy of transcription, how the TL transition, in and out of the active site, is mediated.

Single-molecule, computational, and bulk biochemical data have pointed to many different active site areas as being important for TL mobility. Residues near a C-terminal hinge of the (e.g. E1103) , are thought to be important for stabilizing the open TL conformation, and many mutations in this region have a characteristic increase in elongation rate both for matched and mismatched substrates

Table 3.1: Compiled in vitro transcription rates from Chapter III

Pol II	1mM NTP(s)	k_{obs} (min^{-1})		$t_{1/2}$ (min^{-1})		Approx. Elongation Rate (nt/s)	
		α- amanitin		α- amanitin		α- amanitin	
		-	+	-	+	-	+
WT	A-for C	0.050±0.007	0.029±0.005				
	A*C*G*U	4.8±1.02	0.234±0.03	0.15±0.03	3.0±0.03	5.8	0.14
***rpb9*Δ**	A-for C	0.098±0.017	0.030±0.003				
	A*C*G*U	11.0±1.1	0.620±0.04	0.06±0.01	1.1± 0.07	13.5	0.36
rpb9 (95-97)A	A-for C	0.108±0.023	0.027±0.005				
	A*C*G*U	9.48±2.22	0.498±0.05	0.07±0.02	1.4±0.1	11.6	0.24
rpb1 (707-709)A	A-for C	0.093±0.02	0.043±0.009				
	A*C*G*U	7.92±0.72	0.336±0.05	0.09±0.01	2.0±0.2	9.7	0.20
rpb1 R711A	A-for C	0.094±0.014	0.033±0.007				
	A*C*G*U	7.44±0.78	0.198±0.03	0.09±0.01	3.5±0.3	9.1	0.12
rpb1 S1091C	A-for C	0.097±0.009					
	A*C*G*U	9.9±1.32	0.372±0.03	0.07±0.01	1.8±0.1	12.1	0.22
rpb1 (707-709)A + *rpb9*Δ	A-for C	0.089±0.01					
	A*C*G*U						
rpb1 R711A + *rpb9*Δ	A-for C	0.110±0.017					
	A*C*G*U						
rpb1 S1091C + *rpb9*Δ	A-for C	0.112±0.02					
	A*C*G*U						

(Kaplan et al., 2012; Kaplan, 2008; Kireeva et al., 2008; Walmacq et al., 2009). In contrast, residues in the nucleotide interacting region of the TL are thought to stabilize the closed conformation of the TL in addition to their functions in coordinating catalysis (Kaplan, 2008; Wang et al., 2015) (Refer to Fig. 1.4). In is interesting that, in addition to fidelity, transcriptional start site selection also seems to be a biochemical read-out for TL mutations (Jin and Kaplan, 2015; Kaplan et al., 2012). An upstream shift is observed for fast mutations such as E1103G, while a downstream shift is observed for slow mutations such as H1085Y.

A small subunit at the leading edge of pol II, Rpb9, was also suggested to affect the TL transition through its C-terminal domain based on its similarities with the *rpb1-E1103G* mutation. Similarities included an increase NTP-sequestration, misincorporation rate, and upstream shift in start site (Walmacq et al., 2009). However direct biochemical analysis of a mutation in the proposed interaction pathway yielded a negative result. Previous data from our lab as well as others have implicated Rpb9 in transcription fidelity as well as a host of other functions (surveyed in Chapter I), however we were curious to know if some function of Rpb9 was indeed TL-dependent. To determine this, we took advantage the TL inhibitor α-amanitin, and with it were able to show that this increase in misincoroporation rate associated with a *rpb9*Δ is dependent on free movement of the TL (Fig. 3.1)

Other residues extrinsic of the TL have been suggested by multiple molecular dynamic studies that considered residue conservation, and attempted to model the TL transition pathway via published crystal structures of bacterial and yeast RNAP (Kireeva

et al., 2012; Wang et al., 2015; Wang et al., 2013). In *S. cerevisiae*, residues such as E712 (TL counter-part K1092) and K726, which are located on a loop and adjoining α-21 in Rpb1 subunit of pol II, have been suggested to affect multiple states of the TL. Though, no biochemical evidence until our study has confirmed this. Interestingly, these residues are in close proximity to the *sit1* mutation, *rpb1-G730D* which we and others have biochemically characterized and found to be suppressive of certain phenotypes of fast elongation TL mutations as well as the loss of pol II subunit Rpb9 (Appendix Fig. 2) (Koyama et al., 2010; Walmacq et al., 2012). This same mutation allowed us to take an unbiased approach to identify mutations that might be important for Rpb9 function.

As seen in Fig. 3.3 and 3.4, one mutation in particular *rpb9- (95-97)A* was identified through this approach. This Rpb9 variant mimic the behavior of a *rpb9Δ* in both a misincorporation assay, and for correct nucleotide extension. We also found that the increase in observed rate for misincorporation for Rpb9- (95-97)A was likewise dependent on the TL via α- amanitin (Fig. 3.4). This caused us to scrutinize the published crystal structures available and propose an alternate model for how Rpb9 C-terminal domain might affect TL mobility. Here we suggest an indirect pathway of how Rpb9 affects the TL via a loop connecting α-20 and -21 which we have termed, the anchor loop. We posit that stabilization of the open conformation of the TL via contacts in the AL is partially coordinated by the C-terminal domain of Rpb9 through residues 95-97. This is in contrast to the suggested direct interaction pathway for Rpb9, for which there is no evidence, and would provide an explanation for previous biochemical results, as wells as our own results for TL-dependent function of Rpb9 (Walmacq et al., 2009).

We began testing our model by phenotyping mutations at each proposed interface: Rpb9 and the AL, and the AL and the TL. Based on our model, we reasoned that if these interface residues were important for the function of Rpb9, they should exhibit phenotypes of *rpb9*Δ. Indeed, when we challenged mutations at our proposed interfaces *in vivo*, we found that many of them modulated certain phenotypes of an *rpb9* null such as MPA sensitivity, decreased growth, and the Gal^R phenotypes (Fig. 3.7 and Appendix Fig. 7-9). *In vitro* analysis of selected AL mutations such as *rpb1-R711A, (707-709)A,* and the TL mutation *rpb1-S1091C* revealed an increased misincorporation and matched nucleotide elongation rate, similar to that of *rpb9*Δ. And critically, these same mutants increased misincorporation rate were also dependent on the presence of α-amanitin (i.e. TL mobility) and were no faster in combination with *rpb9*Δ (Fig. 3.8 and Appendix Fig. 10-11). This provides strong evidence for our suggested model.

Interestingly, the selected mutations in Rpb9, AL, and TL are also consistent with a previously described TL mutation, *rpb1-G1097D,* which is located proximal to the C-terminal hinge portion of the TL, transcriptionally fast, and has a strong Gal^R (Kaplan et al., 2012; Kaplan, 2008). The typical trend for previously published mutations in the TL, mutations that are posited to affect TL mobility and catalysis, is a concomitant MPA sensitivity with increased elongation rate (Kaplan et al., 2012; Kaplan, 2008). The Gal^R phenotype however, generally is associated with slower mutations in the TL region, making the mutations in Fig. 3.7 unique along with G1097D. Interestingly, neither R711A, (707-709)A, or S1091C is synthetic lethal with *rpb9Δ*, whereas G1097D is (Appendix Fig. 1). A previous study that analyzed combinations of

mutations in the TL that had opposite effects, i.e. combinations that combined a transcriptionally fast mutation with a transcriptionally slow mutation, found that the mutant combinations are normally additive (Kaplan et al., 2012). In the same study, mutation combinations that had similar defects are normally inviable. We have demonstrated that the defect of Rpb9- (97-97)A is TL-dependent and mutations analyzed in this chapter all share some spectrum of *rpb9Δ* phenotypes. Given that the same mutations are not lethal in combination with *rpb9Δ* and are epistatic in their *in vitro* effects in our assays, these data seem to suggest the possibility that these mutations may be upstream defects, consistent with our model.

This would also be consistent with our observation that the Rpb9- (95-97)A variant is not synthetically lethal with either *rpb1-E1103G* or *rpb1-L1101S* (Appendix Fig. 13). If the AL in conjunction with Rpb9 serves to stabilize the open conformation of the TL, then the most upstream defect in our proposed pathway, is intrinsic changes within the hinges of the TL. In addition, we can also interpret Rpb9- (95-97)A interaction with TL mutations such as E1103G and L1101S, given the fact that full length Rpb9 is present in conjunction with the TL mutations. We have already seen that the first N-terminal 59 amino acids of Rpb9 suppress most of the *in vivo* phenotypes caused by the lack of Rpb9. However, it has also been shown that C-terminal truncation mutant of Rpb9 (Rpb9 1-53) has significantly reduced association with pol II (Chen et al., 2007). Even though mutation of residues 95-97 in Rpb9 increase the transcription rate, they do not affect the contribution of Rpb9 function through the N-terminal domain. Therefore *rpb9- (95-97)A* is simply epistatic with TL hinge mutations whereas Rpb9 (1-

59) is synthetic lethal because reduced function of the N-terminal domain by decreased association, and loss of the C-terminal domain (Appendix Fig. 13). In addition, it could hint that in addition to the transcriptional role we have observed in the above data, the C-terminal domain of Rpb9 may also have another important role. Certainly, the proximity of the AL and the C-terminal domain of Rpb9 to where the extrinsic factor TFIIS and the transcription factor Bye1 bind the jaw domain of pol II provide intriguing targets for analysis (Discussed more in Chapter IV). The interaction of these factors, especially TFIIS, may become more important given the documented role of Rpb9 in proofreading (Knippa and Peterson, 2013).

The results in this chapter argue for a TL-dependence for a portion of Rpb9 function, and provide a novel interaction pathway of how Rpb9 mediates its effect on active site processes through the so-called AL. Mutations in the residues 95-97 in Rpb9, as well as mutations in the AL and corresponding TL residues, provide evidence that the AL is directly important for the TL open conformation. This was ascertained by the *in vitro* epistasis of the mutations in combination with *rpb9*Δ for misincorporation experiments, as well as their increased misincorporation rate dependence on α-amanitin. *In vivo* behavior of mutations at each interaction interface of our model also exhibit varying degrees of phenotypes associated with the loss of Rpb9 are also consistent with our model, as well as molecular dynamic studies that have predicted the effects of mutations in the AL regions on TL transitions (Kireeva et al., 2012; Wang et al., 2015; Wang et al., 2013).

CHAPTER IV

RPB9 N-TERMINAL DOMAIN

Summary

Rpb9, a small non-essential subunit of RNA polymerase II (pol II), has been shown to affect pol II activity in several ways. These functions include a role in the modulation of TL mobility and effects on the TFIIS-mediated proofreading function of pol II. As described in Chapter III, the TL-dependent function of Rpb9 is likely mediated through its C-terminal Zn2 domain. Compared to the C–terminal domain, much less is known about the function of the N-terminal domain of Rpb9. Numerous genetic interactions between Rpb9 and chromatin-related complexes have been reported that are not easily explained based on what is known about the function of Rpb9. In this chapter, I describe preliminary experiments that suggest these genetic interactions are related to a function of the Rpb9 N-terminal domain. These experiments demonstrate that the first ~10 amino acids of Rpb9 are critical to cell viability in the absence of genes encoding SAGA complex components Gcn5 or Spt7, the histone variant H2A.Z, or Swc5, an integral component of the SWR1 complex, which substitutes H2A.Z for H2A in selected nucleosomes. Loss of the same amino acids has an additively negative phenotype with the loss of Bye1, a protein that has been proposed to displace TFIIS at nucleosomes and is important for induction of stress related genes. This suggests that there are at least two pathways in which Rpb9 can affect the passage of pol II through nucleosomal templates.

One pathway involves the N-terminal domain and may be related to the role of Rpb9 in recruiting TFIIF to pol II, and the second involves the C-terminal domain and may be related to a role for Rpb9 in the binding of Bye1 to pol II, which is mutually exclusive with the presence of TFIIS.

Introduction

Rpb9 is composed of three distinct domains, two of which share a structural motif common to several subunits of pol II, the zinc-ribbon fold. They are the N-terminal Zn1 domain, the central linker region, and the C-terminal Zn2 domain. As overviewed in Chapter I and discussed in more detail below, different Rpb9 domains have been implicated in various functions in the cell. The context in which all structural domains of Rpb9 have been studied the most has been transcriptional fidelity. Indeed, Chapter III showed that the C-terminal domain of Rpb9 seems to communicate with the active site of pol II through a molecular pathway that passes through the AL in order to reach the TL. However, the mechanism of Rpb9 in functions other than transcriptional fidelity have remained elusive. This is especially true for various interactions that have been documented with Rpb9 and chromatin-related co-transcriptional complexes.

Rpb9 C-terminal domain

Rpb9 has been implicated in several functions in addition to its role in TL

mobility described in Chapter III. Though there are homologs of Rpb9 in the two other nuclear polymerases (C11 in RNA pol III and A12.2 in RNA pol I), the C-terminal domain of Rpb9 is somewhat different in that it cannot stimulate cleavage, but rather depends on the extrinsic factor TFIIS. Indeed, replacing the Zn2 domain of Rpb9 with that of with C11, which contains an acidic hairpin loop similar to that of domain III of TFIIS, allows pol II to gain the ability to strongly stimulate cleavage, in contrast with the normal intrinsic cleavage of pol II, which is minimal (Cabart et al., 2014; Kettenberger, 2003; Qian et al., 1993; Ruan, 2011). This has been suggested to be an explanation for why C11 is an essential protein and perhaps another layer of control that pol II has gained to control cleavage activity. However, Rpb9, though not directly responsible for activity, does affect TFIIS-mediated cleavage (Knippa and Peterson, 2013). In addition, the Rpb9 C-terminal domain has been implicated in UV-mediated Rpb1 degradation in pathways independent of any Nuceotide Excision Repair pathways (NER) (Chen et al., 2007). Specifically, it was shown that the Rpb9 Zn2 domain is important for Rpb1 ubiquitinylation and subsequent degradation by the 26S proteasome when pol II stalls at sites of DNA damage. The model suggested was that Rpb9 Zn2 was necessary for either sensing of transcriptional senescence or recruitment of degradation factors necessary to remove pol II so that DNA repair can take place and transcription can resume. The C-terminal domain and linker have also been reported to directly interact with the Tfa1 subunit of the basal transcription factor TFIIE in a yeast two-hybrid assay (Van Mullem et al., 2002), but the functional significance of this interaction has not been investigated.

Rpb9 N-terminal domain

In contrast to the C-terminal domain, much less is known mechanistically about the N-terminal domain (Zn1) of Rpb9. Yet, several interesting phenotypes of *rpb9*Δ yeast strains can be suppressed by supplying only the Zn1 domain of Rpb9. Several studies have indicated that the first 45 to 57 amino acids of Rpb9 can suppress, in some cases completely, the severe growth defect (Awrey, 1997; Hemming and Edwards, 2000; Hemming et al., 2000; Koyama, 2007; Li et al., 2006; Van Mullem et al., 2002) and the hypersensitivity to mycophenolic acid (MPA) (Li et al., 2006) associated with *rpb9*Δ strains. This is intriguing, as mutations in pol II exhibiting MPA sensitivity normally are transcriptionally fast mutations (Jin and Kaplan, 2015). The sensitivity associated with the N-terminal domain of Rpb9 seems to be much stronger compared to the sensitivity to MPA observed for C-terminal mutations that we have measured to be transcriptionally fast (see Fig. 3.2). Additionally there is no evidence that N-terminal Rpb9 mutations are transcriptionally fast, and the MPA hypersensitivity seen in the truncations of the N-terminal domain of Rpb9 may be derived from some other type of defect. It is interesting to note that the MPA hypersensitivity of *rpb9*Δ can be mimicked by mutating the coordinating cysteines in the Zinc-ribbon fold of the N-terminal domain (Li et al., 2006). In addition, specific regions of Rpb9 have been shown to be important for association of Rpb9 to pol II. For example, deletion of more than the first 17 amino acids or deletion of the charged residues 65-70 abolished Rpb9 association as measured by a tag pull down assay (Hemming and Edwards, 2000). However, many studies, including experiments to

be presented here, indicate that only the first 59 amino acids of Rpb9 are required to suppress many of the phenotypes of *rpb9*Δ strains (Chen et al., 2007; Hemming and Edwards, 2000).

Several interesting questions arise concerning the N-terminal domain of Rpb9. Can the N-terminal domain alone suppress the synthetic lethality associated with a host of chromatin-related proteins (Table 4.1) and for which there has been no mechanistic interpretation for their interaction with Rpb9? If it is sufficient, what specific residues in the N-terminal domain are important for mediating the interaction between Rpb9 and the particular chromatin modifying protein? Are these interactions direct or indirect (i.e., are the chromatin modifying complexes directly interacting with Rpb9, or is there a mediator between them)?

Introduction to Bye1

Bye1 (Bypass of *ESS1*) is a nuclear protein in *S. cerevisiae* that was originally isolated as a multi-copy suppressor of mutations in *ESS1*, which encodes a peptidyl-prolyl isomerase important for pol II CTD conformation, polymerase pausing, and transcription termination (Hani et al., 1995; Morris et al., 1999; Wu et al., 2003). More specifically, it was shown that overexpression of Bye1 could suppress the temperature sensitivity of *ess1*Δ, but not its increase in pause site read-through or its transcription termination defect (Wu et al., 2003). More recently, it has been shown that Bye1 has a

Table 4.1: Synthetic lethal genetic interactions with *rpb9*Δ

Genes/alleles	Function
TAF9	TFIID subunit (H3)
SPT7	Subunit of SAGA
SPT3	Subunit of SAGA
SOH1	Subunit of the Mediator complex
RTR1	CTD phosphatase
RPO21	Rpb1
RPB4	Subunit of RNA pol II
RNA14	Cleavage and polyadenylation factor
RAD7	DNA damage recognition protein
RAD6	Ubiquitin conjugation enzyme
NGG1	Subunit of SAGA
LGE1	Molecule function unknown
HTZ1	Histone H2a variant
GIM5	Microtubule synthesis
GCN5	Subunit of SAGA
ELP3	Subunit of elongator complex
BRE1	Ubiquitin ligase
ADA2	Subunit of SAGA and ADA complexes
TFA1	TFIIE large subunit
NAB2	polyadenylated RNA-binding protein
PAF1	Component of the Paf1p complex

domain homologous to that of domain II of TFIIS that is required for the binding of TFIIS to the "jaw" domain of pol II (Cheung and Cramer, 2011). This is unique, as there are no other proteins in budding yeast that share this TFIIS-like domain, and, as with TFIIS, the domain is required for Bye1 to associate with the Rpb1 subunit of pol II (Kinkelin et al., 2013; Pinskaya et al., 2014; Wu et al., 2003). Bye1 contains two domains in addition to its central TFIIS-like pol II binding domain and N-terminal nuclear localization signals. The N-terminal Plant Homeo Domain (PHD) is generally associated with proteins that bind chromatin, and it is important for binding to methylated lysines on histone tails (Aasland et al., 1995). Bye1 was recently shown to be associated within the gene bodies of actively transcribed pol II and pol III genes, as well as a much smaller subset of pol II promoter regions. Not surprisingly, the localization of Bye1 to promoters, but not gene bodies, is dependent on the binding of the PHD domain directly trimethylated H3K4 residues (Aasland et al., 1995; Kinkelin et al., 2013). The flanking SPOC (Spen paralogue orthologue C-terminal) C-terminal domain is the third domain of Bye1. The SPOC domain's role in *S. cerevisiae* is not well understood. However, in *H. sapiens*, it has been shown to be important for subunit interactions in transcriptional repression complexes that are critical for cell-signaling pathways, and it may be related to the development of a specific subtype of leukemia (Ariyoshi and Schwabe, 2003; Lee and Skalnik, 2012).

Bye1 in vivo

Genome-wide occupancy analysis, along with various *in vivo* and *in vitro* studies, have combined to increase the understanding of Bye1's function (Braberg et al., 2013; Kinkelin et al., 2013; Pinskaya et al., 2014). Studies have shown that, over expression of Bye1 in yeast lacking *DST1* (the gene encoding TFIIS) enhances the sensitivity of *dst1*Δ cells to 6-azauracil (Wu et al., 2003). In addition, it was reported that the sensitivity of *dst1*Δ cells to high concentrations of caffeine and NaCl, which can affect cell wall integrity, is enhanced in the *bye1*Δ*dst1*Δ double mutant and is even more severe at higher temperatures (34^{o}C) (Kinkelin et al., 2013). This suggests two different modes of action for Bye1: one that opposes TFIIS, as seen through the increase of the *dst1*Δ phenotype with the over expression of Bye1; and the other that is potentially parallel with TFIIS, based on the additive effects of deleting both genes under certain stress conditions. In addition, *bye1*Δ also demonstrates severe synthetic growth defects in combination with the deletion of Paf1 and Tho2 (Kinkelin et al., 2013). Paf1 is a component of the 5 subunit Paf1C complex, which is required not only for the recruitment of the histone methyltransferase Set1 to active genes, but also for ubiquitylation of H2B (Sen et al., 2013). Once present at chromatin templates, Set1 is responsible for trimethylating the K4 residues of H3 tails. Tho2, on the other hand, is a component of the THO complex, which is important for elongation through DNA templates containing tandem repeats, as well as shuttling mRNA from the nucleus to the cytoplasm (Betz et al., 2002; Krogan et al., 2003; Tong et al., 2004). Both Paf and THO

complexes affect the overall efficiency with which pol II can transcribe through a gene body (Costa and Arndt, 2000; Jimeno et al., 2011). Interestingly, SPOC domains have been shown to interact with Set-domain-containing proteins suggesting that Bye1 may recruit complexes (such as Paf) to chromatin by binding H3K4 tails via its PHD domain and recruiting accessory complexes via its SPOC domain (Lee and Skalnik, 2012).

ChIP-chip, as well as conventional ChIP experiments, have outlined several different classes of Bye1 chromatin occupancy *in vivo* (Pinskaya et al., 2014). First, Bye1 is associated with actively transcribed pol II genes, concomitant with the presence of pol II and TFIIS. A second class of Bye1 association is found on pol III class genes together with TFIIS. Third, there was observed a localization of both TFIIS and Bye1 just outside of the telomeres, again absent of pol II. And finally, there was an enrichment of Bye1 at certain pol II promoter regions with active, albeit lower, levels of pol II activity. For the localization of Bye1 at both classes of pol II promoters, there is a direct dependence on H3K4 trimethylation mediated through Set1, as well as active transcription of the gene. However, the localization of Bye1 to coding regions of pol II genes requires only active transcription, but not the H3K4 methylation mark. Interestingly, in both cases Bye1 is co-immunoprecipitated with TFIIS by pol II antibodies, suggesting a potential equilibrium between the binding of TFIIS and the binding of Bye1 (which are mutually exclusive) during active transcription.

Bye1 in vitro

In vitro experiments along with a recent crystal structure of the Bye1 TLD (TFIIS-Like Domain) have shed some light on more specific Bye1 activities. As discussed above, the TLD domain of Bye1 is absolutely required for association with the jaw domain of Rpb1, similar to TFIIS, as determined by co-immunoprecipitation and yeast two-hybrid screening (Pinskaya et al., 2014). From the co-crystal structure however, there are some differences between the binding of Bye1 and TFIIS. First, as pointed out in Kinkelin et al. and seen in Fig. 4.1, in contrast to TFIIS domain II, the linker of Bye1's (α6) TLD domain makes contacts with the AL between residues 703-706 (Specifically there is a hydrogen bond between H706 in the AL and N362 in Bye1, indicated as a red star in Fig. 4.1C), which changes conformation depending on whether Bye1 or TFIIS is bound (Kinkelin et al., 2013). This is intriguing given the role of the AL in TL mobility, and it is possible that Bye1 could affect pol II elongation via this interaction. Second, there are contacts between the N-terminal domain of Rpb5 and a loop located between α3 and α4 of Rpb1. Also seen in Fig. 4.1C, is the proximity of the Rpb9 N-terminal domain which forms a β sheet between Rpb1 residues 1148-1154 (indicated with a red star). Because of the lack of an ordered N-or C-terminal domain of Bye1 in the crystal structure, it is hard to speculate on their spatial location. However, the N-terminal PHD domain would be in the general vicinity of the leading edge of pol II, where it potentially contacts histones tails. In addition, unlike domain III of TFIIS which is directly responsible for RNA transcript cleavage and accesses the active site of

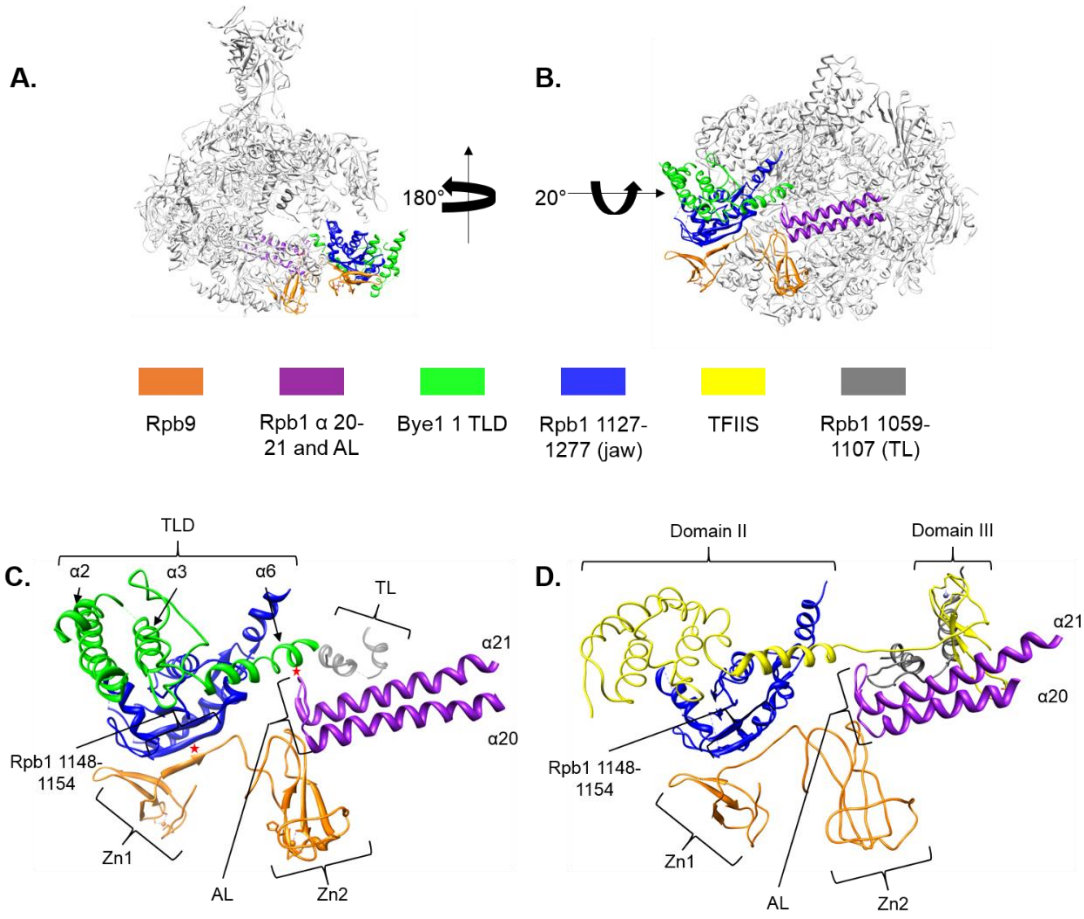

Figure 4.1: Crystal structure of RNA polymerase II with Bye1 and TFIIS

Structures (A) (top view) and (B) are *S. cerevisiae* 12-subunit RNA polymerase II (PDB 4bxz for structures containing Bye1 or 1Y1V for structures containing TFIIS). Different colors indicate different domains or subunits of the polymerase. (C) A zoom-in portion of the polymerase structure depicted in the previous figure illustrating the Bye1 TLD and integral helices (green). Red stars indicate specific interactions between Rpb9 and Rpb1 lobe (residues 1148-1154) or the Anchor Loop (purple) (see text for details). (D)The analogous representation of TFIIS from 1Y1V indicating its position in terms of the same pol II local area.

pol II by inserting into the funnel domain of pol II, the arrangement of the SPOC domain at or near the funnel domain is unclear (Ruan, 2011), though, it seems unlikely that it competes for active site occupancy with the TL.

Experiments that directly probe the effect of Bye1 on pol II activity have been performed; however, the results are somewhat qualitative in nature. One set of experiments looked at Bye1's effect on pol II in the context of a Gcn4-dependent promoter template with pol II derived from cells lacking Bye1 (Kinkelin et al., 2013). In this assay pol II activity was present with and without Bye1 in the presence of the Gcn4 activator. However, only an end-product was monitored only at a single end-point, therefore potential effects of Bye1 on elongation or pausing remain unclear. Similarly, a second set of experiments, which looked at purified pol II assembled into an elongation complex similar to those described in Chapter II, demonstrated that pol II activity with or without the addition of purified Bye1 remains unaffected. In addition, no formation of cleavage products or backtracking was detected, even after the addition of a 100 fold excess of purified Bye1, in contrast to the addition of stoichiometric amount of TFIIS. These experiments again measured only a single end-point, so effects on rate would not have been observed. Thus, there are unanswered questions concerning the possible competition between Bye1 and TFIIS for pol II binding or effects of Bye1 on pol II activity.

Given current known functions of Bye1 and its location above the N-terminal domain of Rpb9, it is intriguing to consider a possible model for how Rpb9 relates to chromatin modifying complexes. Perhaps Rpb9, given its structural location at the

leading edge of pol II, helps form a scaffold along with residues of Rpb1 so that Bye1 can efficiently bind the polymerase complex and interact with histone tails on incoming nucleosomes. In this chapter, I attempt to probe a possible role for Rpb9 and chromatin modifying complexes based on the synthetic lethal interaction between *rpb*Δ and deletions of genes that code for protein components of those complexes. In addition, I also explore the potential relationship between Rpb9 and Bye1 to help shed light on the interactions between pol II and various chromatin modifiers that could be mediated through Rpb9, whether directly or indirectly.

Results

Rpb9 N-terminal domain is required for viability in cells lacking Gcn5, H2A.Z, or Spt7

As noted in Chapter I, Rpb9 is positioned at the leading edge of the polymerase, the N-terminal domain being the leading most structural element (Fig. 4.1C). Deletion of *RPB9* is synthetically lethal with deletions of genes encoding components of several chromatin remodeling complexes, including the Paf1 and SAGA complexes, which are indirectly and directly responsible for histone modifications, respectively. It is therefore easy to imagine that Rpb9 somehow mediates interactions between histones and the core of pol II as the polymerase traverses through chromatin-laden templates. This mediation need not be direct, as the body of pol II is a dynamic landscape for associations with many different complexes. Rather, Rpb9 could, in conjunction with other pol II subunits

or associated factors, help stabilize association of the chromatin modifying complexes. Independent of the molecular details, we wondered if the N-terminal domain of Rpb9 would be sufficient to suppress the synthetic lethality of *rpb9*Δ and deletions of genes encoding components of chromatin-modifying complexes. In addition, knowing that the C-terminal domain can affect TL mobility, we were also curious to see if there were specific genetic interactions with C-terminal Rpb9 mutations, as it has been shown that TL mutants that confer a transcriptionally fast phenotype are synthetically lethal or additively synthetic sick with mutations in components of certain chromatin-modifying complex components (Braberg et al., 2013; Jin and Kaplan, 2015). Specifically, is was shown that the combination of the TL mutation E1103G and the loss of the SAGA complex catalytic component Gcn5 are synthetically lethal (Braberg et al., 2013).

Our experimental strategy was to form a haploid shuffle strain in budding yeast which lacked Rpb9 and the synthetic lethal gene of interest in the genome, but was supplemented with a *URA3* marked plasmid-born copy of wild-type *RPB9*. Then using a standard plasmid shuffle strategy (See Chapter II Methods), we could test a set of Rpb9 variants for suppression of synthetic lethality. We chose three different genes (*GCN5*, *HTZ1*, and *SPT7*) from Table 4.1, all of which are associated with chromatin modification and, when deleted, are synthetically lethal with *rpb9*Δ. Gcn5 and Spt7 are components of the SAGA complex and have been shown to interact with pol II subunits Rpb1-3 and Rpb5 in yeast two-hybrid assays, and together within the SAGA complex function in both negative and positive roles in pol II dependent transcription

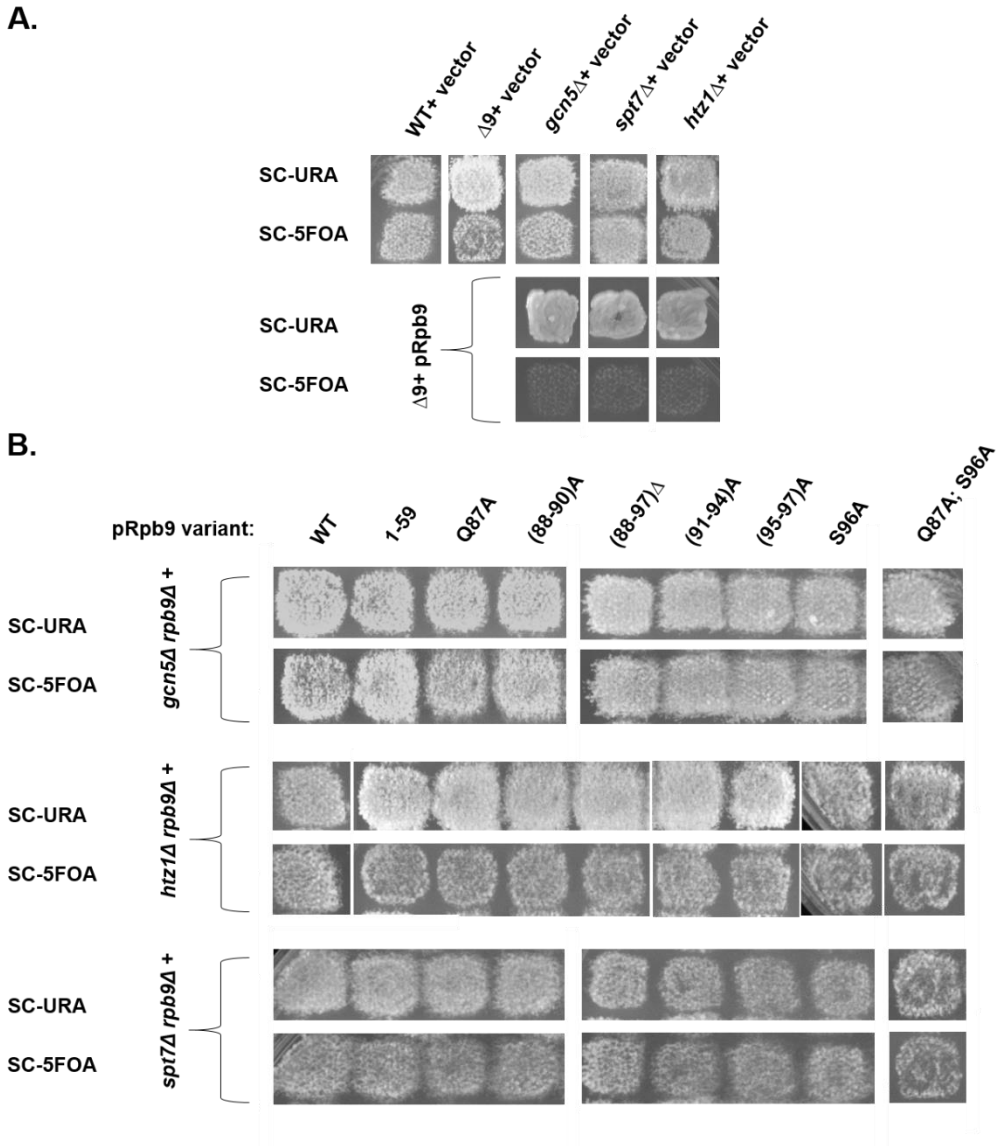

Figure 4.2: Rpb9 C-terminal mutants can suppress synthetic lethality associated with the combination of *rpb9Δ* with *gcn5Δ*, *htz1Δ*, or *spt7Δ*

(A) Background yeast strains created by cross containing a deletion of Rpb9 and one of the selected genes from Table1 are supplemented with a wild-type copy of Rpb9 (pRpb9) on a centromeric plasmid marked with *URA3*. Replica-plating cells onto media containing 5-FOA will result in lethality for cells requiring Rpb9 contained on the *URA3* plasmid (B) In addition to carrying wild-type Rpb9 marked with *URA3*, cells were transformed with variants of Rpb9 on a centromeric plasmid marked with *HIS3* indicated above the panels. Cells were then replica-plated on media containing 5-FOA to determine which Rpb9 variants would suppress the synthetic lethality.

(Garcia-Oliver et al., 2012; Rodriguez-Navarro, 2009; Van Mullem et al., 2002; Wery et al., 2004). Gcn5 is the catalytic component with a histone acetyltransferase activity, while Spt7 is required for formation and stabilization of the complex (Bonnet et al., 2014; Grant et al., 1997; Rodriguez-Navarro, 2009; Spencer, 1989; Sterner et al., 1999). *HTZ1* codes for the histone H2A.Z variant, which is preferentially enriched in promoter-proximal nucleosomes and is important for pol II nucleosome clearance by efficient nucleosome remodeling and proper pol II elongation complex assembly (Jensen et al., 2011; Santisteban et al., 2011; Santisteban et al., 2000; Wan et al., 2009). Also selected was a variety of Rpb9 mutations that span the N- and C-terminal domains of Rpb9 (Fig. 4.2B). These include the C-terminal, transcriptionally fast Rpb9 (95-97)A variant and the variant Rpb9 (1-59) which includes the complete N-terminal domain only. As seen in Fig. 4.2B (SC-5 FOA rows), all of the selected Rpb9 variants were able to suppress the synthetic lethality in *gcn5Δ*, *htz1Δ*, and *spt7Δ* backgrounds. Importantly, the N-terminal Zn1 domain of Rpb9 is sufficient for suppression in every case, suggesting that the relevant portion for the interaction between *RPB9* and *GCN5*, *HTZ1*, and *SPT7* is contained within the N-terminal 59 amino acids of Rpb9. It should also be noted that we did not observe a synthetic lethal interaction with the Rpb9 (95-97)A and *gcn5Δ* as we might have predicted based on the interaction between the TL mutation E1103G and *gcn5Δ* (Braberg et al., 2013). Perhaps this difference reflects two different modes of altering the TL's effect on catalytic rate similar to what has been suggested by single-molecule work by the Bustamante lab (Mejia et al., 2015).

Rpb9 C-terminal mutations interact differently in a gcn5/spt7Δ background versus htz1Δ

To better characterize the extent of the suppression shown in Fig. 4.2, we made 10-fold serial dilutions on various media. We spotted cells on minimal media (SC-His), media containing MPA (in pol II TL mutants seems to related to catalytic speed and transcriptional start site) (SC-His + MPA), and rich media (YPD) (Figs. 4.3-4.5) (Kaplan et al., 2012). In all cases, Rpb9 (1-59) had the most severe growth phenotype out of all the Rpb9 variants tested, though it was never more severe than either single mutant background. However, it should be noted that Rpb9 (1-59) is sufficient to complement the synthetic lethality, and in some instances, can complement a majority of the growth defect in the *rpb9Δ* single mutant (refer to Fig. 3.2). This lack of complete phenotypic suppression may be related to the reduced association of the Rpb9 (1-59) variant, as there is evidence that similar truncations result in decreased affinity (Chen et al., 2007; Hemming and Edwards, 2000). With respect to the *gcn5Δ*/Rpb9 combinations, there is a negative interaction for Rpb9 (88-97)Δ, but not for any other C-terminal mutations both for growth on minimal media and on media containing MPA (Fig. 4.3, 1st and 2nd column of panels). However combinations of Rpb9 variants with deletion of its SAGA complex counterpart Spt7, show no significant interaction with any C-terminal Rpb9 mutations (Fig. 4.5). These epistatic interactions with the C-terminal Rpb9 mutants, particularly the biochemically characterized Rpb9 (95-97)A variant, could

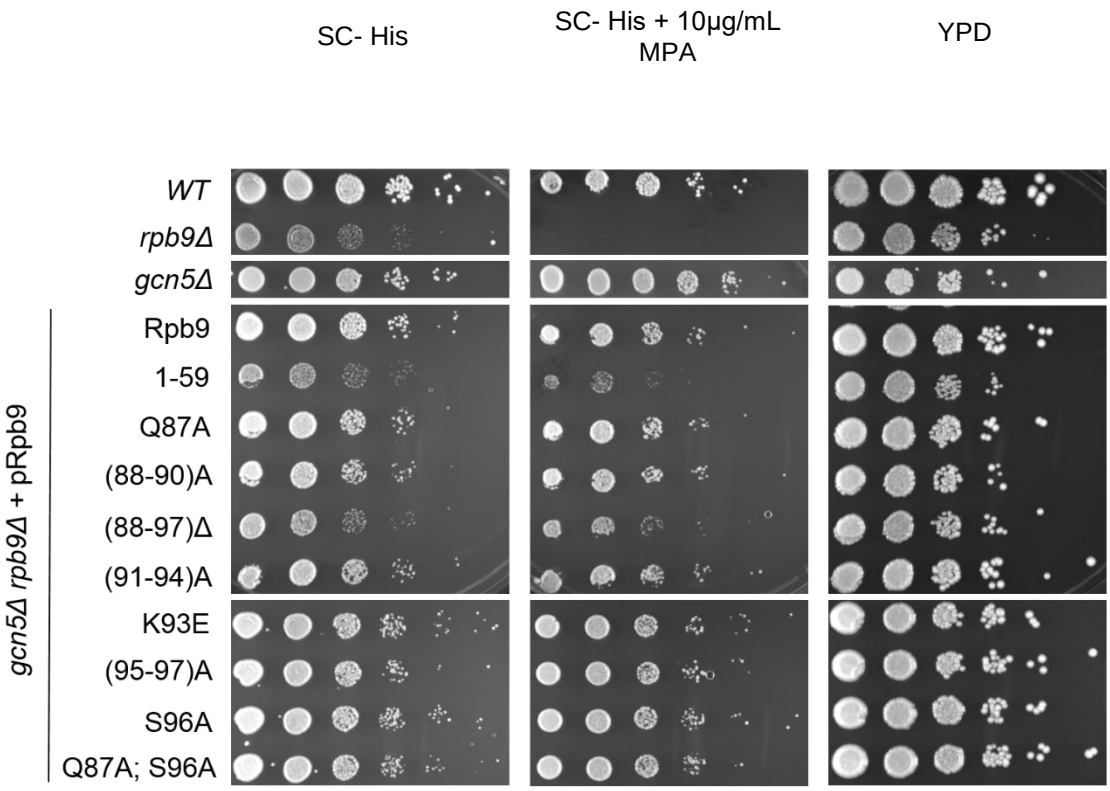

Figure 4.3: C-terminal mutations in a *gcn5Δ* background

Ten-fold serial dilutions of strains isolated from shuffles from previous figure or single deletion control strains carrying vector only (pRS413). Strains were spotted on minimal media (left panels), media containing 10µg/mL MPA (middle panels), or rich media (right panels). Pictures shown are after 3 days of growth.

suggest a potential role for the Rpb9 C-terminus in pol II enzymatic activity, combined with evidence in the literature that lack of Gcn5 affects pol II elongation in certain G-less templates (Tous et al., 2011). Additionally, it should be pointed out that the loss of Gcn5 does not affect the overall stability of the SAGA complex (Grant et al., 1997; Spencer, 1989; Sterner et al., 1999). This argues that the synthetic interactions that we observe between the loss of Rpb9 and either Gcn5 or Spt7, may directly or indirectly depend the histone acetyltransferase activity of SAGA rather than some function that requires direct interaction with the Rpb9 N-terminal domain.

In an *htz1Δ* background, we see a larger contrast in mutant effects with Rpb9 C-terminal mutations. On minimal media (Fig. 4.4, left panels), every Rpb9 variant showed a growth defect similar to an *htz1Δ* or *rpb9Δ* alone. However on rich media, we see both additive and suppressive interactions. For mutations in residues 95-97, or the mutation (88-90)A, or complete loss of the C-terminal domain (1-59) of Rpb9, there is an additive effect with the loss of H2A.Z. However, with the mutations (91-94)A and (88-97)Δ, we observed suppression of either single mutant phenotype. Interestingly, the sensitivity to MPA appears to be suppressed by mutations in residues 95-97 of Rpb9, but Rpb9 (91-94)A and (88-97)Δ appear to have a phenotype similar to wild-type Rpb9 or the *htz1Δ* single mutant (Fig. 4.5 middle panels). It is difficult to interpret these preliminary data given the lack of biochemical data on all of the variants of Rpb9. The one biochemically characterized variant is Rpb9 (95-97)A. This mutation in combination with the loss of H2A.Z appears to be additively negative. This suggests that the Rpb9 N-terminal domain and H2A.Z are important for a pathway that is unrelated to the defect in speed caused by

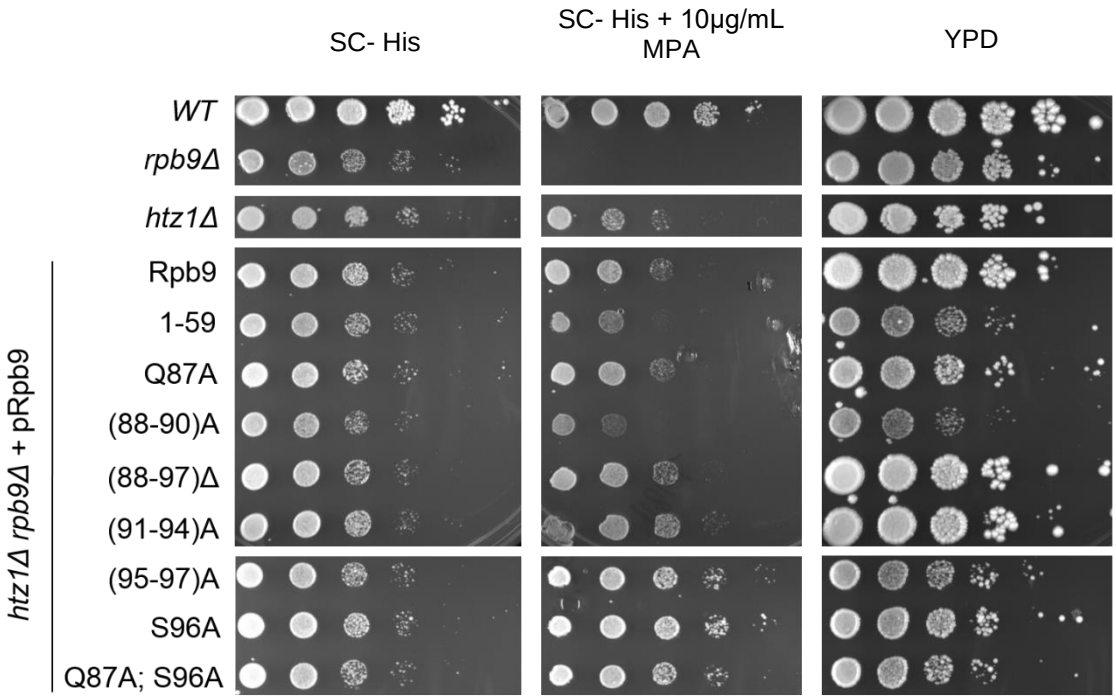

Figure 4.4: Rpb9 C-terminal mutations in a *htz1Δ* background

Ten-fold serial dilution of strains containing Rpb9 C-terminal mutations derived from plasmid shuffle in an *htz1Δ* background (as in previous figure). Strains were spotted on minimal media (left panels), media containing 10µg/mL MPA (middle panels), or rich media (right panels). Pictures shown are after 3 days of growth.

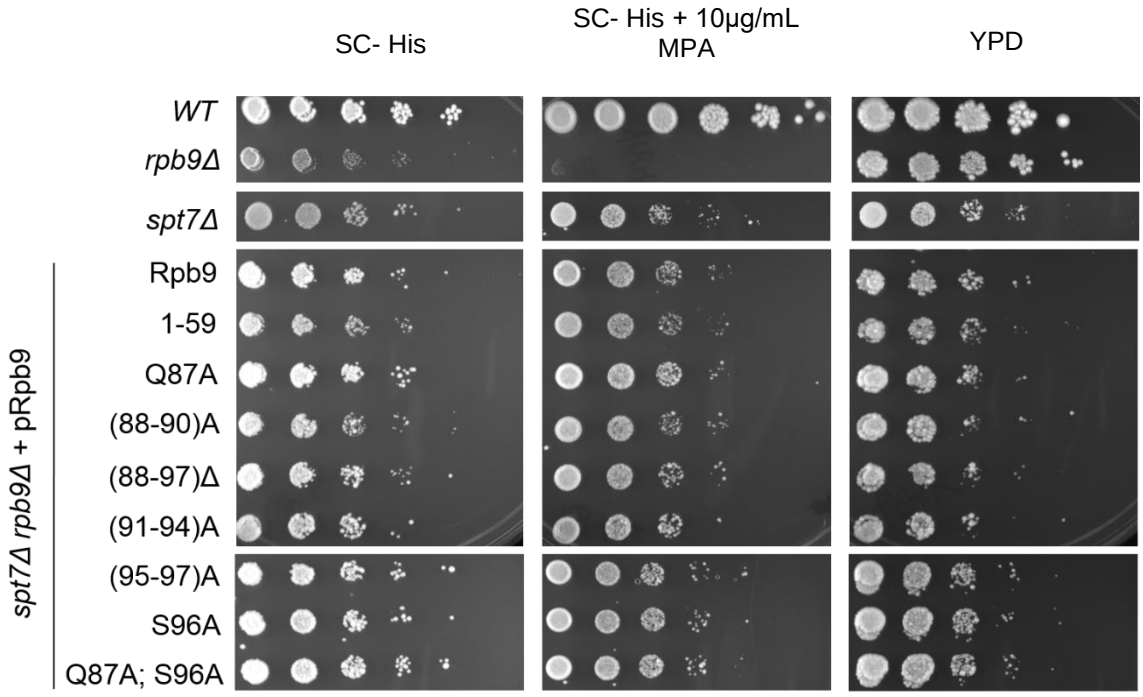

Figure 4.5: Rpb9 C-terminal mutations in a *spt7Δ* background

Ten-fold serial dilution of strains containing Rpb9 C-terminal mutations derived from plasmid shuffle in a *spt7Δ* background (as in previous figure). Strains were spotted on minimal media (left panels), media containing 10µg/mL MPA (middle panels), or rich media (right panels). Pictures shown are after 3 days of growth.

Rpb9 (95-97)A. This would be consistent with experiments showing additive effects in combinations of transcriptionally fast TL mutations like E1103G and *htz1Δ,* as well as other chromatin modifying complex components (Braberg et al., 2013).

Rpb9 residues 1-11 are important for cell viability in the absence of Gcn5, H2A.Z, Spt7, or the SWR1 complex structural component, Swc5

It has previously been shown that deleting the first 11 amino acids of Rpb9 mimics the MPA sensitivity of Rpb9 null cells (Li et al., 2006). We wondered if this MPA sensitivity was reporting on a function of Rpb9 associated with these chromatin modifying complex components, and distinct from the MPA sensitivity associated with pol II mutants that have an increased transcription rate. In order to test this idea and better define structurally the interaction of the Rpb9 N-terminal domain with various proteins important for chromatin remodeling, we combined truncation alleles of *RPB9* that deleted 5 amino acids at a time from the N-terminus of Rpb9 with cells lacking Gcn5, H2A.Z, and Spt7. As seen in Fig. 4.6 (from an experiment performed by A.M. Wadle in our lab), when we shuffled in variants lacking 5, 10, or 15 amino acids from the Rpb9 N-terminal domain, deletion of the first 10 amino acids is sufficient to fully restore the synthetic lethality that we previously observed with deletion of *rpb9*Δ and *gcn5Δ*, *htz1Δ*, and *spt7Δ,* as does the longer 2-16 deletion. It is a possibility that deletion of the first 11 residues of Rpb9 affects the fold of the entire Zn1 domain, as this variant of Rpb9 removes two of the 4 zinc-coordinating cysteines. Interestingly, there seems

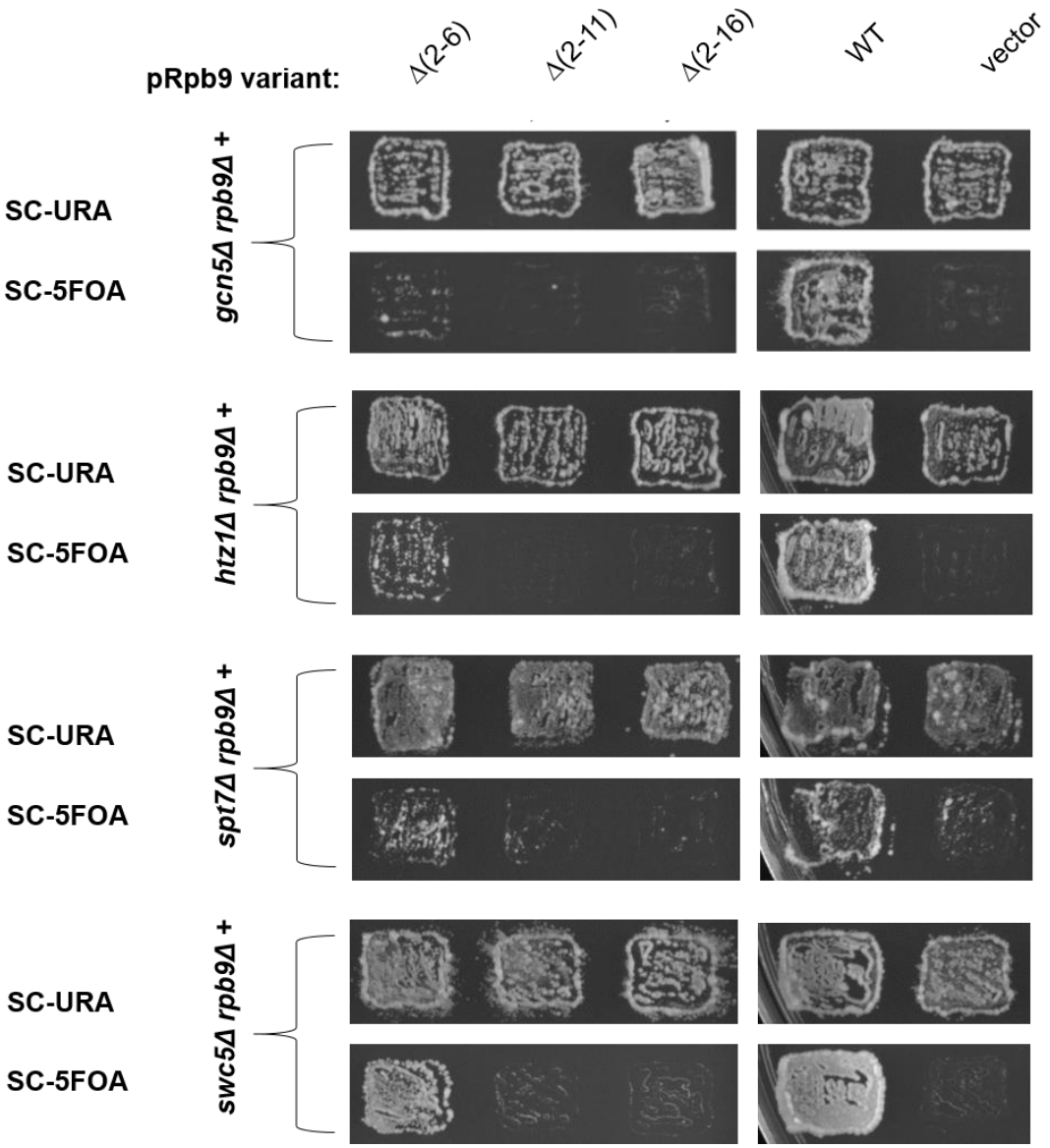

Figure 4.6: Rpb9 N-terminal truncations with *gcn5Δ*, *htz1Δ*, *spt7Δ*, or *swc5Δ* backgrounds

Plasmid shuffle with Rpb9 N-terminal mutants lacking 5, 10, or 15 amino acids from the methionine start in *gcn5Δ*, *htz1Δ*, *spt7Δ*, or *swc5Δ* backgrounds. Plasmid shuffle was done similar to the one done with Rpb9 C-terminal mutants earlier in Chapter IV (Also see Chapter II).

to be an additively negative but not lethal interaction with the 2-6 deletion as well which leaves these cysteines unaffected. Nevertheless, these results suggest that for all three gene deletions, the first ~11 amino acids of Rpb9 are critical. Since Gcn5 and Spt7 represent a catalytic and a structural function within the SAGA complex respectively, and when deleted have the same outcome with loss of the first 10 residues of Rpb9, we similarly wondered if the interaction between Rpb9 and H2A.Z could be recapitulated by deleting a component of the SWR1 complex which is required to insert H2A.Z into nucleosomes. The subunit in SWR1 complex we chose to delete was Swc5. Swc5 is a subunit essential for the function of the SWR1 complex, but is not the subunit which carries out the exchange of the H2A for H2A.Z (Krogan et al., 2003; Mizuguchi et al., 2004; Young, 1991). As seen in Fig. 4.6 (bottom panels), loss of Swc5 is also synthetically lethal in an *rpb9Δ* background. And, like strains lacking H2A.Z, the first 10 residues of Rpb9 are essential for viability. This suggests that the Rpb9 N-terminal domain, through at least the first 10 amino acids, is related to the presence of H2A.Z in nucleosomes specifically.

These experiments suggest a model in which Rpb9 is part of a common hub for pol II-associated factors that are important for negotiation through chromatin. However, to our knowledge, the only evidence of direct interaction Rpb9 and any of the four proteins above was from a Y2H screen that reported an interaction with Spt7, though it is known that the SAGA complex does contact the body of pol II (Wery et al., 2004). Additionally, there is no evidence that any of the components of the SWR1 complex, including Swc5, contact any subunit of pol II. This could argue that if Rpb9 did act in

stabilizing/recruitment/optimal function of the SAGA (Gcn5/Spt7) or SWR1 (H2A.Z/Swc5), then it does so through an intermediary. Alternatively, it could be that Rpb9 N-terminal domain is related to a separate essential pathway that when abrogated through deletion of residues 2-11, is lethal when added to the loss of deposition of H2A.Z or any of the functions related to the SAGA complex.

Loss of Bye1 has no additive effects with dst1Δ, rpb9Δ, or dst1Δrpb9Δ mutations

One attractive candidate that could serve as a link between Rpb9 and chromatin is the protein Bye1. As discussed in the introduction of this chapter, Bye1 has been implicated in two functions within pol II-transcribed genes (Pinskaya et al., 2014). The first role, which is mediated through its TFIIS-like domain, or TLD, is one in which Bye1 binds to pol II that is paused at nucleosomes and displaces TFIIS (Also see Fig. 4.1 C and D). It has been documented that as elongating pol II encounters nucleosomes, it can pause and backtrack, necessitating TFIIS-mediated RNA cleavage for realignment of the RNA 3′-end. Subsequent replacement of TFIIS by Bye1 could aide in reactivation of transcription which has been previously suggested (Pinskaya et al., 2014). The second role is involved with the H3K4 trimethylation-dependent occupancy of Bye1 (through its PHD domain) at promoters of pol II-transcribed genes that are normally transcribed at low levels, but that can be activated under certain stress conditions. The presence of Bye1 is thought to aide in transcriptional activation/initiation at these loci (Kinkelin et al., 2013; Pinskaya et al., 2014). If Rpb9 is related to the function or association of Bye1

with its binding site on the "jaw" domain of Rpb1, then several predications can be made. First, if Rpb9 affects the binding of Bye1 and therefore it's function while localized to pol II, then we would expect that the double knock-out of RPB9 and BYE1 would not be synthetic lethal. Second, if a portion of Bye1 function is dedicated to displacing TFIIS, then *dst1*Δ (*DST1* encodes TFIIS) should be epistatic with *bye1Δ dst1Δ*. Likewise, if the loss of Rpb9 affects Bye1 occupancy and Bye1 affects TFIIS occupancy, then *dst1Δ rpb9Δ* should be epistatic with *bye1Δ dst1Δ rpb9Δ*. Finally, given the proximity of the of the N-terminal domain of Rpb9 to the portion of Rpb1 that binds to the Bye1 TLD, there should be mutations in the N-terminal domain that are epistatic with *bye1*Δ if Rpb9 is necessary for Bye1 association, though the subtle phenotypes of the loss of Bye1 could be masked by the more severe phenotypes of Rpb9 truncations. If, however, mutations in the N-terminal region of Rpb9 are additively negative with the loss of Bye1, it could suggest that Bye1 and the N-terminal domain of Rpb9 are related in that they support separate pathways that function in parallel or redundantly, or that the two suggested functions of Bye1 operate independently and the Rpb9 N-terminal domain is only required for one of the two functions.

In order to explore the interaction between Rpb9 and Bye1, we began by crossing a *bye1Δ* strain into an *rpb9Δ* background and analyzing by tetrad analysis. As seen in Fig. 4.7, the *bye1Δ rpb9Δ* double mutant is not synthetic lethal and bears the growth phenotype of an *rpb9Δ* alone. To confirm this limiting phenotype of the *rpb9Δ* in the *bye1Δ rpb9Δ* combination, we challenged strains carrying the double, or either of the single gene deletions with various stressors within the growth media. Stress agents

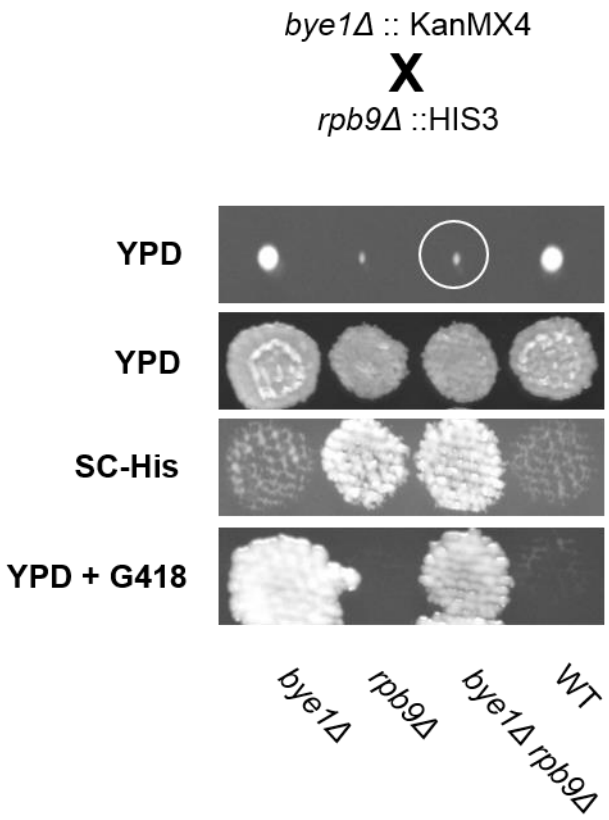

Figure 4.7: Isolation of the *bye1*Δ*rpb9*Δ double mutant

Figure above is a representative dissection of a resultant tetrad of a cross between a yeast strain with *RPB9* deleted from the genome via substitution with the *HIS3* ORF, and a strain with *BYE1* deleted via substitution with the KanMX4 cassette whose gene product confers resistance to the protein synthesis inhibitor G418. The haploid spore containing both gene deletions should be both His^+ and G418 resistant (indicated by white circle). See Chapter II for further details.

included: increased temperature, osmotic stress/cell wall integrity (NaCl and caffeine), nucleotide depleting drugs (6-AU and MPA), and an RNA chain terminator (Cordycepin). Loss of Bye1 does not elicit any of the phenotypes tested (Fig 4.8). On the contrary, in some instances *bye1Δ* confers a resistance to caffeine and MPA at higher concentrations. This is in contrast to *rpb9Δ,* which confers the well-documented hypersensitivity to nucleotide depleting drugs, particularly MPA, even at lower concentrations, as well as sensitivity to elevated temperature and caffeine. The *bye1Δ rpb9Δ* strain has phenotypes identical to *rpb9Δ,* consistent with the idea that the function of Bye1 is dependent on the presence of Rpb9.

It has been reported that deletion of Bye1 increases vegetative growth, consistent with the suppression we see for select phenotypes in our own results (though we did not observe the same growth increase) (Breslow et al., 2008; Kapitzky et al., 2010). We wondered if the resistance to stress seen in *bye1Δ* strains was related to TFIIS, as association with pol II increases under stress conditions (Pinskaya et al., 2014). The sensitivity of *dst1Δ* strains to the various growth conditions is also epistatic with *bye1Δ* (Fig. 4.8). In fact, the triple mutant (*bye1Δ dst1Δ rpb9Δ*) is only as sensitive as *dst1Δ rpb9Δ*. The additively negative affect of combining *rpb9Δ* with *dst1Δ* suggests that there are two differential functions of Rpb9 and TFIIS that are related but independent of each other, which is in agreement with all the *in vivo* literature on the double mutant (Koyama, 2003, 2007; Koyama et al., 2010). This is also consistent with the literature that has shown Rpb9 to affect TFIIS-mediated cleavage (Awrey, 1997; Knippa and Peterson, 2013). The epistasis we observed with the loss of Bye1 and the deletion of

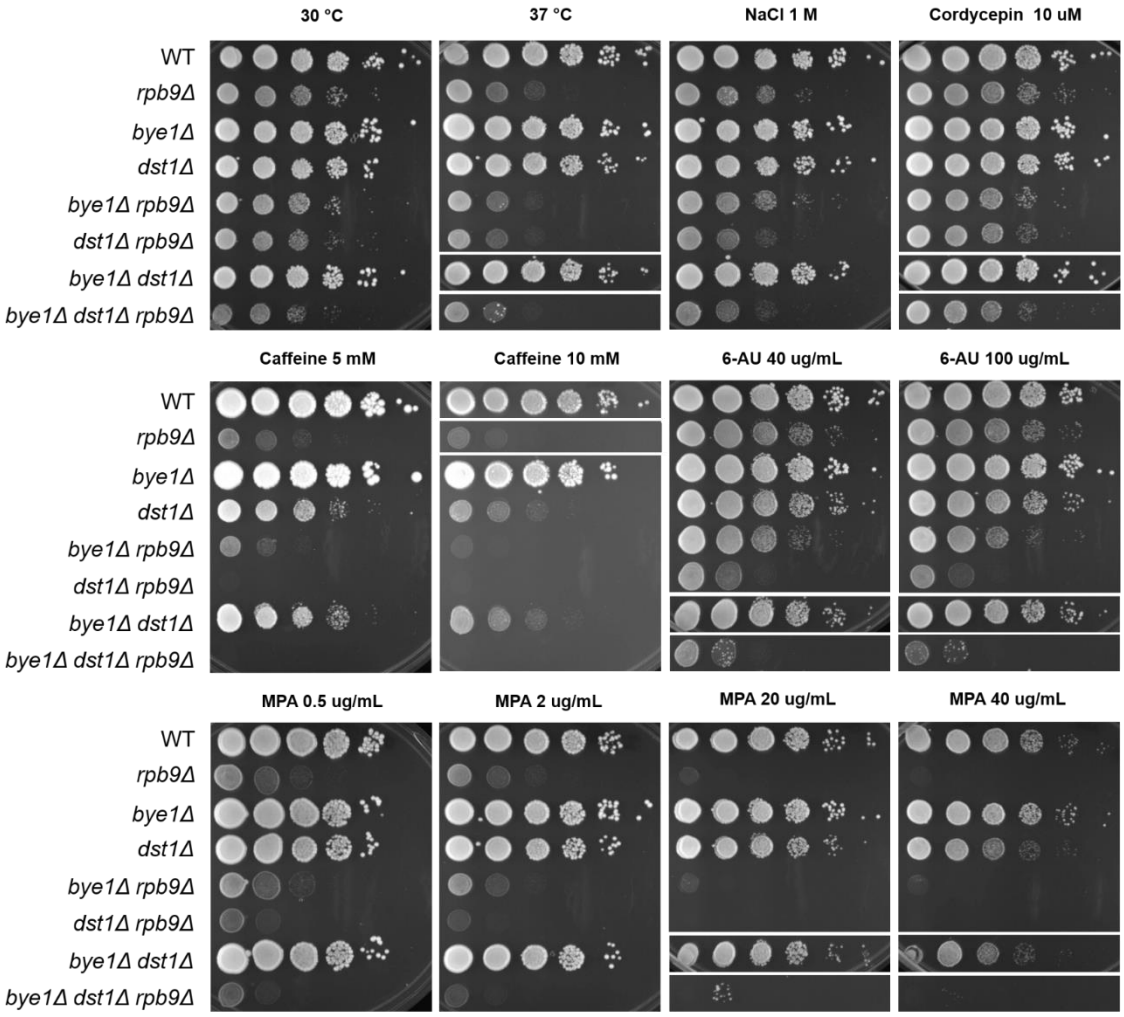

Figure 4.8: Selected stress phenotypes of combinations of *bye1Δ*, *dst1Δ*, and *rpb9Δ*

Ten-fold spot dilutions on rich media of haploid yeast strains carrying the indicated gene deletion created via PCR mediated gene disruption as described in Chapter II. Temperature and chemical phenotypes of varying concentration are indicated above each panel. All picture are shown after 2 days of growth except for the caffeine phenotype which is after 5 days of growth.

RPB9, *DST1*, or both, suggests that there could be a co-dependence of Bye1 on the presence of both Rpb9 and TFIIS. Alternatively, it may be that Bye1 is completely unrelated to the action of Rpb9 and TFIIS and the demonstration of epistasis is because *BYE1* is a redundant non-essential gene. This, however, is much harder to rationalize given the *bona fide* effects of the *bye1Δ in vivo* and *in vitro*.

Overexpression of Bye1 does not suppress phenotypes of dst1Δ or rpb9Δ strains

As noted earlier, Bye1 has been suggested to have a bi-modal function in the cell. In addition, over expression of Bye1 has been shown to increase sensitivity to 6-AU, similar to the deletion of *DST1*, which suggests the existence of a competition between Bye1 and TFIIS for pol II binding (Wu et al., 2003). If the functions of Bye1, both at promoters of genes and during transcription through nucleosomes, are dependent solely on its ability to interact with pol II, and Rpb9 and/or TFIIS modulate these interactions, then it might be expected that overexpression of Bye1 in the absence of either TFIIS or Rpb9 would modulate the phenotypes of both a *dst1Δ* and *rpb9Δ*. Alternatively, the two suggested functions of Bye1 may operate independently, and altering the association of Bye1 with transcribing pol II may not necessarily affect its ability to operate at promoters. In addition, if Bye1 displaces TFIIS, overexpression of Bye1 may make no difference in the context of *dst1Δ* or *rpb9Δ*. To address this, we constructed over-expression plasmids containing wild-type *BYE1*, *RPB9*, *DST1* (TFIIS), or a cleavage deficient variant of *DST1* (TFIIS E291N), and transformed them in combinations with

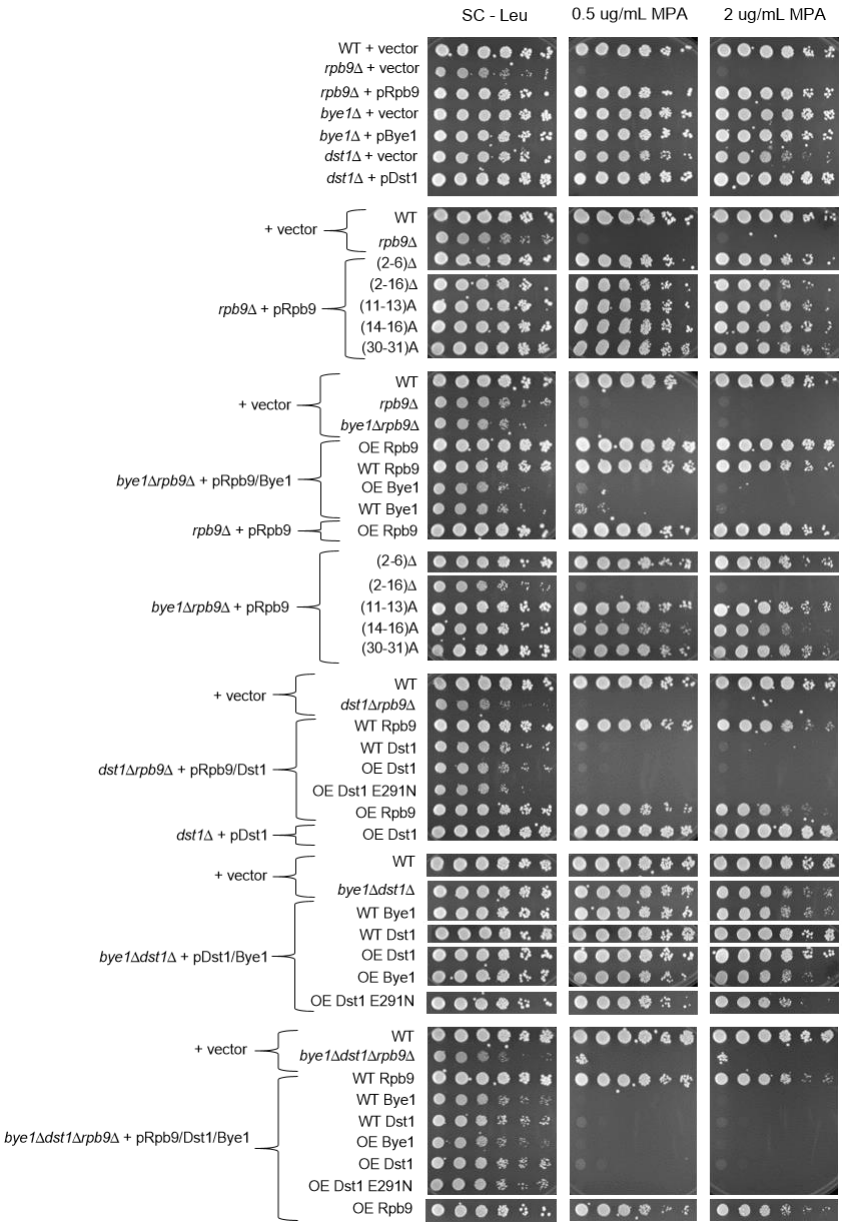

Figure 4.9: Overexpression of Bye1, Rpb9, or TFIIS, and *rpb9* N-terminal mutants in combination with *bye1Δ*, *dst1Δ*, or *rpb9Δ* backgrounds on MPA

Ten-fold spot dilutions of haploid yeast strains carrying the indicated gene deletion and plasmid combination (pRpb9—Rpb9 variants, pBye1— *BYE1*, pDst1—*DST1* or *dst1-E291N*). *Rpb9* N-terminal mutants, *BYE1*, *DST1*, or the cleavage-null *dst1* mutant were cloned into a centromeric plasmid (WT), as well as a high copy number 2μ plasmid (OE) , and transformed into the indicated background strain (indicated by brackets surrounding what is contained on the vector). Pictures are shown after 3 days of growth.

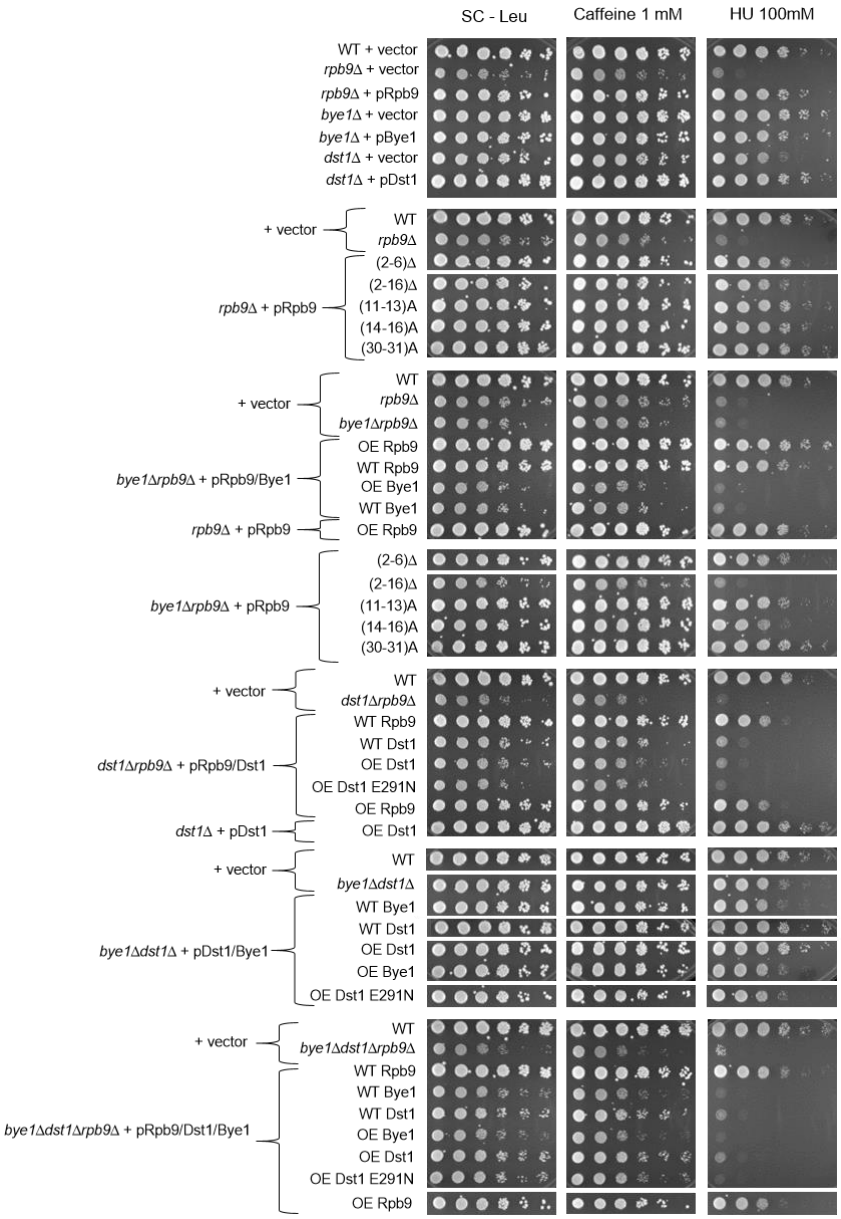

Figure 4.10: Overexpression of Bye1, Rpb9, or TFIIS, and *rpb9* N-terminal mutants in combination with *bye1Δ*, *dst1Δ*, or *rpb9Δ* backgrounds on caffeine or hydroxyurea

Ten-fold spot dilutions of haploid yeast strains carrying the indicated gene deletion and plasmid combination (As in previous figure). Pictures are shown after 3 days of growth on minimal media containing caffeine or hydroxyurea.

bye1Δ, *dst1Δ* or *rpb9Δ*. As seen in Figs. 4.9 and 4.10 (3rd, 6th, and 7th rows of panels), overexpression of Bye1 does not exacerbate or suppress any phenotype in the *dst1Δ* or *rpb9Δ* backgrounds. Nor does the overexpression of the cleavage inactive *dst1* mutant. Much like the behavior observed in Fig. 4.8, only wild-type Rpb9 or TFIIS can restore the growth defect of the *bye1Δ rpb9Δ* or *bye1Δ dst1Δ*, respectively (Figs. 4.9 and 4.10, 3rd and 6th row of panels). However, the absence Rpb9 and TFIIS is limiting in every phenotype both in the *dst1Δ rpb9Δ* (compared to *dst1Δ* or *rpb9Δ* alone) double mutant, and *bye1Δ dst1Δ rpb9Δ* triple mutant (Figs. 4.9 and 4.10, bottom row of panels), with overexpression of wild-type Rpb9 having the greatest suppression of the growth defects, sensitivity to MPA, caffeine, and the DNA synthesis inhibitor hydroxyl urea (HU).

These results provide several interesting conclusions. First, if both Bye1 and TFIIS's occupancy of pol II is mutually exclusive and Bye1 functions at the polymerase is solely to displace TFIIS, then we would expect a.) Deletion of *BYE1* would be epistatic to a *dst1Δ rpb9Δ* double mutant b.) overexpression of Bye1 alone would mimic some of the phenotypes of a *dst1Δ*, and c.) overexpression of Bye1 in a *dst1Δ* background would have no additional effect on the resulting phenotype. Published findings (Pinskaya et al., 2014; Wu et al., 2003) and Figs. 4.8-4.10 are in agreement with this model. Second, we also observed that overexpression of Bye1 did not enhance the phenotype of a strain lacking Rpb9, suggesting that displacing TFIIS by Bye1 is dependent on the presence of Rpb9. Lastly, in a *bye1Δ* background, overexpression of the cleavage deficient E291N mutant of TFIIS could not suppress sensitivity to any of the phenotypes tested suggesting that the defect observed through loss of TFIIS through

deletion or potentially through displacement by Bye1, relates to the cleavage function of TFIIS. However, more direct experiments are needed to explore the specific interaction between TFIIS (E291N) and Bye1, as *bye1Δ* may also suppress some of the phenotypes of the cleavage deficient mutation. It is important to note that these experiments seem to relate more to the effect of Bye1 on the function of TFIIS, rather than function(s) of Bye1 that may be independent of but important for pol II.

Mutations in the N-terminal domain of Rpb9 are more sensitive to stress in combination with bye1Δ

Experiments up to this point seem to hint at a model where Bye1 competitively affects TFIIS occupancy, and Bye1 association could be affected by Rpb9. We also saw that Rpb9 interacts with a general class of pol II associated factors relating to chromatin via its first ~ 16 amino acids. We wondered if, like the SAGA or H2A.Z factors, Bye1 also interacted with Rpb9 via this N-terminal domain. To test this, we looked at the effect of Rpb9 N-terminal mutations or truncations in a *bye1Δ* background. If the Rpb9 N-terminal domain is important for the interaction with Bye1, then we might expect that N-terminal mutations of Rpb9 would be epistatic with the loss of Bye1. Alternatively, if N-terminal Rpb9 mutations are additively negative with the loss of Bye1, it would argue that the defect that we see with the loss of Rpb9 in the context of Gcn5, H2A.Z, Spt7, Swc5, is distinct from the defect caused by the loss of Rpb9 in a *bye1Δ*. In addition, it would also argue that the region critical for the Rpb9/Bye1 interaction resides in the C-

terminal region of Rpb9. All the Rpb9 N-terminal variants tested have no growth defect on minimal media (Figs. 4.9 and 4.10 (2^{nd} row of panels)). However, the truncation variants (2-6)Δ and (2-16)Δ show a hypersensitivity to MPA at low concentrations, as well as a sensitivity to HU. The scanning mutations (14-16)A and (30-31)A also demonstrate a slight sensitivity to HU and MPA, respectively. If Rpb9 affects the association/function of Bye1 via its N-terminal domain, we might have expected resistance in the phenotypes tried, as seen in the *bye1Δ* only (Refer to Fig. 4.8). But, here we do not. Indeed, when we combine these Rpb9 variants with a *bye1Δ* we see the strain becomes additively more sensitive to the drugs or growth conditions tested, especially the (2-16)Δ truncation (Figs. 4.9 and 4.10, 4^{th} row of panels). What is interesting is that the more conservative mutation in Rpb9 (14-16)A also demonstrates an additive phenotype with the loss of Bye1. It would interesting to know whether these residues are important for Rpb9 interactions with SAGA or SWR1 complex components as well as their behavior with over-expression of Bye1. Taken together however, these results suggest that again the C-terminal domain of Rpb9 is important for the interaction of Bye1. A potential relationship between Bye1, the Rpb9 C-terminal domain, and TFIIS will be discussed in the section bellow.

Discussion

The small, non-essential subunit Rpb9 has been implicated in several functions of eukaryotic RNA polymerase II. More recently, clear biochemical evidence has given

insight into Rpb9's role in error detection by slowing the extension of a mismatched base, proofreading through enhancement of TFIIS-mediated cleavage, and modulation of the TL dynamic through the so-called Anchor Loop and Rpb9's C-terminal domain as described in Chapter III (Knippa and Peterson, 2013). However, much has been left unexplained about all the other non-polymerase interactions that are not necessarily related to the C-terminal Zn2 domain of Rpb9, or the active site of pol II. Table 4.1 illustrates a collection of the interacting proteins that are synthetic lethal upon deletion of *RPB9*, meaning that they are potentially critical in the same functional pathway. At a glance, none of the listed proteins or complex components seems to lend itself to a clear link to Rpb9. One thing many of them have in common is that they are important for pol II navigating chromatin templates, and, in some instances, as with the SAGA complex and its component proteins, affect the pol II CTD phosphorylation state, which is important for recruitment of various factors that mature the nascent RNA as pol II transitions from the 5'- to the 3'- end of the gene (Wyce et al., 2007).

To better understand these interactions between Rpb9 and these chromatin-related complexes, as well as all the synthetic lethal interactions in general, we analyzed a subset of them in the context of mutations in Rpb9 that spanned the majority of the length of the protein. Interestingly, we found that the N-terminal domain is required for cell viability in combination with deletion of *GCN5*, *HTZ1*, or *SPT7*. In addition, depending on the stress introduced, C-terminal mutations in Rpb9 behaved differently in the absence of SAGA complex components compared to the histone H2A variant, H2A.Z. For the deletion of the SAGA complex components, we observed epistasis with

the Rpb9 (95-97)A variant which we have shown to be transcriptionally fast. This is in contrast to the loss of H2A.Z, which is additively negative with this variant of Rpb9. This argues that the function of the SAGA complex is potentially dependent on both the function of the N-terminal domain as well as the catalytic role of Rpb9's C-terminal domain. Whereas the Rpb9-dependent function of H2A.Z may be limited to the N-terminal domain only. Interestingly, disrupting the SAGA complex via deletion of Spt7 or specifically deleting the histone acetyltransferase activity through Gcn5, yields the same outcome. Given that the loss of Gcn5 does not destabilize the SAGA complex as a whole (Grant et al., 1997; Sterner et al., 1999), it suggests that the defect caused by abrogating the SAGA complex or the N-terminal domain of Rpb9, relates to the histone acetyltransferase activity of the SAGA Complex. Upon further analysis, we found that the first ~11 amino acids of Rpb9's N-terminal domain were absolutely required for cell viability for the initial three synthetic lethal genes tested. In addition, we also identified a new synthetic lethal gene, *SWC5*. Similar to the relationship between the catalytically active component of the SAGA complex Gcn5 and the structural component Spt7, we found that the absence of Swc5, an integral component of the SWR1 complex which functions to substitute H2A for H2A.Z (Mizuguchi et al., 2004), was equivalent to the loss of H2A.Z and also dependent on the first ~11 amino acids of Rpb9. This suggests that the defect caused by the absence of H2A.Z or the Rpb9 N-terminal domain, is related to the presence of H2A.Z in chromatin.

Recent literature on Bye1, a protein with a pol II binding domain very similar to that of the transcription factor TFIIS, provided us a testable hypothesis of how Rpb9

might directly interact with chromatin, as none of the synthetic lethal genes analyzed had. Bye1 contains a TFIIS-like domain that is required for its association to pol II, as shown in a recent crystal structure and *in vivo* studies (Kinkelin et al., 2013; Pinskaya et al., 2014). Interestingly, in addition to its ability to bind the polymerase, it has been implicated in both the induction of stress-response genes by binding to tri-methylated histones at their promoters, as well as a proposed function in displacing TFIIS in order to promote productive transcription (Pinskaya et al., 2014). Given its location proximal to the N-terminal domain of Rpb9 (Refer to Fig. 4.1C), we wondered if Bye1 association could be affected by the loss of Rpb9 or TFIIS. Our initial experiments (Figs. 4.8-4.10) allowed us to make several interesting observations. First, in addition to not being synthetically lethal with *rpb9Δ*, deletion of *BYE1* does not result in enhancement of any of the phenotypes we tested. Rather, we found that absence of Bye1 made cells more resistant to stress in some cases. One possible interpretation of this observation is based on the proposed action of Bye1 in displacing TFIIS. TFIIS is preferentially enriched at genes under stress conditions (Pokholok et al., 2002). Increasing TFIIS occupancy at pol II by eliminating the competition with Bye1 could render cells more resistant to stress. This is in agreement with published observations in which overexpression of Bye1 renders cells more sensitive to 6-AU, and deletion of Bye1 leads to increased growth in the presence of 6-AU (Breslow et al., 2008). However, here we did not observe any effect of Bye1 over-expression on the MPA sensitivity of *rpb9Δ* or *dst1Δ* strains, but we have not examined Bye1 over-expression in other genetic backgrounds. The subtle phenotypes observed for the *bye1Δ* are completely dependent on the presence of TFIIS

and Rpb9. Indeed, over expression of Bye1 in either a *dst1*Δ or *rpb9*Δ background had no effect on sensitivity to MPA, Caffeine, or HU. Lastly, combining the N-terminal mutants of Rpb9 with *bye1Δ* were additively negative when compared to either single mutant. Specifically, the truncation Rpb9 (2-16)Δ and the scanning mutation Rpb9 (14-16)A demonstrated the largest increase in phenotype. These results imply that it is the C-terminal and/or the linker, and not the N-terminal domain of Rpb9 that is potentially important for Bye1 association with pol II. It also argues that the mechanism of Rpb9 and Bye1, however related to chromatin template navigation, is distinct from the pathways for which the N-terminal portion of Rpb9 is critical.

Model for Rpb9/Bye1 interaction

Nucleosomes provide a natural barrier to transcription. One of the proposed functions of Bye1 is to locate to pol II via interaction with trimethylated H3K4 in a nucleosome. This is done in order to displace TFIIS which has localized to pol II in response to the stalling of pol II at the nucleosomal barrier (Kireeva et al., 2005). It has been suggested that displacing TFIIS, which functions to cleave and realign the 3'-end of the RNA, allows the TL to gain access to the active and resume productive elongation. In addition, it has been shown that the loss of Rpb9 affects TFIIS-mediated cleavage without affecting TFIIS binding (Awrey, 1997). Crystal structures containing TFIIS bound to pol II show that the TL and domain III of TFIIS, which contains the acidic residues essential for RNA cleavage activity, cannot concomitantly occupy the

active site (Kettenberger et al., 2004). Quench-flow kinetic analysis has shown that the absence of Rpb9 increases nucleotide sequestration at the active sight, consistent with the idea that Rpb9 functions, at least in part, by delaying TL closure (Walmacq et al., 2009). The evidence presented in Chapter III that the effect of Rpb9 on TL closure is mediated through its C-terminal domain and the AL of Rpb1, as well as the preliminary results from this chapter, are consistent with a model in which Rpb9 can affect TFIIS function in two different ways. The first way would be through the AL-TL interaction. Rpb9 in this case would function to delay the closure of the TL, which would reduce the competition between the TL and TFIIS for active site occupancy and enhance TFIIS-mediated cleavage. The second component of the model would be that Rpb9 is required for efficient Bye1 association with pol II, which competes with TFIIS for pol II occupancy. This would negatively affect proofreading, but balance the competition between the TL and TFIIS.

This model makes a number of predictions that could be tested in future experiments. Mutations in the C-terminal area of Rpb9 should have phenotypes similar to *bye1Δ*. Indeed, we have observed MPA resistance in some mutations of the C-terminal domain, which would be consistent with constitutive *IMD2* expression (Fig. 3.2). This effectively would increase the allowed binding of TFIIS, and perhaps exacerbate the effect of the TFIIS E291N mutation. In addition, if the AL affects the dynamic of the TL, then mutations in the AL would also increase the competition between the TL and domain III of TFIIS, providing a second mode for Rpb9 to affect TFIIS function at the pol II active site. A similar mechanism has been proposed between

GreA/B and the TL in bacteria (Dangkulwanich et al., 2014; Roghanian et al., 2011). With our predictions based on this model, experiments with combinations of mutants could be performed that look directly at TFIIS occupancy of pol II subject to competition with Bye1, as well as experiments that analyze whether mutations in the C-terminal domain of Rpb9 affect both Bye1 and TFIIS occupancy, given that they bind similarly. It may be that the effect of mutating the C-terminal domain of Rpb9 and the AL simultaneously affects both Bye1 and TFIIS association, though deletion of all of Rpb9 seems to affect cleavage but not association of TFIIS (Awrey, 1997). It would be interesting to know whether Rpb9 and Bye1 affect other functions of TFIIS, which include formation of the preinitiation complex (Kim et al., 2007), suppressing pausing (Schweikhard et al., 2014), and interactions with the SAGA complex through Spt8 and the Mediator complex through several subunits (Wery et al., 2004). In addition, it has been suggested that the Rpb9 pol III homolog C11, which contains a C-terminal domain similar to TFIIS domain III, functions in termination in *S. pombe* (Iben et al., 2011). It would interesting to know if Rpb9 affected termination for pol II through TFIIS occupancy. Regardless, the experiments necessary to test this model would be straightforward in their approach.

Global model for Rpb9 and transcriptionally related complexes

The preliminary data with Bye1 and Rpb9 suggest that the Rpb9 N-terminal domain is operating in a mechanism distinct from Bye1 and distinct from the function of

its C-terminal domain. A study on the pol III Rpb9 homolog C11, showed that several conserved hydrophobic residues in the N-terminal Zn2 domain of C11 are important for the binding the pol III dimeric termination factor C53/37 (Homologous to Rap30/74 dimer in humans and a paralogous to pol II TFIIF (Kuhn et al., 2007). These four conserved residues reside within the first ~34 amino acids of Rpb9, and three are within the first 16 amino acids of N-terminal domain of Rpb9, C11, and the pol I Rpb9 homolog A12.2 (refer to Fig. 4.11). It is intriguing that several of these residues are located within the N-terminal portion of Rpb9 that we have shown to be critical for cell viability with the synthetic lethal genes we have analyzed so far. This was exciting given that it has been documented that deletion of Rpb9 drastically affects the association of TFIIF to pol II (Khaperskyy et al., 2008; Ziegler et al., 2003). Furthermore, a large-scale crosslinking/MS study on the association of TFIIF and pol II demonstrated that Rpb9 crosslinks to the largest subunit of TFIIF (Tfg1) within the first 20 amino acids of the N-terminal Zn1 domain (Chen et al., 2010). In addition, the analysis also showed that regions of Rpb1 and Rpb2 that are adjacent to Rpb9 residues that contact Tfg1, also contact Tfg1 and Tfg2. This suggests that Rpb9 N-terminal domain, in combination with other core subunits in the local area, provide an interaction surface for the TFIIF complex to associate with the body of the polymerase. .

TFIIF also has connections with some of the genes whose deletion is synthetic lethal with *rpb9*Δ. Of the 22 documented synthetic lethal genes (Table 4.1), 8 also physically interact with TFIIF subunits, whether directly or indirectly (Table 4.2). Of those, 5 specifically contact the main body of TFIIF through either Tfg1 or Tfg2, and

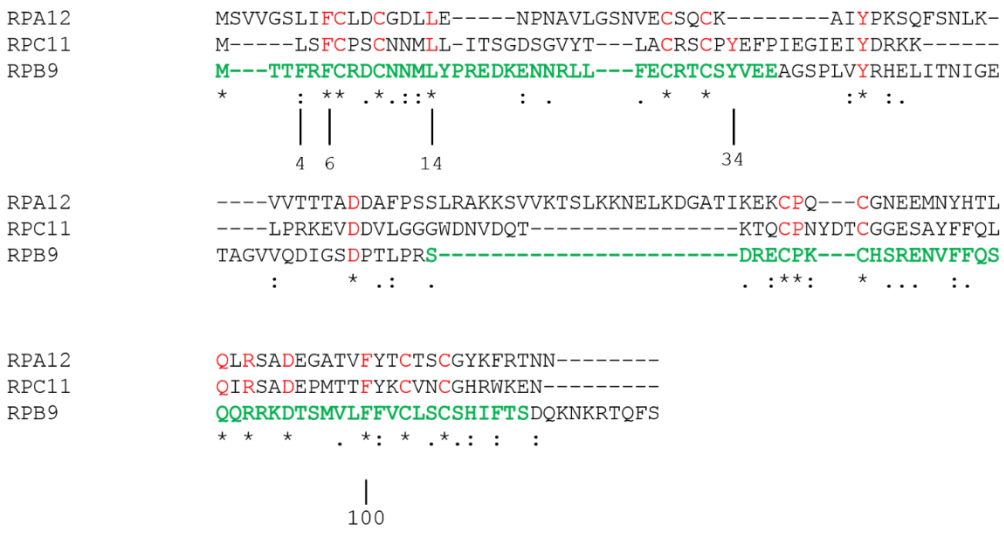

Figure 4.11: Protein alignment of Rpb9 and its pol I and III paralogs

Sequence alignment of *S. cerevisiae* Rpb9 homologs C11 and A12 from pol III and pol I, respectively. Alignment was generated using ClustalOmega. Asterisks indicate complete conservation, colons indicate residue character conservation, and a single period indicates residue shape conservation. Highlighted in green is the amino acid sequence of Rpb9 and numbers indicate conserved residues important potentially for TFIIF (Rpb9) and C53/37 (C11) biding (See text for details).

that Rpb1, Rpb4, and Paf1, have been shown to co-immunopurify with Tfg1 or Tfg2 (Wade and Jaehning, 1996; Wade et al., 1996). In addition, we also noticed that many of the synthetic lethal genes from Table 4.2 also interacted with components of complexes such as SAGA, Paf1, or SWR1. It is intriguing to consider a model where perhaps TFIIF is important for mediating the association or function of these complexes. Given that we suspect the N-terminal domain of Rpb9 to affect TFIIF association to pol II, perhaps this would provide a molecular link between Rpb9 and these various pol II-associated complexes. It has already been demonstrated, through Y2H and various proteomics approaches, that the Rpb1 subunit of pol II contacts subunits of TFIIF, as well as SAGA and Paf1(Krogan et al., 2002; Lee et al., 2011; Pascual-Garcia et al., 2008). Importantly, synthetic lethal genes that contact TFIIF, in some instance contact subunits of every complex analyzed. This is in addition to any affects that would be caused by altering any functions of TFIIF.

This model makes several predictions. If Rpb9 affects the association of TFIIF, there should be alleles of *TFG1* and *TFG2* with phenotypes similar to those of *rpb9*Δ, and there are documented alleles of these genes that exhibit MPA sensitivity at concentrations that exhibit MPA sensitivity similar to that of *rpb9-(2-16)Δ* (Jin and Kaplan, 2015). In addition, these mutations fall in the area that crosslinks to Rpb9 N-terminal domain (residues 120-130, 400-420 in Tfg1, and 260-280 in Tfg2) (Chen et al., 2010). The adjacent areas in Rpb2 (270-280, 340-350) also demonstrate similar phenotypes (Kubicek et al., 2013). TFIIF mutants have also been shown to affect start site selection, as have mutations in the TL and truncations in the C-terminal domain of

Rpb9 (Jin and Kaplan, 2015; Khaperskyy et al., 2008; Shandilya et al., 2012; Sun et al., 1996; Ziegler et al., 2003). In fact, combinations of upstream start site-shifting TFIIF mutations can suppress the downstream defect of downstream shifting TL mutants, and exacerbate the defect of upstream shifting mutants (Jin and Kaplan, 2015). Importantly, these same TFIIF mutants do not suppress the growth defect of these same start site-shifting TL mutants. These results argue for a role of TFIIF that is independent of its function in start site selection and the TL, perhaps the one we have suggested above concerning co-transcriptional complexes. Nevertheless, we would predict minimally that the TL-dependent, C-terminal function of Rpb9 would affect start site selection as gain of function TL mutations. However, an additional Rpb9 N-terminal pathway with TFIIF may also exist to affect start site selection.

In summary, there is compelling evidence that mutations in the lobe region of pol II affect TFIIF association. Given that TFIIF interacts with many of the genes that are synthetic lethal with Rpb9, we propose that in addition to the defects cause by decreased association of TFIIF, decreased association of TFIIF also globally affects the function of transcription complexes that temporally associate with the polymerase at all stages of transcription, which are depicted Fig. 4.12. If mutations in Rpb9 can alter the interaction of TFIIF with pol II, which has a broad range of effects that collectively confer a severe growth defect in *rpb9*Δ strains, it would explain why *rpb9*Δ has a growth defect more severe than that of other fast polymerase mutations. Synthetic lethality results when any of a number of processes, already partially disrupted by the absence of Rpb9, is further disrupted with a second mutation. This predicts that at least some genes that are

Figure 4.12: General timeline of synthetic lethal interacting genes of Rpb9 in the context of all stages of the transcription cycle

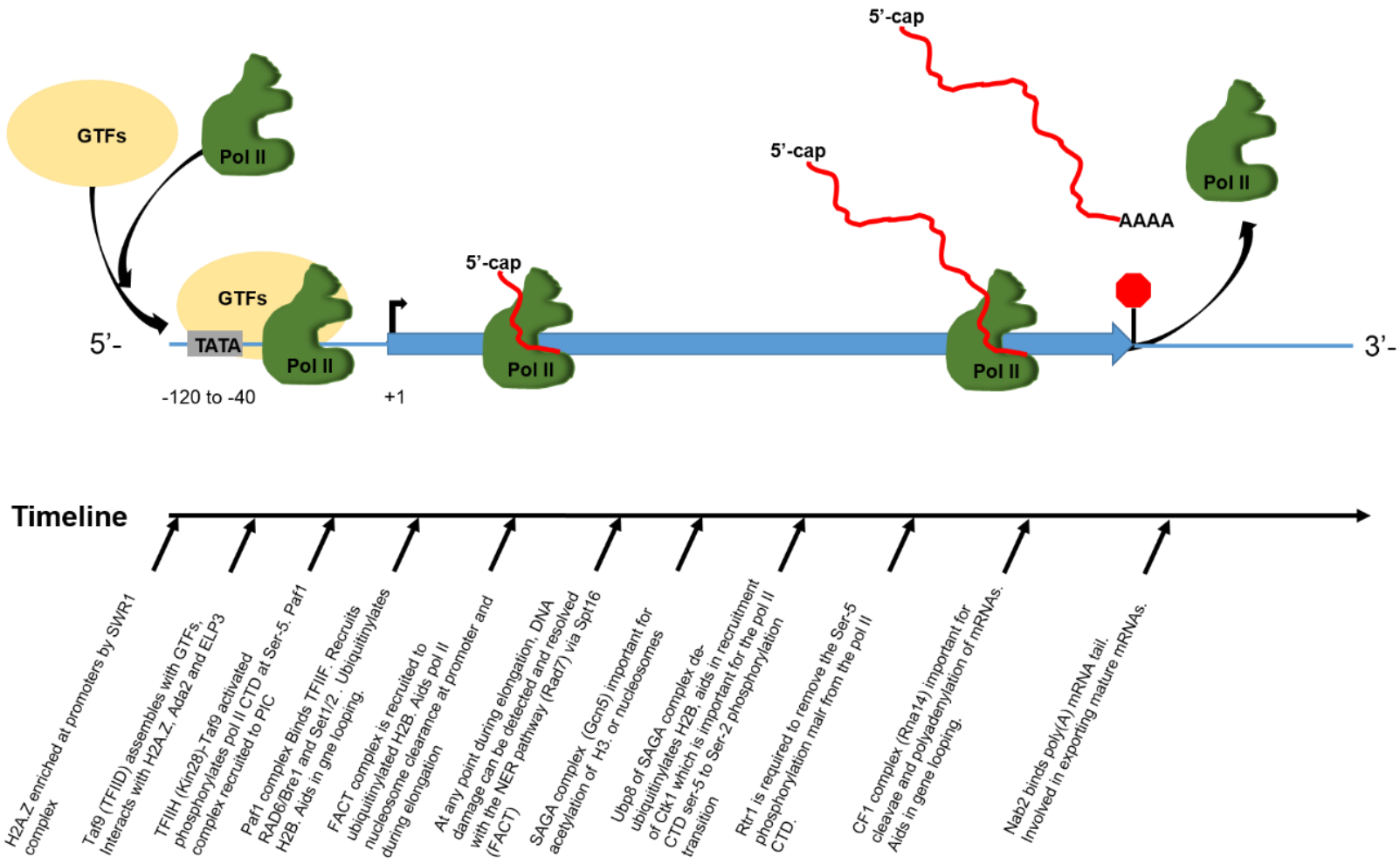

synthetically lethal with *rpb9*Δ should be synthetically lethal with each other in a *RPB9* background, and indeed *paf1*Δ is synthetically lethal with deletion of several of the subunits of SAGA (Ingvarsdottir et al., 2005; Milgrom et al., 2005). This is in contrast to the mechanism of Bye1, which seems to be related to the C-terminal function of Rpb9 and a balanced competition with TFIIS.

CHAPTER V

SUMMARY, FUTURE DIRECTIONS, AND FINAL REMARKS

The pol II subunit Rpb9, though non-essential, has been shown to be important for various functions in the cell, not the least of which is transcriptional fidelity (Knippa and Peterson, 2013; Walmacq et al., 2009). Maintenance of accurate transcription is critical to faithful conversion of the information stored in DNA into the functional units of the cell. Transcriptional fidelity has been a point of much study and in pol II, it seems to be governed in part by a mobile domain at the heart of the active site, termed the TL. The TL moves in and out of the active site at different stages of the nucleotide addition cycle. As discussed in Chapter I, the TL has been implicated in selection of the correct substrate base, induction of pausing post-misincorporation, and most notably the balance of the catalytic speed of the polymerase which effects both selection and proofreading (Kaplan, 2008; Larson et al., 2012; Mejia et al., 2015; Wang et al., 2015; Wang et al., 2013). Among the other documented phenotypes associated with the loss of Rpb9, it was noticed that pol II lacking Rpb9 had similar *in vitro* behavior to TL mutants which were posited to affect the TL transition from the closed position, required for substrate addition, to the open position which allows for translocation and another substrate NTP to enter the active site (Walmacq et al., 2009). Increasing the trapping of substrates at the active site by increasing the fraction of time the TL spends in the closed state can have a direct effect on fidelity, and it was proposed that Rpb9 affects fidelity by directly affecting the TL transition. However, when this model was tested by measuring the

effect on fidelity of a specific mutation in the C-terminal domain of Rpb9, a negative result was obtained (Walmacq et al., 2009). This left the specific mechanism of Rpb9 function, and its relationship to the TL, an open question.

One of my initial project goals was to define the role of the TL in Rpb9 function, and answer this question. From Chapter III, an approach was used that took advantage of the TL inhibitor α-amanitin (Kaplan, 2008). We reasoned that if any of the *in vitro* characteristics of *rpb9*Δ were dependent on TL movement, then they should be affected by the TL immobilization caused by the presence of α-amanitin. Indeed, as seen in Chapter III, this was observed to be the case for the increased misincorporation rate for pol IIΔ9, consistent with the idea that in this context, the effect of *rpb9*Δ was TL-dependent. In parallel, we were also using a classic genetic approach to elucidate functions of Rpb9 by exploiting the *rpb9*Δ suppressor *rpb1-G730D*. We were able to localize the interaction of this pol II mutant to residues 95-97 in Rpb9. The location of these residues in the crystal structures relative to the open conformation of the TL, as well as the ability of the *rpb9- (95-97)A* mutation to phenocopy *rpb9*Δ both *in vivo* and *in vitro*, led us to propose a new model of how the Rpb9 C-terminal domain might function through the TL.

Our new model suggests that it is not a direct interaction by which Rpb9 stabilizes the open conformation of the TL, but rather an indirect interaction pathway way through a loop connecting α-20 and α -21 which we have termed the anchor loop (AL). The results in Chapter III demonstrated that mutations that occur on either side of an interaction surface between Rpb9 and the AL (*rpb9- (95-97)A/rpb1- R711A*) or

between the AL and TL (*rpb1- (707-709A)/ rpb1- S1091C*), mimicked properties of *rpb9*Δ *in vivo* and *in vitro*. Importantly, these same mutations in the AL and TL were epistatic *in vitro* in combination with *rpb9*Δ, and likewise dependent on TL mobility as ascertained through the use of α-amanitin. This suggests that they are in the same functional pathway, are upstream defects, and give credence to our model.

These results are also consistent with molecular dynamic studies that utilized published crystal structures (Kireeva et al., 2012; Wang et al., 2013) to model the movement of the TL between the open and closed positions. These studies predicted that Rpb1 residues E712 (in α-21) and K1092 (in the TL), would be important for the TL transition (Wang et al., 2013). Indeed, my preliminary *in vitro* transcription assays indicate that E712A is transcriptionally slow (data not shown), which correlates with the predicted *in vitro* phenotype from the molecular dynamics studies. We have also examined residues S751 and K752, which are not part of the TL, but do interact with the γ- phosphate group of the incoming substrate at the pol II active site and also behave as predicted from (Wang et al., 2013). In addition to the residues we have biochemically characterized here, it would be beneficial to systematically introduce mutations in the AL/ α- 21 helix region based on the observation that mutations in this region can have both gain of function and loss of function phenotypes (Wang et al., 2013). Certainly the Rpb9 residue S112, which hydrogen bonds with Rpb1-Q698 would be an excellent candidate to study, as it also pertains to our model and resides in an area of Rpb9 that was missing in a truncated form of Rpb9 that altered transcriptional start site selection (TSS) (Sun et al., 1996). As noted in Chapter I, TSS seems to be a common read-out for

TL defects. Knowing the effect of all of our *rpb9* or AL mutations on TSS would generally be useful information to have, given our interpretation of their function.

In Chapter III, it was also observed that the mutation *rpb9- (95-97)A* was not synthetic lethal with either TL mutants *rpb1-E1103G* or *-L1101S*, while the *rpb9- (1-59)* mutation was. As pointed out in the discussion of Chapter III, this could be an indication that there are additional functions in the C-terminal domain of Rpb9 beyond the TL-dependent role we have defined for it. Certainly, one aspect that we have not fully addressed is the effect of any of the Rpb9 or AL mutations on the extrinsic cleavage factor TFIIS. Indeed, in the crystal structure PDB 1Y1V (Kettenberger, 2003), TFIIS spatially is in close proximity to the AL and has a hydrogen bonding interaction at residue H706 in Rpb1. It would be interesting to see if, in addition for the role we suggest here for the AL, the AL also affects TFIIS function or association. Affecting TFIIS occupancy could in addition affect TL occupancy in the active site. This has previously been suggested to be the case for the TFIIS bacterial homolog GreA (Dangkulwanich et al., 2014; Roghanian et al., 2011). One simple and straightforward experiment would be to over-express TFIIS in the context of the Rpb9-(95-97)A variant or any of the AL mutants defined in this work. If the AL or the C-terminal of Rpb9 has any effect on TFIIS function we might predict that over expression of TFIIS would suppress some of the AL or Rpb9 C-terminal mutant phenotypes.

It is important to point out that this function of the Rpb9 C-terminal domain on TL function distinguishes it from its pol I and III counterparts. As discussed in the introduction, both C11 and A12.2, the pol I and III homologs, respectively, have C-

terminal domains more closely related to domain III of the pol II cleavage factor TFIIS (Cramer et al., 2008). This domain of TFIIS is responsible for displacing the TL and stimulating cleavage at the active site, as are the C-terminal domains of C11 and A12.2 (Alic et al., 2007; Kettenberger et al., 2004; Kuhn et al., 2007). From various structural studies and experiments from this work, we have shown that the Rpb9 C-terminal domain has a novel function in affecting TL mobility, rather than directly stimulating cleavage (Kettenberger et al., 2004; Ruan, 2011). This model of how the C-terminal domain of Rpb9 functions provides an explanation for the increase in transcriptional speed of pol II lacking Rpb9. In addition, as has been suggested for the bacterial counterpart of TFIIS (GreA) (Roghanian et al., 2011), we can also suggest a model of how Rpb9 C-terminal domain may affect the competition between TFIIS and the TL for active site occupancy through the AL. Rpb9, through the AL, would stabilize the open TL, which would balance the ability of TFIIS to gain access to the active site. Interestingly, it has been reported from our lab that Rpb9 does affect TFIIS-mediated transcript cleavage (Knippa and Peterson, 2013). Perhaps these results also reflect this balance between transcriptional speed through the TL, and cleavage through TFIIS.

It is interesting to consider why pol II depends on TFIIS for efficient removal of transcription errors, while pol I and pol III contain integral subunits that promote much more rapid proofreading (Alic et al., 2007; Kuhn et al., 2007). As described in Chapter I, pol I and III transcribe genes that are of limited variety, and, compared to pol II, they have a faster rate of elongation (refer to Table 1.1). This faster speed may make it advantageous for pol I and polIII to carry an endogenous means of transcript cleavage

rather than the remote, slower system utilized by pol II. In addition, in the case of pol III, the cleavage activity of C11 is specifically needed for transcription termination (Iben et al., 2011). This in contrast to pol II where the variety of templates and promoters might demand a more modular approach that would allow different types of regulatory molecules to interact with pol II depending on the context. The same argument could be made with various mRNAs that require pol II pausing or co-transcriptional processing. One specific example of this modular behavior may be present in the apparent competition between Bye1 and TFIIS described in Chapter IV, which is discussed further below.

Only within the last ~10 years has the C-terminal domain of Rpb9 been suggested to be important for Rpb9 function (Li et al., 2006). This is due in part to the original interpretation of MPA sensitivity being linked specifically to elongation rate, which for intrinsic TL mutations seems to be the case. However, from our work we see two very distinct types of MPA sensitivity derived from mutations in Rpb9, one derived from the N-terminal domain, the other from the C-terminal domain. The results shown in Fig. 3.3, as well as some reported by others (Hemming et al., 2000; Koyama, 2007; Li et al., 2006), have shown that the N-terminal residues [Rpb9- (1-59) in this work] are sufficient to suppress many of the growth and drug sensitivity phenotypes associated with *rpb9*Δ strains (which inadvertently makes the identification of C-terminal mutations very hard), and that functions of Rpb9 at the pol II active site seem to localize to the C-terminal domain (Koyama, 2007; Koyama et al., 2010; Li et al., 2006). This, as pointed out in Chapter III, makes the MPA sensitivity of *rpb9- (95-97)A* unique. However, even

though the N-terminal domain seems important for many of the phenotypes of *rpb9*Δ, currently its mechanistic details remain unclear. Even less is known concerning the genetic interactions between Rpb9 and a variety of non-polymerase subunits of chromatin modifying complexes (Table 4.1). In Chapter IV, I attempted to elucidate a role for Rpb9 in terms of the chromatin modifying complexes, and suggested that they seem to be related to the N-terminal domain of Rpb9.

To probe the question of these genetic interactions between *RPB9* and the genes in Table 4.1, we asked what structural portion of Rpb9 is able to rescue the synthetic lethality associated with the combination of *rpb9*Δ and the loss of each of these genes. We initially began our investigation with *HTZ1*, *SPT7*, and *GCN5*. As seen in Chapter IV, the first 59 amino acids of Rpb9 were sufficient to suppress the synthetic lethality, suggesting that the N-terminal domain of Rpb9 was important for the function of the H2A.Z variant (*HTZ1*) or SAGA complex components (*GCN5* and *SPT7*). Further analysis revealed that C-terminal alterations in Rpb9, specifically the (95-97)A variant, differentially interacted with these mutations. In the case of *htz1*Δ *rpb9-(95-97)A* mutant strain, we observed a double mutant phenotype which was worse than either *htz1*Δ or *rpb9- (95-97)A* alone on rich media. This might be expected given that the synthetic lethality associated with the *htz1*Δ *rpb9Δ* double mutant is completely suppressed by the Rpb9 N-terminal domain (Rpb9- (1-59)), and that the N- and C-terminal functions of Rpb9 seem to be separable. In addition, deletion of *SWC5*, which encodes a structural component of the SWR1 complex, responsible for insertion of H2A.Z into nucleosomes, was similarly lethal with the loss of Rpb9. This lethality could also be rescued by the

presence of Rpb9- (1-59) and suggests that the interaction of Rpb9 with H2A.Z depends on the presence of H2A.Z in the nucleosome. The combination of *gcn5*Δ or *spt7*Δ with C-terminal *rpb9* mutants in contrast, were epistatic in some phenotypes, suggesting that any function of Rpb9 that is SAGA complex related may also be related to transcriptional speed and/or some other function of the Rpb9 C-terminal domain. As discussed previously, the interaction of Rpb9- (95-97)A and TFIIS, which directly interacts with the SAGA component Spt8 (Wery et al., 2004), remains unstudied. In addition, it would be interesting to know whether any component of the SWR1 complex makes contacts through Rpb9 directly. Perhaps this could be assayed initially through a Y2H screen.

N-terminal deletions in Rpb9 suggested that the first 11-16 amino acids are critical for cell viability in the absence of the selected chromatin-related genes. These residues localize to the same spatial region of the Rpb9 N-terminus, suggesting that there may be an intermediary that interacts with this region to allow communication between pol II (through the N-terminal domain of Rpb9 on the leading edge of the polymerase) and nucleosomes. One primary candidate for this intermediary is the transcription factor Bye1. Bye1 had been previously shown to bind to pol II through a TFIIS-like binding domain, which is unique given that it is the only other known protein in yeast which has this domain (Kinkelin et al., 2013; Pinskaya et al., 2014). Structurally, Bye1 contains a histone binding motif (PHD domain) and a less understood protein binding domain (SPOC domain). A recent crystal structure of Bye1 with pol II (Kinkelin et al., 2013), showed that Bye1 binds the Rpb1 jaw domain just above the N-terminal domain of

Rpb9, suggesting Rpb9 may affect Bye1 association with the polymerase and impact the progression of pol II through chromatin templates.

Preliminary experiments with *bye1*Δ demonstrated that the mutant phenotype was dependent on the presence of either Rpb9 or TFIIS. This is not surprising in terms of TFIIS, considering that the occupancy of Bye1 and TFIIS are most likely mutually exclusive, and competition for pol II binding between Bye1 and TFIIS has been proposed to be a function of Bye1 (Pinskaya et al., 2014; Wu et al., 2003). As pol II encounters a nucleosome, stalls, and is reactivated by TFIIS, it has been suggested that TFIIS must be displaced so that transcription can resume (Pinskaya et al., 2014). This raised the possibility that the competition between Bye1 and TFIIS indirectly affects the TL occupancy of the active site, given that domain III of TFIIS inserts into the active site, displacing the TL during cleavage (Kettenberger, 2003). This notion is somewhat supported by the negative interactions observed in Rpb9 N-terminal truncations in a *bye1*Δ background, and that in the Bye1/pol II crystal structure, the Bye1 TLD domain hydrogen bonds with the AL. Experiments that examine the phenotypes of C-terminal Rpb9 mutants with *bye1*Δ, as well as directly examining the effect of Rpb9 mutations on Bye1 binding to pol II, must be done. In addition, given the suggested competition of Bye1 and TFIIS, which may also depend on Rpb9 and/or the AL, it would interesting to see how Bye1 and Rpb9 C-terminal mutants affect RNA cleavage *in vitro*.

In addition to the possibility of a communication line between Rpb9 and chromatin via Bye1, it has been shown that the pol III Rpb9 homolog (C11) is important for association of the pol III termination factor C53/37 (Iben et al., 2011). This

termination factor is a paralog of the basal transcription for TFIIF in pol II. More importantly, the residues that are important for the hydrophobic binding surface in C11 are conserved in Rpb9 (and A12.2), three of which fall into the first 20 amino acids of Rpb9 (A12.2 as well). This was intriguing as a recent large-scale protein cross-linking analysis of a pol II/TFIIF complex revealed contacts between both large subunits of TFIIF and the same region of the Rpb9 N-terminal domain (Chen et al., 2010). Furthermore it has previously been documented that deletion of Rpb9 virtually eliminates TFIIF association with pol II *in vitro* (Ziegler et al., 2003). As described in Chapter IV, this suggested the possibility that the Rpb9 N-terminal domain (along with adjacent residues from Rpb1 and Rpb2) could mediate TFIIF interactions with pol II.

If this hypothesis is correct, it has several very important implications. First, if the Rpb9 N-terminal domain is important at least in part for TFIIF association, as has been suggested for the N-terminal domain of C11, then it could provide a link between the global association hub that is pol II, and many chromatin modifying complexes. These complexes, as pointed out in Chapter IV, either directly interact with TFIIF (Paf1) or are dependent on some upstream signal mediated by the presence of TFIIF at pol II (Rad6/Bre1). Second, Rpb9 could have an alternate pathway to modulate pol II catalytic activity given that TFIIF by itself, or synergistically with TFIIS, can affect the passage of pol II through pause sites and nucleosomal barriers, which is important for transcription efficiency (Ishibashi et al., 2014; Schweikhard et al., 2014). Lastly, TFIIF has been suggested to have a TL-independent role in TSS selection (Jin and Kaplan, 2015), perhaps providing a secondary path for Rpb9 to affect the selection of a TSS.

Certainly, there is evidence for this model already, as a study in which it was found that Rpb2 mutations in the area adjacent to the Rpb9 N-terminal domain residues that may be important for TFIIF binding, phenocopy certain TFIIF mutants which are deficient in pol II association (Kubicek et al., 2013). It will be very important for our lab to look at TFIIF/Rpb9 mutant combinations in the near future to test this model, which is important given its global implications in co-transcriptional pol II-associated complexes. If the Rpb9 N-terminal domain does affect TFIIF association, we could initially probe this by over-expressing both subunits of TFIIF in yeast (Tfg1/2) and observe whether or not the over-expression could suppress any of the phenotypes we have observed in the N-terminal domain of Rpb9. We could also couple these simple *in vivo* experiments with more detailed biochemical tests that observe TSS, such as a primer extension assays. This would allow us to observe whether or not the N-terminal domain can affect start site selection through a TL/Rpb9 C-terminal domain independent pathway.

In closing, presented above are potential future directions for the pol II subunit Rpb9. This body of work has described a role of the C-terminal domain in terms of the mobile active site domain, the TL. It will be interesting to see the forward progress of research on Rpb9, given the relatively minimal collection of data on its N-terminal structural functions. Four our lab, Rpb9 has been a remarkable tool to look into the function of pol II. Because it is non-essential, we can study the changes induced in pol II by its absence. In addition, we have seen that it reports on at least two different types of interactions—those in the active site, and those on the exterior of pol II. My hope is that this body of work has conveyed the significance of Rpb9 in the context of pol II.

REFERENCES

Aasland, R., Gibson, T.J., and Stewart, A.F. (1995). The PHD finger: implications for chromatin-mediated transcriptional regulation. Trends Biochem Sci *20*, 56-59.

Abbondanzieri, E.A., Greenleaf, W.J., Shaevitz, J.W., Landick, R., and Block, S.M. (2005). Direct observation of base-pair stepping by RNA polymerase. Nature *438*, 460-465.

Alic, N., Ayoub, N., Landrieux, E., Favry, E., Baudouin-Cornu, P., Riva, M., and Carles, C. (2007). Selectivity and proofreading both contribute significantly to the fidelity of RNA polymerase III transcription. Proc Natl Acad Sci U S A *104*, 10400-10405.

Archambault, J., Jansma, D.B., Kawasoe, J.H., Arndt, K.T., Greenblatt, J., and Friesen, J.D. (1998). Stimulation of transcription by mutations affecting conserved regions of RNA polymerase II. J Bacteriol *180*, 2590-2598.

Ariyoshi, M., and Schwabe, J.W. (2003). A conserved structural motif reveals the essential transcriptional repression function of Spen proteins and their role in developmental signaling. Genes Dev *17*, 1909-1920.

Arndt, K.T., Styles, C.A., and Fink, G.R. (1989). A suppressor of a HIS4 transcriptional defect encodes a protein with homology to the catalytic subunit of protein phosphatases. Cell *56*, 527-537.

Awrey, D.E., Weilbaecher, R.G., Hemming, S.A., Orlicky, S.M., Kane, C.M., Edwards, A.M. (1997). Transcription elongation through DNA arrest sites. A multistep process involving both RNA polymerase II subunit RPB9 and TFIIS Journal of Biological Chemistry *272*, 14747-14754.

Bai, L., Shundrovsky, A. and Wang, M.D. (2004). Sequence-dependent kinetic model for transcription elongation by RNA polymerase. Journal of Molecular Biology *344*, 335-349.

Bar-Nahum, G., Epshtein, V., Ruckenstein, A.E., Rafikov, R., Mustaev, A., and Nudler, E. (2005). A ratchet mechanism of transcription elongation and its control. Cell *120*, 183-193.

Batada, N.N., Westover, K.D., Bushnell, D.A., Levitt, M., and Kornberg, R.D. (2004). Diffusion of nucleoside triphosphates and role of the entry site to the RNA polymerase II active center. Proc Natl Acad Sci U S A *101*, 17361-17364.

Baudin, A., Ozier-Kalogeropoulos, O., Denouel, A., Lacroute, F., and Cullin, C. (1993). A simple and efficient method for direct gene deletion in Saccharomyces cerevisiae. Nucleic Acids Res *21*, 3329-3330.

Betz, J.L., Chang, M., Washburn, T.M., Porter, S.E., Mueller, C.L., and Jaehning, J.A. (2002). Phenotypic analysis of Paf1/RNA polymerase II complex mutations reveals connections to cell cycle regulation, protein synthesis, and lipid and nucleic acid metabolism. Mol Genet Genomics *268*, 272-285.

Bonnet, J., Wang, C.Y., Baptista, T., Vincent, S.D., Hsiao, W.C., Stierle, M., Kao, C.F., Tora, L., and Devys, D. (2014). The SAGA coactivator complex acts on the whole transcribed genome and is required for RNA polymerase II transcription. Genes Dev *28*, 1999-2012.

Borukhov, S., Sagitov, V., and Goldfarb, A. (1993). Transcript cleavage factors from E. coli. Cell *72*, 459-466.

Braberg, H., Jin, H., Moehle, E.A., Chan, Y.A., Wang, S., Shales, M., Benschop, J.J., Morris, J.H., Qiu, C., Hu, F., *et al.* (2013). From structure to systems: high-resolution, quantitative genetic analysis of RNA polymerase II. Cell *154*, 775-788.

Brachmann, C.B., Davies, A., Cost, G.J., Caputo, E., Li, J., Hieter, P., and Boeke, J.D. (1998). Designer deletion strains derived from Saccharomyces cerevisiae S288C: a useful set of strains and plasmids for PCR-mediated gene disruption and other applications. Yeast *14*, 115-132.

Breslow, D.K., Cameron, D.M., Collins, S.R., Schuldiner, M., Stewart-Ornstein, J., Newman, H.W., Braun, S., Madhani, H.D., Krogan, N.J., and Weissman, J.S. (2008). A comprehensive strategy enabling high-resolution functional analysis of the yeast genome. Nature methods *5*, 711-718.

Brueckner, F., Armache, K., Cheung, A., Damsma, C., Kettenberger, H., Lehmann, E., Sydow, J., Cramer, P. (2009). Structure-function studies of the RNA polymerase II elongation complex. Acta Crystallographica *D65*, 112-120.

Brueckner, F., and Cramer, P. (2008). Structural basis of transcription inhibition by alpha-amanitin and implications for RNA polymerase II translocation. Nat Struct Mol Biol *15*, 811-818.

Bucheli, M.E., and Buratowski, S. (2005). Npl3 is an antagonist of mRNA 3' end formation by RNA polymerase II. EMBO J *24*, 2150-2160.

Bucheli, M.E., He, X., Kaplan, C.D., Moore, C.L., and Buratowski, S. (2007). Polyadenylation site choice in yeast is affected by competition between Npl3 and polyadenylation factor CFI. RNA *13*, 1756-1764.

Burton, Z.F., Feig, M., Gong, X.Q., Zhang, C., Nedialkov, Y.A., and Xiong, Y. (2005). NTP-driven translocation and regulation of downstream template opening by multi-subunit RNA polymerases. Biochemistry and cell biology = Biochimie et biologie cellulaire *83*, 486-496.

Cabart, P., Jin, H., Li, L., and Kaplan, C.D. (2014). Activation and reactivation of the RNA polymerase II trigger loop for intrinsic RNA cleavage and catalysis. Transcription *5*, e28869.

Chedin, S., Riva, M., Schultz, P., Sentenac, A., and Carles, C. (1998). The RNA cleavage activity of RNA polymerase III is mediated by an essential TFIIS-like subunit and is important for transcription termination. Genes Dev *12*, 3857-3871.

Chen, X., Ruggiero, C., and Li, S. (2007). Yeast Rpb9 plays an important role in ubiquitylation and degradation of Rpb1 in response to UV-induced DNA damage. Mol Cell Biol *27*, 4617-4625.

Chen, Z.A., Jawhari, A., Fischer, L., Buchen, C., Tahir, S., Kamenski, T., Rasmussen, M., Lariviere, L., Bukowski-Wills, J.C., Nilges, M., *et al.* (2010). Architecture of the RNA polymerase II-TFIIF complex revealed by cross-linking and mass spectrometry. EMBO J *29*, 717-726.

Cheung, A.C., and Cramer, P. (2011). Structural basis of RNA polymerase II backtracking, arrest and reactivation. Nature *471*, 249-253.

Conaway, J.W.C.a.R.C. (2000). Light at the End of the Channel. Science *288*, 632-633
Costa, P.J., and Arndt, K.M. (2000). Synthetic lethal interactions suggest a role for the Saccharomyces cerevisiae Rtf1 protein in transcription elongation. Genetics *156*, 535-547.

Cramer, P. (2002). Multisubunit RNA polymerases Curr Opin Struct Biol *12*, 89-97.
Cramer, P., Armache, K.J., Baumli, S., Benkert, S., Brueckner, F., Buchen, C., Damsma, G.E., Dengl, S., Geiger, S.R., Jasiak, A.J., *et al.* (2008). Structure of eukaryotic RNA polymerases. Annual review of biophysics *37*, 337-352.

Dangkulwanich, M., Ishibashi, T., Bintu, L., and Bustamante, C. (2014). Molecular mechanisms of transcription through single-molecule experiments. Chemical reviews *114*, 3203-3223.

Duan, R., Rhie, B.H., Ryu, H.Y., and Ahn, S.H. (2013). The RNA polymerase II Rpb4/7 subcomplex regulates cellular lifespan through an mRNA decay process. Biochem Biophys Res Commun.

Erie, D.A., Hajiseyedjavadi, O., Young, M.C., von Hippel, P.H. (1993). Multiple RNA polymerase conformations and Gre A: control of the fidelity of transcription. Science *262*, 867-873.

Fernandez-Tornero, C., Moreno-Morcillo, M., Rashid, U.J., Taylor, N.M., Ruiz, F.M., Gruene, T., Legrand, P., Steuerwald, U., and Muller, C.W. (2013). Crystal structure of the 14-subunit RNA polymerase I. Nature *502*, 644-649.

Fish, R.N., and Kane, C.M. (2002). Promoting elongation with transcript cleavage stimulatory factors. Biochim Biophys Acta *1577*, 287-307.

Garcia-Oliver, E., Garcia-Molinero, V., and Rodriguez-Navarro, S. (2012). mRNA export and gene expression: The SAGA-TREX-2 connection. Biochim Biophys Acta *1819*, 555-565.

Ghazy, M.A., Brodie, S.A., Ammerman, M.L., Ziegler, L.M., and Ponticelli, A.S. (2004). Amino acid substitutions in yeast TFIIF confer upstream shifts in transcription initiation and altered interaction with RNA polymerase II. Mol Cell Biol *24*, 10975-10985.

Gibney, P.A., Fries, T., Bailer, S.M., and Morano, K.A. (2008). Rtr1 is the Saccharomyces cerevisiae homolog of a novel family of RNA polymerase II-binding proteins. Eukaryot Cell *7*, 938-948.

Gnatt, A.L., Cramer, P., Fu, J., Bushnell, D.A., and Kornberg, R.D. (2001). Structural basis of transcription: an RNA polymerase II elongation complex at 3.3 A resolution. Science *292*, 1876-1882.

Grant, P.A., Duggan, L., Cote, J., Roberts, S.M., Brownell, J.E., Candau, R., Ohba, R., Owen-Hughes, T., Allis, C.D., Winston, F., *et al.* (1997). Yeast Gcn5 functions in two multisubunit complexes to acetylate nucleosomal histones: characterization of an Ada complex and the SAGA (Spt/Ada) complex. Genes Dev *11*, 1640-1650.

Greger, I.H., Aranda, A., and Proudfoot, N. (2000). Balancing transcriptional interference and initiation on the GAL7 promoter of Saccharomyces cerevisiae. Proc Natl Acad Sci U S A *97*, 8415-8420.

Greger, I.H., and Proudfoot, N.J. (1998). Poly(A) signals control both transcriptional termination and initiation between the tandem GAL10 and GAL7 genes of Saccharomyces cerevisiae. EMBO J *17*, 4771-4779.

Hampsey, M. (1998). Molecular Genetics of the RNA Polymerase II General Transcriptional Machinery. Microbiology and Molecular Biology Reviews *62*, 465–503.

Hani, J., Stumpf, G., and Domdey, H. (1995). Ptf1 Encodes an Essential Protein in Saccharomyces-Cerevisiae, Which Shows Strong Homology with a New Putative Family of Ppiases. Febs Lett *365*, 198-202.

Hausner, W., Lange, U., and Musfeldt, M. (2000). Transcription factor S, a cleavage induction factor of the archaeal RNA polymerase. J Biol Chem *275*, 12393-12399.

Hemming, S.A., and Edwards, A.M. (2000). Yeast RNA polymerase II subunit RPB9. Mapping of domains required for transcription elongation. J Biol Chem *275*, 2288-2294.

Hemming, S.A., Jansma, D.B., Macgregor, P.F., Goryachev, A., Friesen, J.D., and Edwards, A.M. (2000). RNA polymerase II subunit Rpb9 regulates transcription elongation in vivo. J Biol Chem *275*, 35506-35511.

Hull, M.W., McKune, K., and Woychik, N.A. (1995). RNA polymerase II subunit RPB9 is required for accurate start site selection. Genes Dev *9*, 481-490.

Hyle, J.W., Shaw, R.J., and Reines, D. (2003). Functional distinctions between IMP dehydrogenase genes in providing mycophenolate resistance and guanine prototrophy to yeast. J Biol Chem *278*, 28470-28478.

Iben, J.R., Mazeika, J.K., Hasson, S., Rijal, K., Arimbasseri, A.G., Russo, A.N., and Maraia, R.J. (2011). Point mutations in the Rpb9-homologous domain of Rpc11 that impair transcription termination by RNA polymerase III. Nucleic Acids Res *39*, 6100-6113.

Ingvarsdottir, K., Krogan, N.J., Emre, N.C., Wyce, A., Thompson, N.J., Emili, A., Hughes, T.R., Greenblatt, J.F., and Berger, S.L. (2005). H2B ubiquitin protease Ubp8 and Sgf11 constitute a discrete functional module within the Saccharomyces cerevisiae SAGA complex. Mol Cell Biol *25*, 1162-1172.

Ishibashi, T., Dangkulwanich, M., Coello, Y., Lionberger, T.A., Lubkowska, L., Ponticelli, A.S., Kashlev, M., and Bustamante, C. (2014). Transcription factors IIS and IIF enhance transcription efficiency by differentially modifying RNA polymerase pausing dynamics. Proc Natl Acad Sci U S A *111*, 3419-3424.

Izban, M.G.a.L., D.S. (1993). The increment of SII-fascilitated transcript cleavage varies dramatically between elongation competent and incompetent RNA polymerase II ternary complexes. Journal of Biological Chemistry *268*, 12874-12885.

Izban, M.G.a.L., D.S. (1992). The RNA polymerase II ternary complex cleaves the nascent transcript in a 3' to 5' direction in the presence of elongation factor SII. Genes and Development *6*, 1342-1356.

Jensen, K., Santisteban, M.S., Urekar, C., and Smith, M.M. (2011). Histone H2A.Z acid patch residues required for deposition and function. Mol Genet Genomics *285*, 287-296.

Jimeno, S., Tous, C., Garcia-Rubio, M.L., Ranes, M., Gonzalez-Aguilera, C., Marin, A., and Aguilera, A. (2011). New suppressors of THO mutations identify Thp3 (Ypr045c)-Csn12 as a protein complex involved in transcription elongation. Mol Cell Biol *31*, 674-685.

Jin, H.Y., and Kaplan, C.D. (2015). Relationships of RNA Polymerase II Genetic Interactors to Transcription Start Site Usage Defects and Growth in Saccharomyces cerevisiae. G3-Genes Genom Genet *5*, 21-33.

Jin, J., Bai, L., Johnson, D.S., Fulbright, R.M., Kireeva, M.L., Kashlev, M., Wang, M.D. (2011). Synergistic action of RNA polymerases in overcoming the nucleosomal barrier. Nature Structural & Molecular Biology *17*, 745-752.

Jonas, S., and Izaurralde, E. (2015). Towards a molecular understanding of microRNA-mediated gene silencing. Nature reviews Genetics *16*, 421-433.

Kapitzky, L., Beltrao, P., Berens, T.J., Gassner, N., Zhou, C., Wuster, A., Wu, J., Babu, M.M., Elledge, S.J., Toczyski, D., *et al.* (2010). Cross-species chemogenomic profiling reveals evolutionarily conserved drug mode of action. Molecular systems biology *6*, 451.

Kaplan, C.D. (2010). The architecture of RNA polymerase fidelity. BMC Biology *8*, 85.

Kaplan, C.D., Holland, M.J., and Winston, F. (2005). Interaction between transcription elongation factors and mRNA 3'-end formation at the Saccharomyces cerevisiae GAL10-GAL7 locus. J Biol Chem *280*, 913-922.

Kaplan, C.D., Jin, H., Zhang, I.L., and Belyanin, A. (2012). Dissection of Pol II trigger loop function and Pol II activity-dependent control of start site selection in vivo. PLoS Genet *8*, e1002627.

Kaplan, C.D., Larsson, K., Kornberg, R.D. (2008). The RNA Polymerase II Trigger Loop Functions in Substrate Selection and Is Directly Targeted by α-Amanitin. Molecular Cell *30*, 547-556.

Kettenberger, H., Armache, K.J., and Cramer, P. (2004). Complete RNA polymerase II elongation complex structure and its interactions with NTP and TFIIS. Mol Cell *16*, 955-965.

Kettenberger, H., Armache, K., and Cramer, P. (2003). Complete RNA polymerase II elongation complex structure and its interactions with NTP and TFIIS. Molecular Cell *114*, 347-257.

Khaperskyy, D.A., Ammerman, M.L., Majovski, R.C., and Ponticelli, A.S. (2008). Functions of Saccharomyces cerevisiae TFIIF during transcription start site utilization. Mol Cell Biol *28*, 3757-3766.

Kim, B., Nesvizhskii, A.I., Rani, P.G., Hahn, S., Aebersold, R., and Ranish, J.A. (2007). The transcription elongation factor TFIIS is a component of RNA polymerase II preinitiation complexes. Proc Natl Acad Sci U S A *104*, 16068-16073.

Kinkelin, K., Wozniak, G.G., Rothbart, S.B., Lidschreiber, M., Strahl, B.D., and Cramer, P. (2013). Structures of RNA polymerase II complexes with Bye1, a chromatin-binding PHF3/DIDO homologue. Proc Natl Acad Sci U S A *110*, 15277-15282.

Kireeva, M.L., Hancock, B., Cremona, G.H., Walter, W., Studitsky, V.M., and Kashlev, M. (2005). Nature of the nucleosomal barrier to RNA polymerase II. Mol Cell *18*, 97-108.

Kireeva, M.L., Lubkowska, L., Komissarova, N., and Kashlev, M. (2003). Assays and affinity purification of biotinylated and nonbiotinylated forms of double-tagged core RNA polymerase II from Saccharomyces cerevisiae. Methods Enzymol *370*, 138-155.

Kireeva, M.L., Nedialkov, Y.A., Cremona, G.H., Purtov, Y.A., Lubkowska, L., Malagon, F., Burton, Z.F., Strathern, J.N., and Kashlev, M. (2008). Transient reversal of RNA polymerase II active site closing controls fidelity of transcription elongation. Mol Cell *30*, 557-566.

Kireeva, M.L., Opron, K., Seibold, S.A., Domecq, C., Cukier, R.I., Coulombe, B., Kashlev, M., and Burton, Z.F. (2012). Molecular dynamics and mutational analysis of the catalytic and translocation cycle of RNA polymerase. BMC biophysics *5*, C.

Knippa, K., and Peterson, D.O. (2013). Fidelity of RNA polymerase II transcription: Role of Rbp9 in error detection and proofreading. Biochemistry *52*, 7807-7817.

Koyama, H., Ito, T., Nakanishi, T., Kawamura, N., Sekimizu, K. (2003). Transcription elongation factor S-II maintains transcriptional fidelity and confers oxidative stress resistance Genes to Cells *8*, 779-788.

Koyama, H., Ito, T., Nakanishi, T., Kawamura, N., Sekimizu, K. (2007). Stimulation of RNA polymerase II transcript cleavage activity contributes to maintain transcriptional fidelity in yeast Genes to Cells *12*, 547-559.

Koyama, H., Ueda, T., Ito, T., and Sekimizu, K. (2010). Novel RNA polymerase II mutation suppresses transcriptional fidelity and oxidative stress sensitivity in rpb9Delta yeast. Genes Cells *15*, 151-159.

Krogan, N.J., Dover, J., Wood, A., Schneider, J., Heidt, J., Boateng, M.A., Dean, K., Ryan, O.W., Golshani, A., Johnston, M., *et al.* (2003). The Paf1 complex is required for histone H3 methylation by COMPASS and Dot1p: linking transcriptional elongation to histone methylation. Mol Cell *11*, 721-729.

Krogan, N.J., Kim, M., Ahn, S.H., Zhong, G., Kobor, M.S., Cagney, G., Emili, A., Shilatifard, A., Buratowski, S., and Greenblatt, J.F. (2002). RNA polymerase II elongation factors of Saccharomyces cerevisiae: a targeted proteomics approach. Mol Cell Biol *22*, 6979-6992.

Kubicek, C.E., Chisholm, R.D., Takayama, S., and Hawley, D.K. (2013). RNA polymerase II mutations conferring defects in poly(A) site cleavage and termination in Saccharomyces cerevisiae. G3 *3*, 167-180.

Kuhn, C.D., Geiger, S.R., Baumli, S., Gartmann, M., Gerber, J., Jennebach, S., Mielke, T., Tschochner, H., Beckmann, R., and Cramer, P. (2007). Functional architecture of RNA polymerase I. Cell *131*, 1260-1272.

Kulish, D.a.S., K. (2001). TFIIS enhances transcriptional elongation through an artificial site *in vivo* Molecular Cell Biology *21*, 4162-4168.

Lange, U., and Hausner, W. (2004). Transcriptional fidelity and proofreading in Archaea and implications for the mechanism of TFS-induced RNA cleavage. Molecular microbiology *52*, 1133-1143.

Larson, M.H., Zhou, J., Kaplan, C.D., Palangat, M., Kornberg, R.D., Landick, R., and Block, S.M. (2012). Trigger loop dynamics mediate the balance between the transcriptional fidelity and speed of RNA polymerase II. Proc Natl Acad Sci U S A *109*, 6555-6560.

Lee, J.H., and Skalnik, D.G. (2012). Rbm15-Mkl1 interacts with the Setd1b histone H3-Lys4 methyltransferase via a SPOC domain that is required for cytokine-independent proliferation. PLoS One *7*, e42965.

Lee, K.K., Sardiu, M.E., Swanson, S.K., Gilmore, J.M., Torok, M., Grant, P.A., Florens, L., Workman, J.L., and Washburn, M.P. (2011). Combinatorial depletion analysis to assemble the network architecture of the SAGA and ADA chromatin remodeling complexes. Molecular systems biology *7*, 503.

Li, S., Ding, B., Chen, R., Ruggiero, C., and Chen, X. (2006). Evidence that the transcription elongation function of Rpb9 is involved in transcription-coupled DNA repair in Saccharomyces cerevisiae. Mol Cell Biol *26*, 9430-9441.

Liu, N., Peterson, C.L., Hayes, J.J. (2011). Swi/Snf- and RSC- Catalyzed Nucleosome Mobilization Requires Internal DNA Loop Transclocation within Nucleosome. Molecular and Cellular BIology *31*, 4165-4175.

Malagon, F., Kireeva, M.L., Shafer, B.K., Lubkowska, L., Kashlev, M., and Strathern, J.N. (2006). Mutations in the Saccharomyces cerevisiae RPB1 gene conferring hypersensitivity to 6-azauracil. Genetics *172*, 2201-2209.

Martinez-Rucobo, F.W., and Cramer, P. (2013). Structural basis of transcription elongation. Biochim Biophys Acta *1829*, 9-19.

Mason, P.B., and Struhl, K. (2005). Distinction and relationship between elongation rate and processivity of RNA polymerase II in vivo. Mol Cell *17*, 831-840.

Matsuzaki, H., Kassavetis, G.A., and Geiduschek, E.P. (1994). Analysis of RNA chain elongation and termination by Saccharomyces cerevisiae RNA polymerase III. J Mol Biol *235*, 1173-1192.

McKune, K., Moore, P.A., Hull, M.W., and Woychik, N.A. (1995). Six human RNA polymerase subunits functionally substitute for their yeast counterparts. Mol Cell Biol *15*, 6895-6900.

McKune, K., P. A. Moore, M. W. Hull, and N. A. Woychik. (1995). Six human RNA polymerase subunits functionally substitute for their yeast counterparts. Mol Cell Biol *15*, 6895–6900.

Mejia, Y.X., Nudler, E., and Bustamante, C. (2015). Trigger loop folding determines transcription rate of Escherichia coli's RNA polymerase. Proc Natl Acad Sci U S A *112*, 743-748.

Milgrom, E., West, R.W., Jr., Gao, C., and Shen, W.C. (2005). TFIID and Spt-Ada-Gcn5-acetyltransferase functions probed by genome-wide synthetic genetic array analysis using a Saccharomyces cerevisiae taf9-ts allele. Genetics *171*, 959-973.

Mizuguchi, G., Shen, X., Landry, J., Wu, W.H., Sen, S., and Wu, C. (2004). ATP-driven exchange of histone H2AZ variant catalyzed by SWR1 chromatin remodeling complex. Science *303*, 343-348.

Morris, D.P., Phatnani, H.P., and Greenleaf, A.L. (1999). Phospho-carboxyl-terminal domain binding and the role of a prolyl isomerase in pre-mRNA 3'-End formation. J Biol Chem *274*, 31583-31587.

Morris, K.V., and Mattick, J.S. (2014). The rise of regulatory RNA. Nature reviews Genetics *15*, 423-437.

Mullenders, L. (2015). DNA damage mediated transcription arrest: Step back to go forward. DNA repair.

Nesser, N.K., Peterson, D.O., and Hawley, D.K. (2006). RNA polymerase II subunit Rpb9 is important for transcriptional fidelity in vivo. Proc Natl Acad Sci U S A *103*, 3268-3273.

Opalka, N., Chlenov, M., Chacon, P., Rice, W.J., Wriggers, W., and Darst, S.A. (2003). Structure and function of the transcription elongation factor GreB bound to bacterial RNA polymerase. Cell *114*, 335-345.

Orphanides, G.a.R., D. (2000). RNA polymerase II elongation through chromatin. Nature *407*, 471-475.

Pascual-Garcia, P., Govind, C.K., Queralt, E., Cuenca-Bono, B., Llopis, A., Chavez, S., Hinnebusch, A.G., and Rodriguez-Navarro, S. (2008). Sus1 is recruited to coding regions and functions during transcription elongation in association with SAGA and TREX2. Genes Dev *22*, 2811-2822.

Pinskaya, M., Ghavi-Helm, Y., Mariotte-Labarre, S., Morillon, A., Soutourina, J., and Werner, M. (2014). PHD and TFIIS-Like domains of the Bye1 transcription factor determine its multivalent genomic distribution. PLoS One *9*, e102464.

Pokholok, D.K., Hannett, N.M., and Young, R.A. (2002). Exchange of RNA polymerase II initiation and elongation factors during gene expression in vivo. Mol Cell *9*, 799-809.

Qian, X.Q., Jeon, C.J., Yoon, H.S., Agarwal, K., and Weiss, M.A. (1993). Structure of a New Nucleic-Acid-Binding Motif in Eukaryotic Transcriptional Elongation-Factor Tfiis. Nature *365*, 277-279.

Reins, D., Conaway, R.C., Conaway, J.W. (1999). Mechanism and regulation of transcriptional elongation by RNA polymerase II. Current Opinion in Cell Biology *11*, 342-346.

Rodriguez-Navarro, S. (2009). Insights into SAGA function during gene expression. EMBO reports *10*, 843-850.

Roghanian, M., Yuzenkova, Y., and Zenkin, N. (2011). Controlled interplay between trigger loop and Gre factor in the RNA polymerase active centre. Nucleic Acids Res *39*, 4352-4359.

Roth, S.Y., Denu, J.M., Alls, C.D. (2001). Histone acetyltransferases. . Annual Review Biochemistry *70*, 81-120.

Ruan, W., Lehmann, E., Thomm, M., Kostrewa, D., Cramer, P. (2011). Evolution of two modes of intrinsic RNA polymerase transcript cleavage. Journal of Biological Chemistry *286*, 18701–18707.

Santisteban, M.S., Hang, M., and Smith, M.M. (2011). Histone variant H2A.Z and RNA polymerase II transcription elongation. Mol Cell Biol *31*, 1848-1860.

Santisteban, M.S., Kalashnikova, T., and Smith, M.M. (2000). Histone H2A.Z regulats transcription and is partially redundant with nucleosome remodeling complexes. Cell *103*, 411-422.

Saxowsky, T.T.a.D., P.W. (2006). RNA polymerase encounters with DNA damage: transcription-coupled repair or transcriptional mutagenesis? Chemistry Review *106*, 474-488.

Schweikhard, V., Meng, C., Murakami, K., Kaplan, C.D., Kornberg, R.D., and Block, S.M. (2014). Transcription factors TFIIF and TFIIS promote transcript elongation by RNA polymerase II by synergistic and independent mechanisms. Proc Natl Acad Sci U S A *111*, 6642-6647.

Sen, R., Lahudkar, S., Durairaj, G., and Bhaumik, S.R. (2013). Functional analysis of Bre1p, an E3 ligase for histone H2B ubiquitylation, in regulation of RNA polymerase II association with active genes and transcription in vivo. J Biol Chem *288*, 9619-9633.

Shandilya, J., Wang, Y., and Roberts, S.G. (2012). TFIIB dephosphorylation links transcription inhibition with the p53-dependent DNA damage response. Proc Natl Acad Sci U S A *109*, 18797-18802.

Shaw, R.J., Bonawitz, N.D., and Reines, D. (2002). Use of an in vivo reporter assay to test for transcriptional and translational fidelity in yeast. J Biol Chem *277*, 24420-24426.

Sigurdsson, S., Dirac-Svejstrup, A.B., and Svejstrup, J.Q. (2010). Evidence that transcript cleavage is essential for RNA polymerase II transcription and cell viability. Mol Cell *38*, 202-210.

Simchen, G., Winston, F., Styles, C.A., and Fink, G.R. (1984). Ty-mediated gene expression of the LYS2 and HIS4 genes of Saccharomyces cerevisiae is controlled by the same SPT genes. Proc Natl Acad Sci U S A *81*, 2431-2434.

Sosunov, V., Sosunova, E., Mustaev, A., Bass, I., Nikiforov, V., and Goldfarb, A. (2003). Unified two-metal mechanism of RNA synthesis and degradation by RNA polymerase. EMBO J *22*, 2234-2244.

Spencer, J.F.T., Spencer, D.M., and Bruce, I.J. (1989). Yeast Genetics: A Manual of Methods (Berlin: Springer-Verlag).

Sterner, D.E., Grant, P.A., Roberts, S.M., Duggan, L.J., Belotserkovskaya, R., Pacella, L.A., Winston, F., Workman, J.L., and Berger, S.L. (1999). Functional organization of the yeast SAGA complex: distinct components involved in structural integrity, nucleosome acetylation, and TATA-binding protein interaction. Mol Cell Biol *19*, 86-98.

Sun, Z.W., Tessmer, A., and Hampsey, M. (1996). Functional interaction between TFIIB and the Rpb9 (Ssu73) subunit of RNA polymerase II in Saccharomyces cerevisiae. Nucleic Acids Res *24*, 2560-2566.

Svetlov, V., Vassylyev, D.G., Artsimovitch, I. (2004). Descrimination against deoxyribonucleotide substrates by bacterial RNA polymerase. Journal of Biological Chemistry *279*, 38087-38090.

Sydow, J.F., Brueckner, F., Cheung, A.C., Damsma, G.E., Dengl, S., Lehmann, E., Vassylyev, D., Cramer, P. (2009a). Structural basis of transcription: mismatch-specific fidelity mechanims and paused RNA polymerase II with frayed RNA. Molecular Cell *34*, 710-721.

Sydow, J.F.a.C., P. (2009b). RNA polymerase fidelity and transcriptional proofreading Current Opinion in Structural Biology *19*, 732-739.

Thomas, M.J., Platas, A.A., Hawley, D. K. (1998). Transcripional fidelity and proofreading by RNA polymerase II. Cell *93*, 627-637.

Tong, A.H., Lesage, G., Bader, G.D., Ding, H., Xu, H., Xin, X., Young, J., Berriz, G.F., Brost, R.L., Chang, M., *et al.* (2004). Global mapping of the yeast genetic interaction network. Science *303*, 808-813.

Toulokhonov, I., Zhang, J., Palangat, M., and Landick, R. (2007). A central role of the RNA polymerase trigger loop in active-site rearrangement during transcriptional pausing. Mol Cell *27*, 406-419.

Tous, C., Rondon, A.G., Garcia-Rubio, M., Gonzalez-Aguilera, C., Luna, R., and Aguilera, A. (2011). A novel assay identifies transcript elongation roles for the Nup84 complex and RNA processing factors. EMBO J *30*, 1953-1964.

Turowski, T.W., and Tollervey, D. (2015). Cotranscriptional events in eukaryotic ribosome synthesis. Wiley interdisciplinary reviews RNA *6*, 129-139.

van Leeuwen, F.W., Fischer, D.F., Benne, R., and Hol, E.M. (2000). Molecular misreading. A new type of transcript mutation in gerontology. Ann N Y Acad Sci *908*, 267-281.

Van Mullem, V., Wery, M., Werner, M., Vandenhaute, J., and Thuriaux, P. (2002). The Rpb9 subunit of RNA polymerase II binds transcription factor TFIIE and interferes with the SAGA and elongator histone acetyltransferases. J Biol Chem *277*, 10220-10225.

Vassylyev, D.G., Vassylyev, M.N., Zhang, J., Palangat, M., Artsimovitch, I., Landick, R. (2007). Structural basis for substrate loading in bacterial polymerase. Nature *448*, 163-168.

Viktorovskaya, O.V., Engel, K.L., French, S.L., Cui, P., Vandeventer, P.J., Pavlovic, E.M., Beyer, A.L., Kaplan, C.D., and Schneider, D.A. (2013). Divergent contributions of conserved active site residues to transcription by eukaryotic RNA polymerases I and II. Cell Rep *4*, 974-984.

Wade, P.A., and Jaehning, J.A. (1996). Transcriptional corepression in vitro: a Mot1p-associated form of TATA-binding protein is required for repression by Leu3p. Mol Cell Biol *16*, 1641-1648.

Wade, P.A., Werel, W., Fentzke, R.C., Thompson, N.E., Leykam, J.F., Burgess, R.R., Jaehning, J.A., and Burton, Z.F. (1996). A novel collection of accessory factors associated with yeast RNA polymerase II. Protein expression and purification *8*, 85-90.

Walmacq, C., Cheung, A.C., Kireeva, M.L., Lubkowska, L., Ye, C., Gotte, D., Strathern, J.N., Carell, T., Cramer, P., and Kashlev, M. (2012). Mechanism of translesion transcription by RNA polymerase II and its role in cellular resistance to DNA damage. Mol Cell *46*, 18-29.

Walmacq, C., Kireeva, M.L., Irvin, J., Nedialkov, Y., Lubkowska, L., Malagon, F., Strathern, J.N., and Kashlev, M. (2009). Rpb9 subunit controls transcription fidelity by delaying NTP sequestration in RNA polymerase II. J Biol Chem *284*, 19601-19612.

Wan, Y., Saleem, R.A., Ratushny, A.V., Roda, O., Smith, J.J., Lin, C.H., Chiang, J.H., and Aitchison, J.D. (2009). Role of the histone variant H2A.Z/Htz1p in TBP

recruitment, chromatin dynamics, and regulated expression of oleate-responsive genes. Mol Cell Biol *29*, 2346-2358.

Wang, B., Opron, K., Burton, Z.F., Cukier, R.I., and Feig, M. (2015). Five checkpoints maintaining the fidelity of transcription by RNA polymerases in structural and energetic details. Nucleic Acids Res *43*, 1133-1146.

Wang, B., Predeus, A.V., Burton, Z.F., and Feig, M. (2013). Energetic and structural details of the trigger-loop closing transition in RNA polymerase II. Biophysical journal *105*, 767-775.

Wang, D., Bushnell, D., Westover, K., Kaplan, C., and Kornberg, R. (2006). Structural basis of transcription: role of the trigger loop in substrate specificity and catalysis. Cell *127*, 941-954.

Wang, D.a.H., D.K. (1993). Identification of a 3' to 5' exonuclease activity associated with human RNA polymerase II. PNAS *90*, 843-847.

Watson, J.D., and Crick, F.H. (1953). Molecular structure of nucleic acids; a structure for deoxyribose nucleic acid. Nature *171*, 737-738.

Wery, M., Shematorova, E., Van Driessche, B., Vandenhaute, J., Thuriaux, P., and Van Mullem, V. (2004). Members of the SAGA and Mediator complexes are partners of the transcription elongation factor TFIIS. EMBO J *23*, 4232-4242.

Westover, K.D., Bushnell, D.A., and Kornberg, R.D. (2004). Structural basis of transcription: nucleotide selection by rotation in the RNA polymerase II active center. Cell *119*, 481-489.

Woychik, N.A., and R. A. Young, ed. (1994). Exploring RNA polymerase II structure and function (New York Raven Press).

Woychik, N.A., Liao, S.M., Kolodziej, P.A., and Young, R.A. (1990). Subunits shared by eukaryotic nuclear RNA polymerases. Genes Dev *4*, 313-323.

Wu, X., Rossettini, A., and Hanes, S.D. (2003). The ESS1 prolyl isomerase and its suppressor BYE1 interact with RNA pol II to inhibit transcription elongation in Saccharomyces cerevisiae. Genetics *165*, 1687-1702.

Wyce, A., Xiao, T., Whelan, K.A., Kosman, C., Walter, W., Eick, D., Hughes, T.R., Krogan, N.J., Strahl, B.D., and Berger, S.L. (2007). H2B ubiquitylation acts as a barrier to Ctk1 nucleosomal recruitment prior to removal by Ubp8 within a SAGA-related complex. Mol Cell *27*, 275-288.

Young, R.A. (1991). RNA polymerase II. Annu Rev Biochem *60*, 689–715.
Zhang, G.C., EA ; Minakhin, L ; Richter, C ; Severinov, K ; Darst, SA (1999). Crystal structure of Thermus aquaticus core RNA polymerase at 3.3 angstrom resolution. Cell *98*, 811.

Ziegler, L.M., Khaperskyy, D.A., Ammerman, M.L., and Ponticelli, A.S. (2003). Yeast RNA polymerase II lacking the Rpb9 subunit is impaired for interaction with transcription factor IIF. J Biol Chem *278*, 48950-48956.

APPENDIX

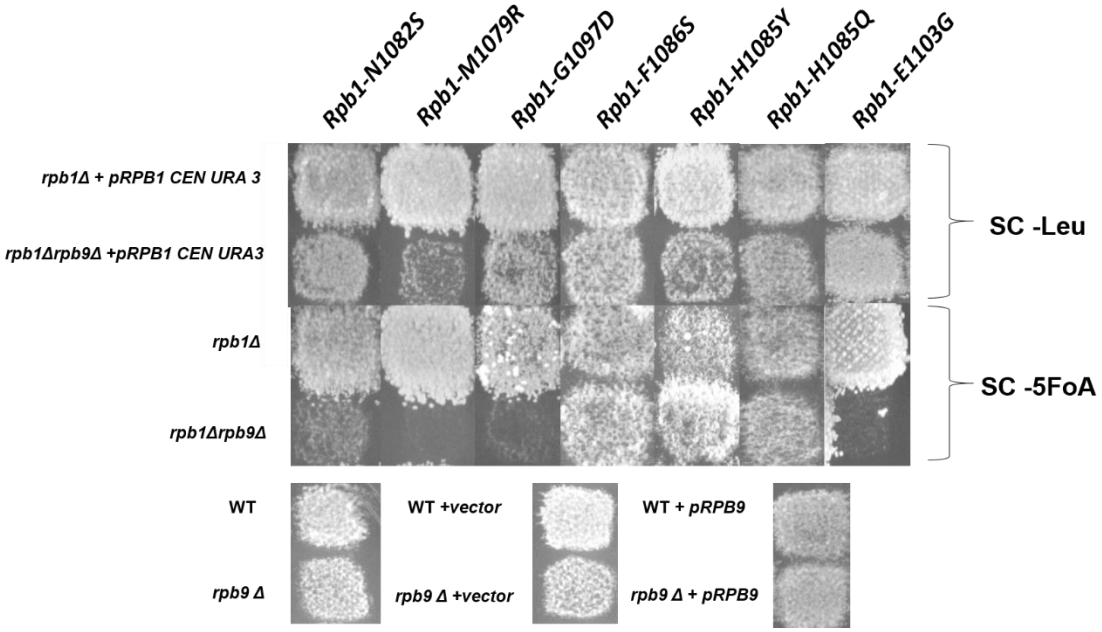

Figure A.1: Interactions of Trigger Loop mutants and *rpb9Δ*

Yeast strains lacking genomic RPB1 and RPB9 are supplemented with *RPB1* on a *URA3* marked plasmid. Strains are then transformed with varying alleles of *RPB1* with mutations in various areas of the TL on a *LEU2* marked plasmid. If selected TL mutations are lethal with the loss of Rpb9, then cells with be forced to maintain the *RPB1 CEN URA3* plasmid. Plating of these cells to 5-FOA will then result in cell death.

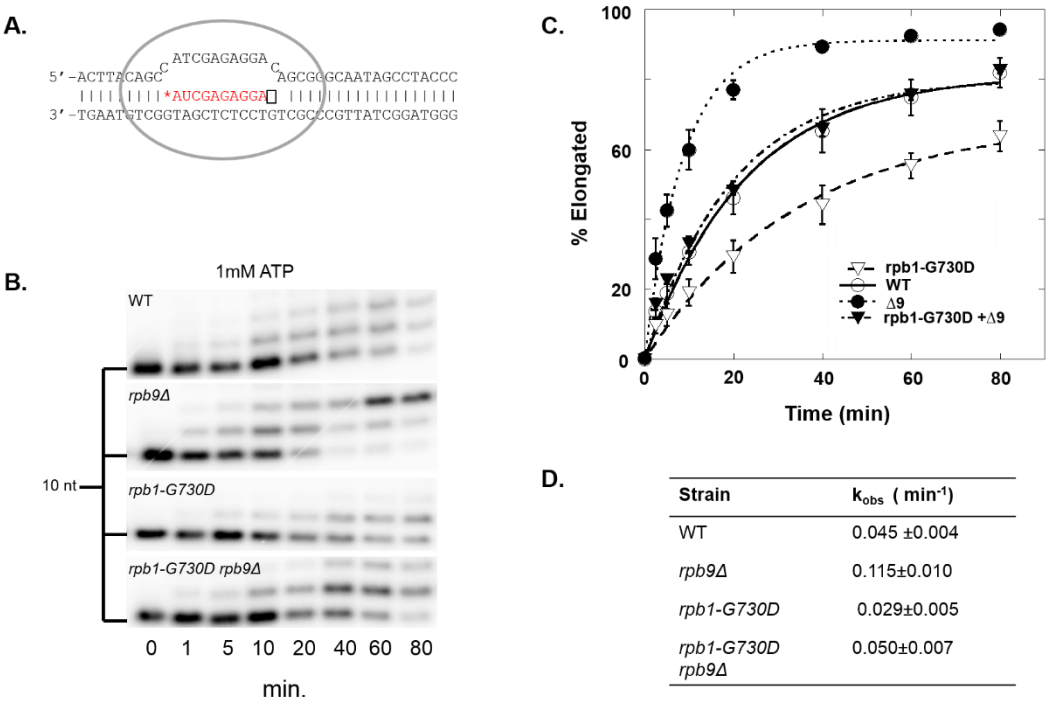

Strain	k_{obs} (min^{-1})
WT	0.045 ±0.004
rpb9Δ	0.115±0.010
rpb1-G730D	0.029±0.005
rpb1-G730D rpb9Δ	0.050±0.007

Figure A.2: The effect of the *rpb1- G730D* mutation on the pol IIΔ9 misincorporation rate.

(A) The EC complex with template/non-template DNA combinations used for misincorporation assay as well as the pre-annealed 5'-^{32}P labeled RNA (red) as in Fig. 3.1. (B) ATP 1mM was added to ECs immobilized from WCEs with pol II, *rpb1-G730D* pol II, pol IIΔ9, or *rpb1-G730D* pol IIΔ9, and the extension of the RNA to 11 nucleotides (nt) or greater was monitored over time via a 20% polyacrylamide gel. The *rpb1* mutation was introduced into cells as in Appendix Fig. 1. (C and D)The fraction extended to 11 or greater nts in B was plotted and fit to a single exponential function to obtain an observed rate for misincorporation, indicated by each curve. The fraction elongated was divided by the extent of the reaction as determined by curve fit.

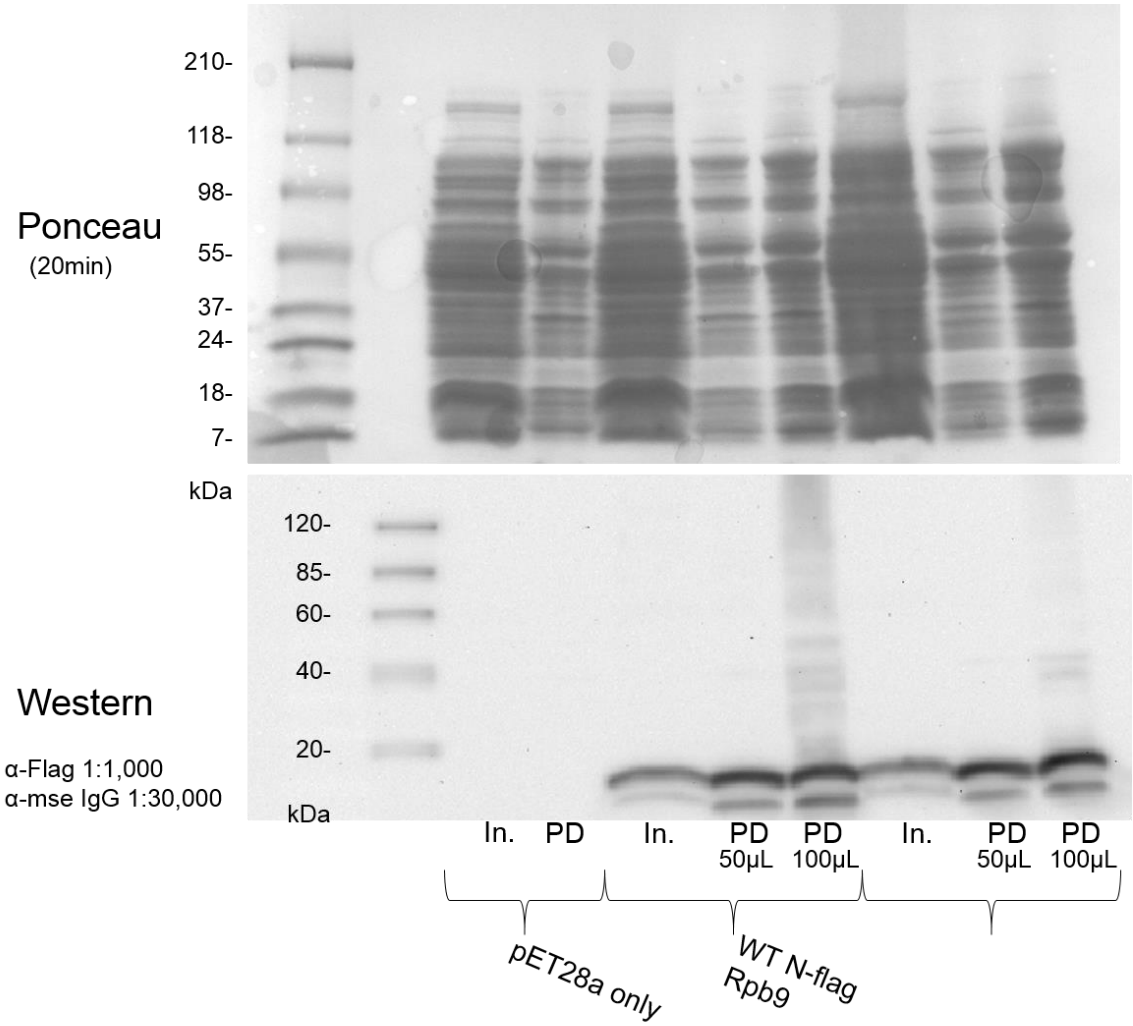

Figure A.3: Bacterial expression of wild-type and the (95-97)A variant of Rpb9 for purification

Rpb9 or Rpb9- (95-97)A with an N-terminal 6X-His and Flag-epitope tag was expressed as described in the methods chapter in a pET28a vector bacterial expression system. Lysates in varying amounts (post-induction with IPTG) derived from bacteria with vector only, or expressing recombinant Rpb9 were added to Ni^{2+} - NTA beads and probed with an α-Flag antibody to determine success of expression. Bracketed at the bottom of both panels is the strains loading of each lane. (In.) indicates crude lysate, while (PD) indicates lysate added to beads. The top panel shows the Panceau (2mg/mL in 1% acetic acid) stained nitrocellulose membrane after transfer from SDS PAGE. Standard band sizes are indicated on the left. Bottom panel is the resulting Western blot with a strong band approximately ~14kDa which corresponds to the size of recombinant Rpb9. The faster migrating band below are degradation products.

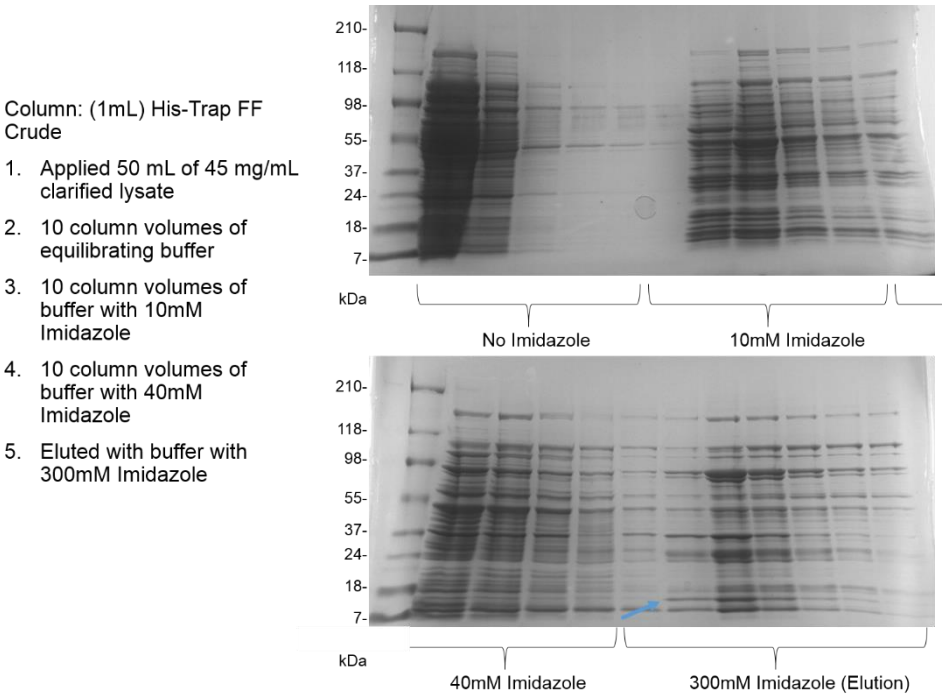

Figure A.4: Initial purification steps and elution profile of recombinant Rpb9 from bacterial lysates.

Lysates of bacteria expressing Rpb9 or Rpb9- (95-97)A were added to a His-Trap FF Crude column and washed in imidazole gradients as described in materials and methods. Final elution concentration corresponds with appearance of a protein band the approximate size of Rpb9 (blue arrow) as detected by a Coomassie stained SDS PAGE gel.

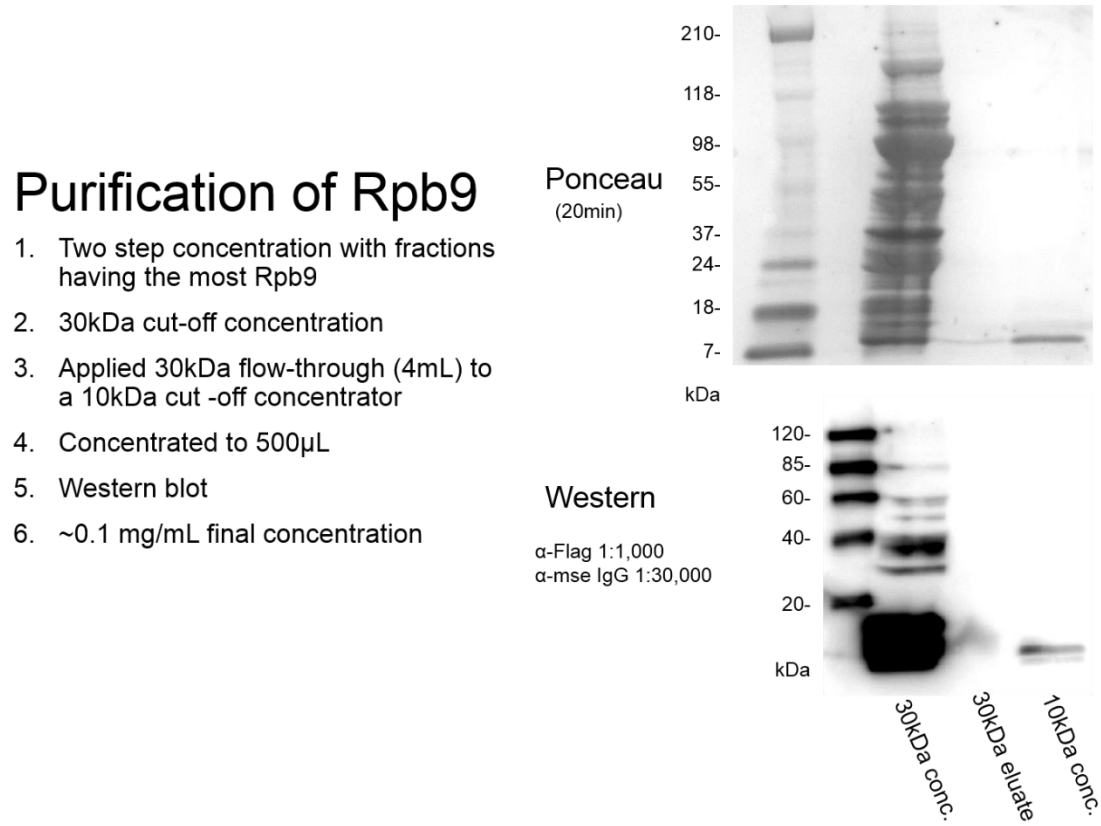

Figure A.5: Final purification step of Rpb9 or Rpb9- (95-97)A purification

Fractions from His-Trap FF column were pooled and applied to a 30kDa cut-off spinal column. Flow-through was then added to a 10kDa cut-off spin column and concentrated to 500 µL volume and analyzed by Western which demonstrated a single band of a size approximate to Rpb9 that is also detected by an α-Flag probe.

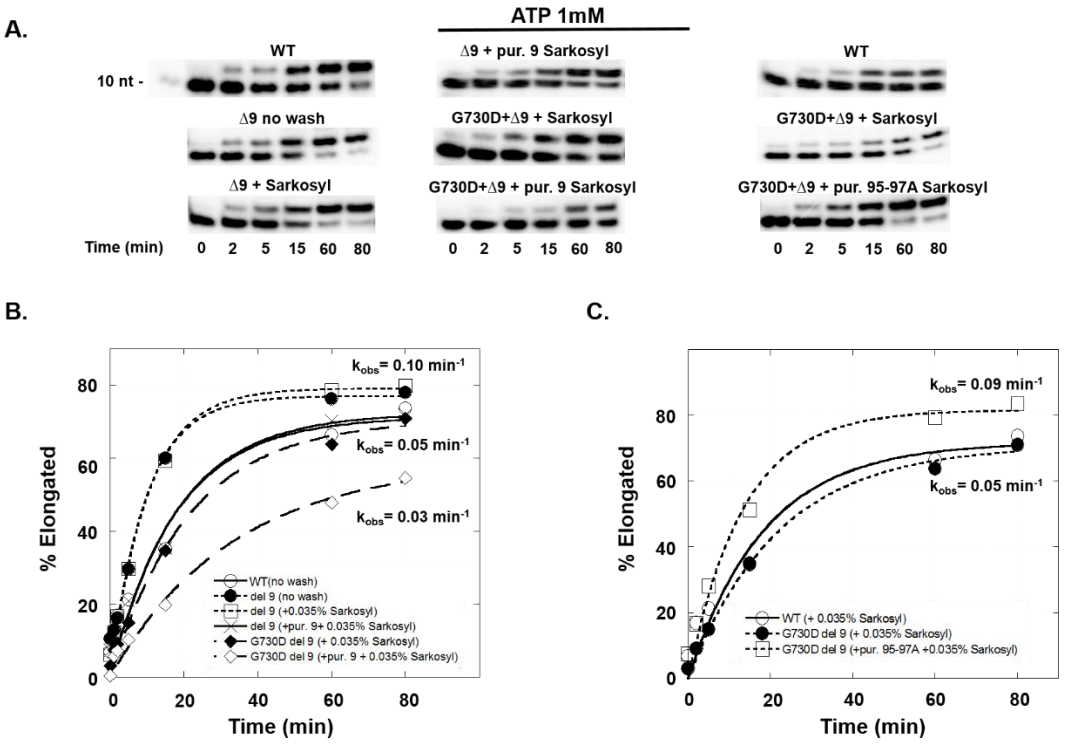

Figure A.6: Misincorporation rate of pol II ECs reconstituted by addition of purified Rpb9, or Rpb9- (95-97)A

Purified recombinant Rpb9 or Rpb9- (95-97)A was added back to ECs immobilized from WCEs derived from strains with pol II lacking Rpb9 and/or the *rpb1-G730D* mutation in amounts 20 times the published K_D. Preparation of ECs was identical to that of Fig. 3.1 except that we found an addition wash of 0.035% Sarkosyl was necessary for assembly. (A) ATP 1mM was added to indicated ECs and the extension of the RNA to 11 nucleotides (nt) or greater was monitored over time via a 20% polyacrylamide gel. (B and C)The fraction extended to 11 or greater nts in A was plotted and fit to a single exponential function to obtain an observed rate for misincorporation. Indicated on the graphs are the average rates in each grouping (i.e, pol IIΔ9 and Rpb9- (95-97)A + pol IIΔ9 have a k_{obs} ~0.10 min^{-1}, while pol II (WT), Rpb9 + pol IIΔ9, and *rpb1-G730D* pol IIΔ9 all have a k_{obs} ~0.05 min^{-1}).

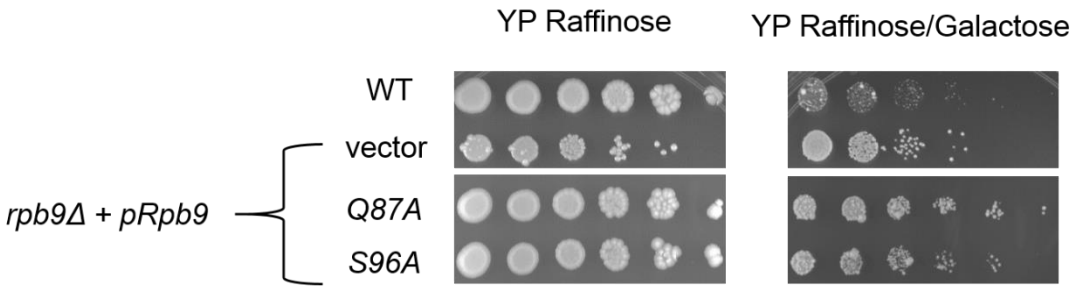

Figure A.7: Gal^S phenotype of selected *RPB9* C-terminal mutations *rpb9- Q87A/-S96A*

10-fold serial dilutions of indicated Rpb9 mutations. Performed as in Fig. 3.7.

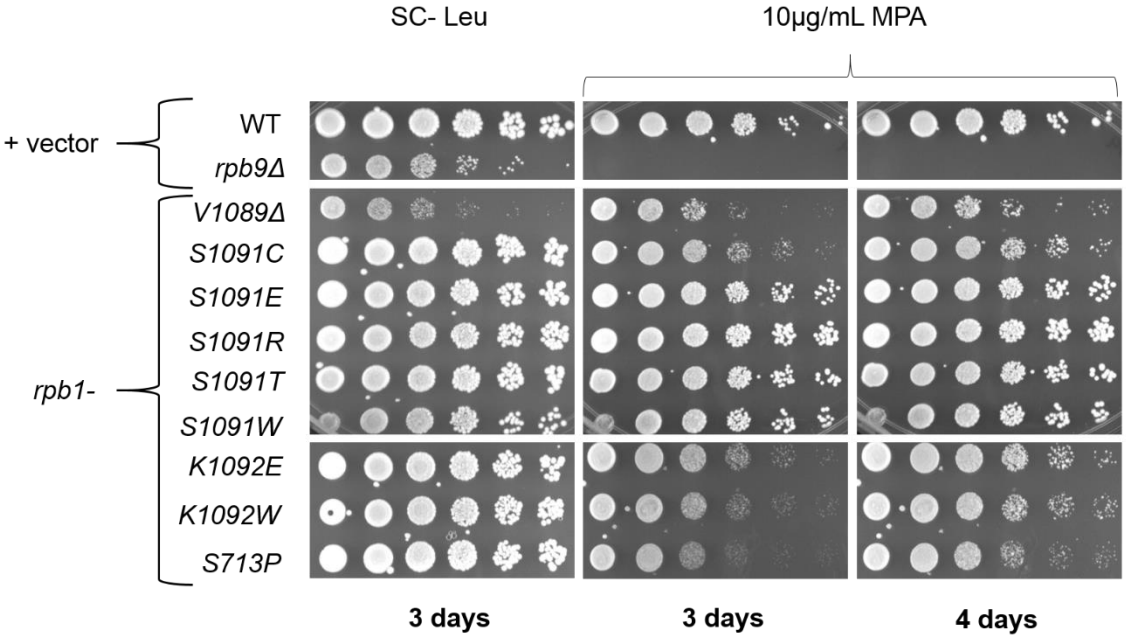

Figure A.8: Selected phenotypes of mutations at the AL-TL interface

10-fold serial dilutions of indicated AL-TL mutations as described in Chapter III. Cells were spotted from saturated liquid culture on the indicated media and monitored for growth for the indicated days. Performed as in Fig. 3.7, Rpb1 mutations where derived from shuffles as described in materials and methods and Fig. A1.

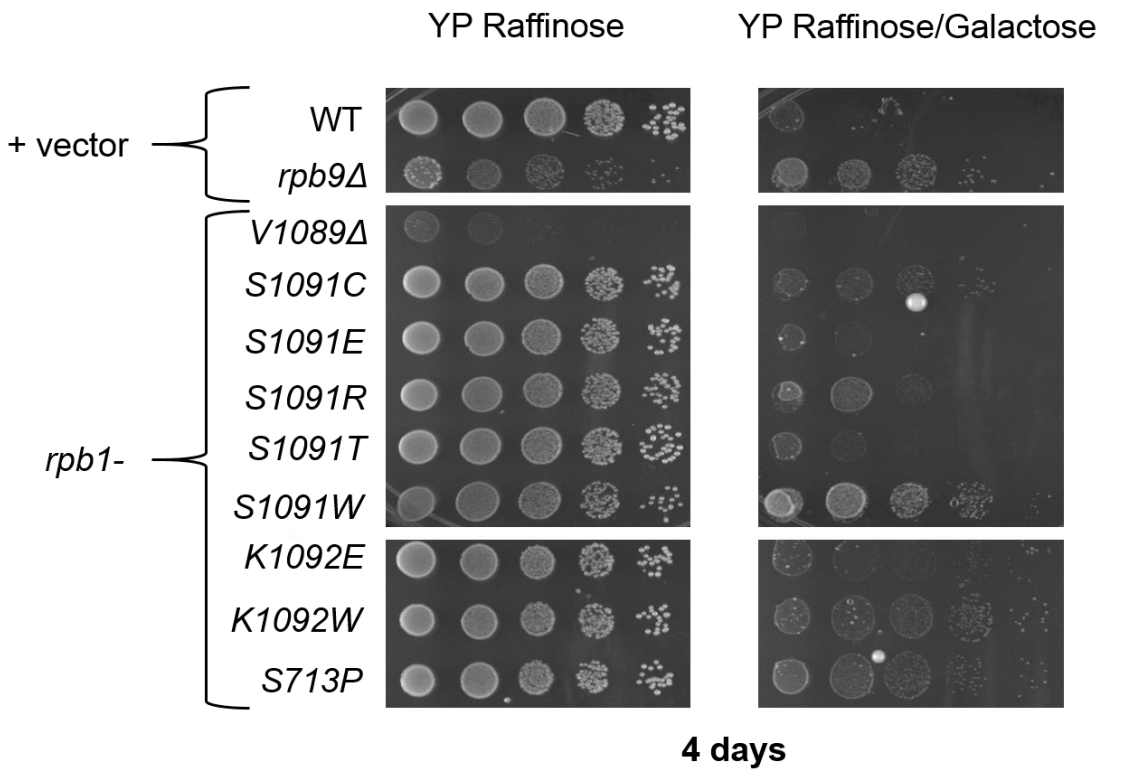

Figure A.9: Gal^S phenotypes of mutations at the AL-TL interface

10-fold serial dilutions of indicated AL-TL mutations as described in Chapter III. Identical strains and preparation to Fig. A8 and Fig. 3.7.

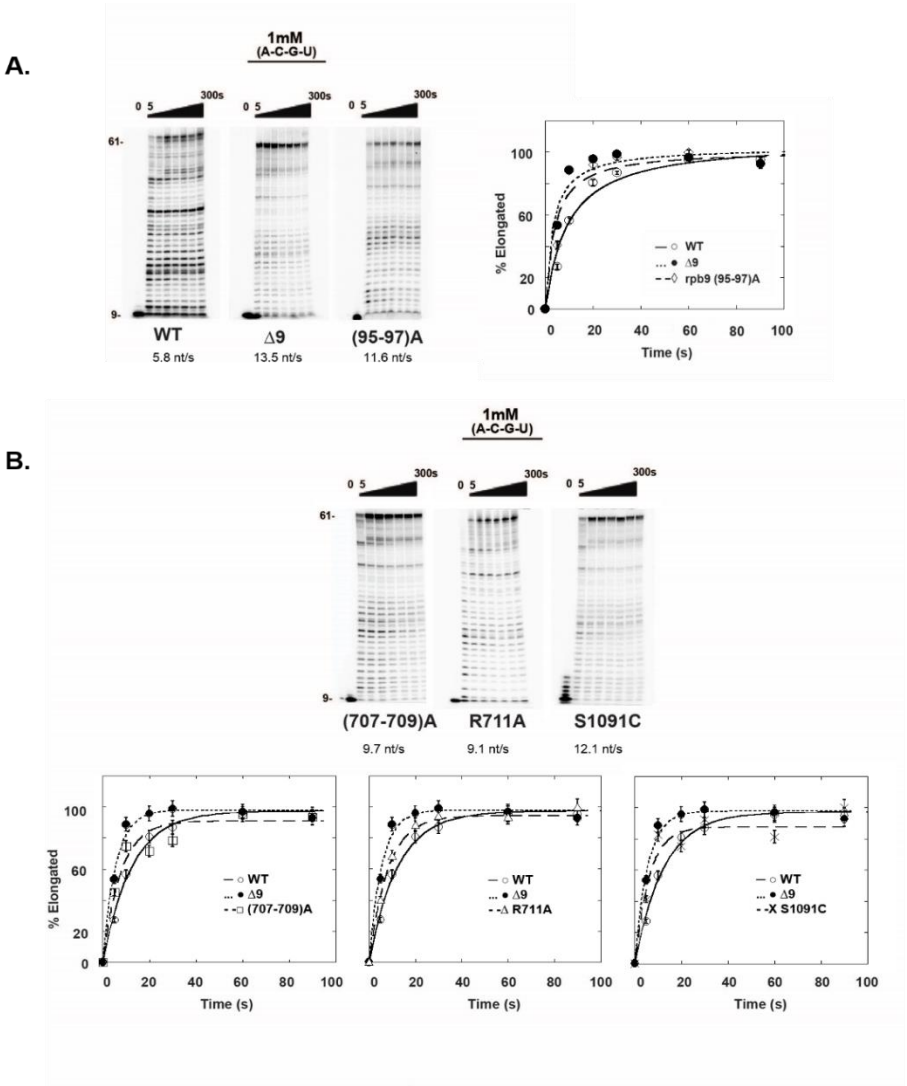

Figure A.10: Average correct nucleotide extension rate of Rpb9, AL, and TL mutants

The EC complex with template/non-template DNA combinations used to determine the average correct nucleotide extension rate as in Fig. 3.2 except that ECs were assemble from WCEs rather than purified pol II. A-, C,-, G, and UTP 1mM were simultaneously added to ECs derived from strains with indicated pol II mutation. The fraction of RNA extended to 61 nt (forming a product of 51nt) was plotted and fit with a non-linear equation to determine the half-time. The extension rate in nt/s was determined by dividing the 25 nts by the half-time and is indicated below each representative gel. (A) Estimation of the correct nucleotide extension rate for the Rpb9 variant, Rpb9- (95-97)A. (B) Estimation of the correct nucleotide extension rate for the AL mutations *rpb1- (707-709)A* and -*R711A*, as well as the TL mutation *rpb1-S1091C*.

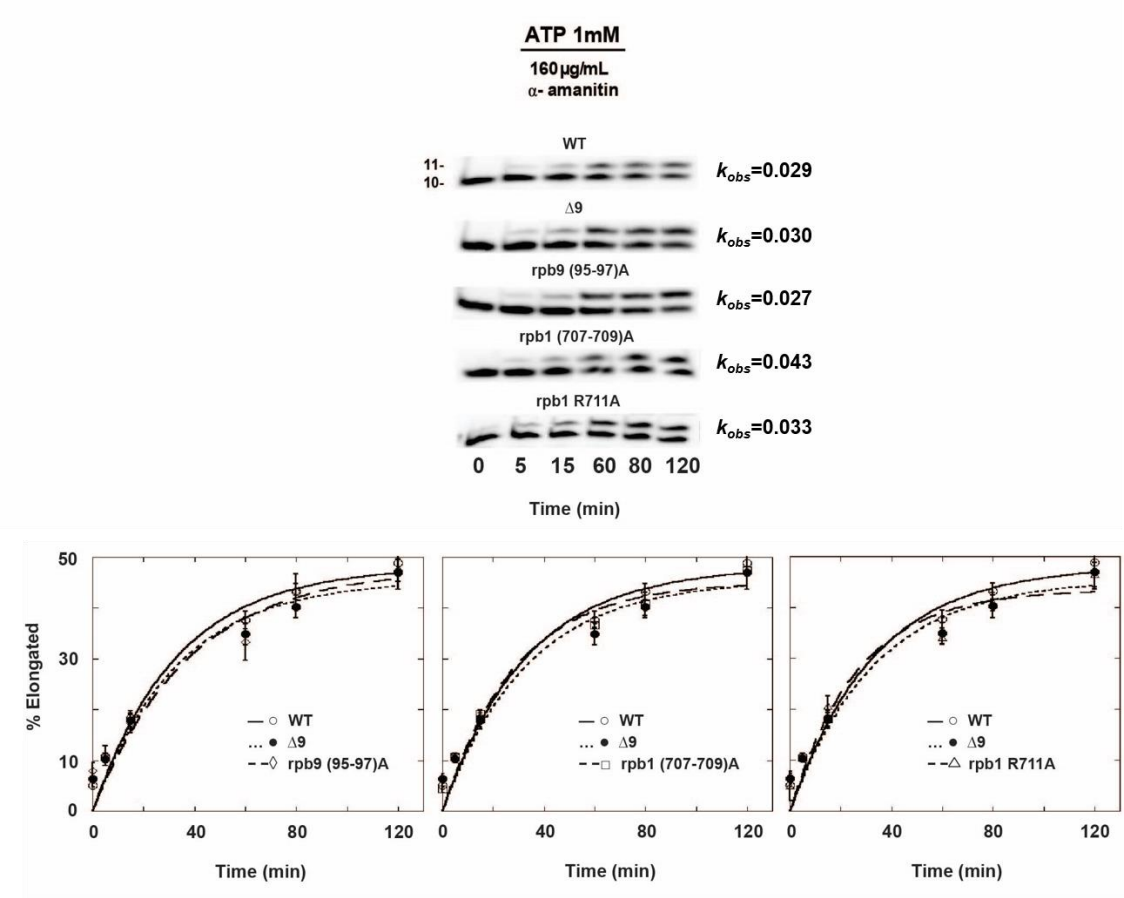

Figure A.11: The rate increase for an ATP misincorporation caused by mutations in the AL is dependent on α-amanitin

Complexes were formed as described in Fig. 3.4. ATP 1mM was added to ECs with indicated pol II mutation alone or ECs pre-incubated with α-amanitin, and the extension of the RNA to 11 nucleotides (nt) or greater was monitored over time via a 20% polyacrylamide gel. The fraction extended to 11 nts was plotted and fit to a single exponential function to obtain an observed rate for misincorporation, indicated by each representative *in vitro* assay and compiled in Table 3.1.

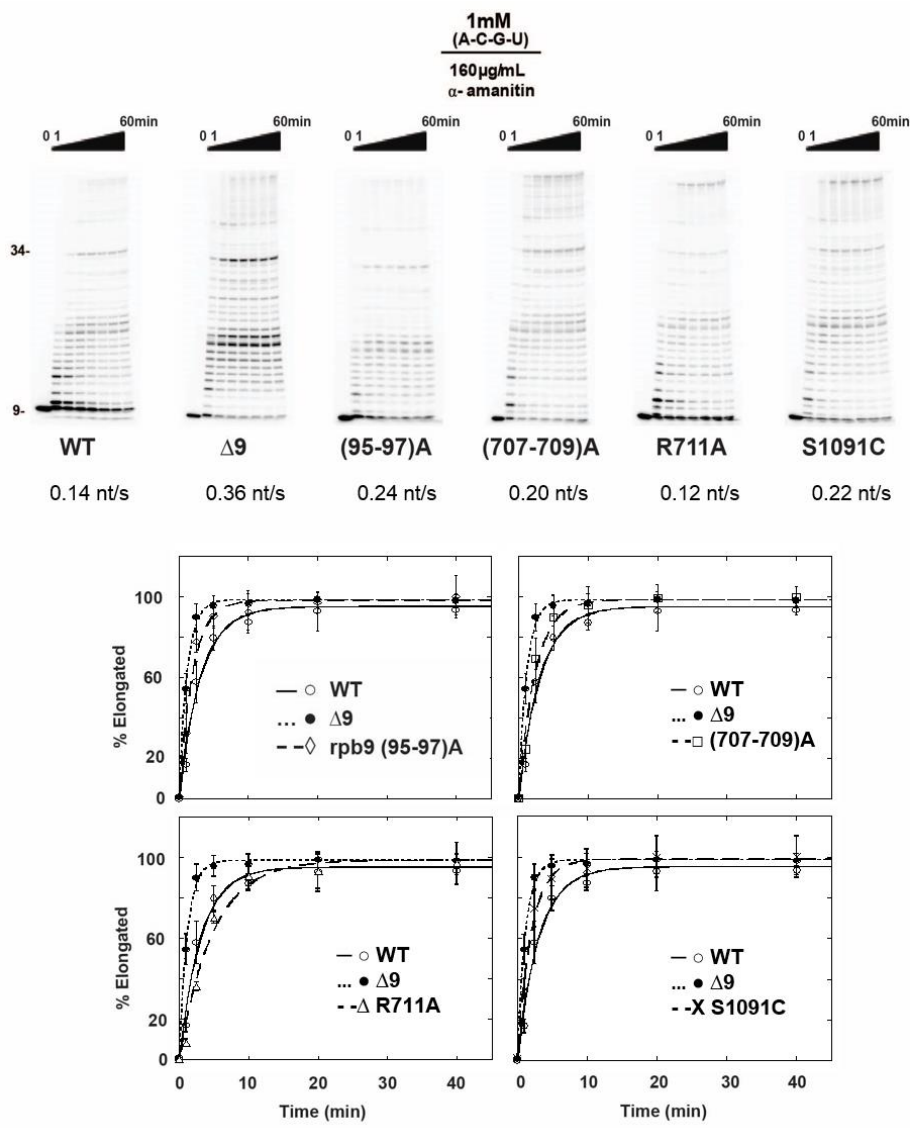

Figure A.12: Average correct nucleotide extension rate of Rpb9, AL, and TL mutants in the presence of α- amanitin

The EC complex with template/non-template DNA combinations used to determine the average correct nucleotide extension rate as in Chapter III, Fig. 2 except that ECs were assemble from WCEs rather than purified pol II. A-, C,-, G, and UTP 1mM were simultaneously added to ECs derived from strains with indicated pol II mutation that were pre-incubated with α- amanitin for 15 minutes. The fraction of RNA extended to 34 nts or greater for α-amanitin experiments was plotted and fit with a non-linear equation to determine the half-time. The extension rate in nt/s was determined by dividing the length of the extension product n- nucleotides long by the half-time. Elongation rates are indicated below each representative gel and compiled in Table 3.1

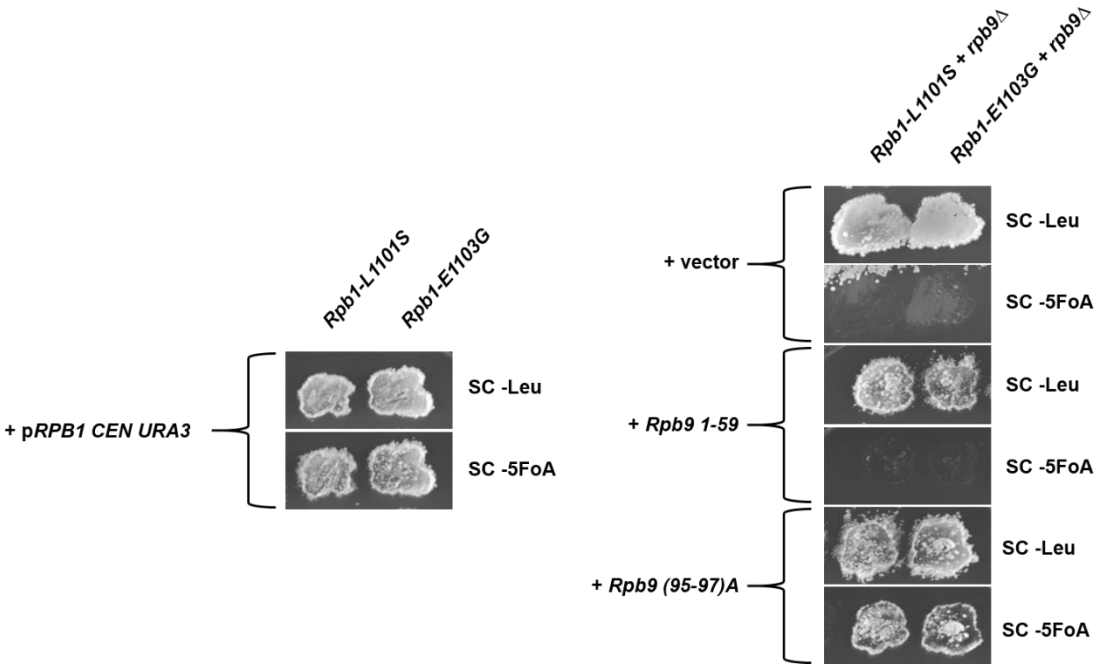

Figure A.13: Interactions of Trigger Loop mutants, *rpb1- L1101S* and - *E1103G* with *rpb9- (1-59)* and - *(95-97)A*

Shuffles performed as in Fig. A1. See Chapter III for description.